



Stephanie Ortiz Collazos

**Physical-chemical studies of the effect
of antibiotic incorporation in the
structure and molecular organization of
clinical-grade lung surfactant
monolayers and membrane models at
the air-water interface**

Tese de Doutorado

Thesis presented to the Programa de Pós-graduação em Química of PUC-Rio in partial fulfillment of the requirements for the degree of Doutor em Química.

Advisor: Prof. André Silva Pimentel

Rio de Janeiro
December 2018



Stephanie Ortiz Collazos

**Physical-chemical studies of the effect
of antibiotic incorporation in the
structure and molecular organization of
clinical-grade lung surfactant
monolayers and membrane models at
the air-water interface**

Thesis presented to the Programa de Pós-graduação em Química of PUC-Rio in partial fulfillment of the requirements for the degree of Doutor em Química. Approved by the undersigned Examination Committee.

Prof. André Silva Pimentel

Orientador

Departamento de Química – PUC-Rio

Profa. Sonia Renaux Louro

Departamento de Física – PUC-Rio

Prof. Luciano Caseli

UNIFESP

Prof. Carlos A. Gomes Soares

UFRJ

Prof. Katty Gyselle de Holanda e Silva

UFRJ

Prof. Marcio da Silveira Carvalho

Vice Dean of Graduate Studies

Centro Técnico Científico – PUC-Rio

Rio de Janeiro, December 17th, 2018

All rights reserved.

Stephanie Ortiz Collazos

Graduated in Chemistry at the University of Atlantico in 2013 and obtained her M.Sc. Degree in Chemistry from Pontifical Catholic University of Rio de Janeiro in 2015.

Bibliographic data

Ortiz Collazos, Stephanie

Physical-chemical studies of the effect of antibiotic incorporation in the structure and molecular organization of clinical-grade lung surfactant monolayers and membrane models at the air-water interface / Stephanie Ortiz Collazos; advisor: André Silva Pimentel. –2018.

112 f. : il. color. ; 30 cm

Tese (doutorado) – Pontifícia Universidade Católica do Rio de Janeiro, Departamento de Química, 2018.

Inclui bibliografia

1. Química – Teses. 2. Filmes de Langmuir 3. Surfactante pulmonar 4. Claritromicina 5. Levofloxacina 6. Modelos de membrana I. Pimentel, André Silva. II. Pontifícia Universidade Católica do Rio de Janeiro. Departamento de Química. III. Título.

CDD:540

A Cristina e Arman,
for their support and encouragement

Acknowledgements

First, I would like to thank my Lord God.

I would like to thank my supervisor, Prof. Dr. André Silva Pimentel, for providing me with research support, collaborations and coaching in his group.

I would like to thank Prof. Dr. Karen Edler, for her support in our neutron scattering project, which I developed in her group during for 4 months at the University of Bath.

I would like to thank CNPq for my pre-doctoral fellowship and CAPES for a sandwich doctorate scholarship (88881.132891/2016-01) which allowed me to develop part of my research.

I would like to thank Prof. Dr. Osvaldo Novaes de Oliveira Jr, Dr. Paulo Henrique de Souza Picciani and Dr. Carlos Augusto Gomes Soares by their assistance in this work.

I would like to thank Nathally B. Oliveira, Jéssica Cavaleiro, Evelina D. Estrada-López, Alline A. Pedreira, Lucas M. P. Souza, Felipe R. Souza and Antonio Augusto Malfatti Gasperini for their support in the development of this work.

I would like to thank the thesis committee for kindly accept the invitation, for their flexibility and great contributions to this thesis.

Last but not least, I would to thank my boyfriend Arman Esmaili for his love and support, to my family and to my friends from PUC-Rio/University of Bath for keeping me sane and nurtured with healthy relationships.

This study was financed in part by the Coordenação de Aperfeiçoamento de Pessoal de Nível Superior - Brasil (CAPES) - Finance Code 001.

Abstract

Collazos, Stephanie Ortiz; Pimentel, André Silva (Advisor). **Physical-chemical studies of the effect of antibiotic incorporation in the structure and molecular organization of clinical-grade lung surfactant monolayers and membrane models at the air-water interface.** Rio de Janeiro, 2018. 112p. Tese de Doutorado - Departamento de Química, Pontifícia Universidade Católica do Rio de Janeiro.

The lipo-proteic surfactant system acting at the alveolar interface is of vital importance for keeping functional the respiratory mechanics. Its impairments are associated with several pulmonary infections. Drug delivery systems based on animal-derived lung surfactants are complex making it difficult to understand the individual role of guest molecules in membrane interactions. Here we present a characterization of a clinical-grade porcine lung surfactant extract mixed with the antibiotics Levofloxacin and Clarithromycin, using a multi-technique approach – in conjunction with the Langmuir-monolayer methodology– consisting of surface pressure-area isotherms, Brewster angle microscopy (BAM), polarization modulation-infrared reflection-adsorption spectroscopy (PM-IRRAS), neutron reflectometry (NR), *in vitro* assays, and molecular dynamics simulations. The effect of both antibiotics in the structure of porcine lung surfactant monolayers as well as in DPPC monolayers was examined. It was revealed that the stability/integrity of the monolayers is preserved in the presence of both drugs. The mixed antibiotic/lung surfactant systems enhance the antibacterial activity against Gram-positive (*Bacillus cereus*) and Gram-negative (*Escherichia coli*) bacteria. These findings provide new insights into the optimization of efficient drug delivery systems for the treatment of pathological conditions at the respiratory level.

Keywords

Lung surfactant; Curosurf; Levofloxacin; Clarithromycin.

Resumo

Collazos, Stephanie Ortiz; Pimentel, André Silva. **Estudos físico-químicos sobre o efeito da incorporação de antibióticos na estrutura e organização molecular de monocamadas de surfactante pulmonar de grau clínico e em modelos de membrana na interface ar-água.** Rio de Janeiro, 2018. 112p. Tese de Doutorado - Departamento de Química, Pontifícia Universidade Católica do Rio de Janeiro.

O surfactante pulmonar é um sistema lipo-proteico que atua na interface alveolar com vital importância para manter funcional a mecânica respiratória. Os comprometimentos na sua função estão associados a diversas infecções pulmonares. Os sistemas de administração de fármacos baseados em surfactantes pulmonares derivados de animais são complexos, dificultando a compreensão do papel individual das moléculas hóspedes nas suas interações com a membrana. Aqui apresentamos uma caracterização de um extrato surfactante de pulmão porcino de grau clínico misturado com os antibióticos Levofloxacina e Claritromicina, usando uma abordagem multi-técnica – em conjunto com a metodologia de monocamadas de Langmuir– consistindo de isotermas de pressão de superfície-área, microscopia de ângulo de Brewster (BAM), espectroscopia de reflexão-absorção do infravermelho com modulação da polarização (PM-IRRAS), reflectometria de nêutrons (NR), ensaios *in vitro* e simulações de dinâmica molecular. Avaliou-se o efeito de ambos os antibióticos na estrutura das monocamadas de surfactantes de origem porcino bem como em monocamadas de DPPC. Foi revelado que a estabilidade / integridade das monocamadas é preservada na presença de ambas as drogas. Os sistemas mistos de antibiótico / surfactante pulmonar aumentam a atividade antibacteriana contra bactérias Gram-positivas (*Bacillus cereus*) e Gram-negativas (*Escherichia coli*). Essas descobertas fornecem novas percepções sobre a otimização de sistemas eficientes de administração de medicamentos para o tratamento de condições patológicas no nível respiratório.

Palavras-chave

Surfactante pulmonar; Curosurf; Levofloxacina; Claritromicina.

Table of contents

1 Introduction.....	16
2 Theoretical foundation	18
2.1 Lung surfactant: Composition, structure, and function	18
2.2 Exogenous lung surfactant as a drug delivery system	22
2.3 Antibiotics and model lung surfactant monolayers	23
2.3 About the layout of this manuscript	30
3 Materials and methods	31
3.1 Langmuir monolayers	31
3.1.1 Curosurf experiments	31
3.1.2 DPPC experiments	32
3.2 Brewster angle microscopy	32
3.3 Polarization-modulation infrared reflection absorption spectroscopy ..	33
3.4 Neutron reflectometry experiments in DPPC monolayers	33
3.5 Molecular dynamics simulations	34
3.6 Antibacterial activity quantification	35
4 Interaction of Levofloxacin with lung surfactant at the air-water interface	37
4.1 Introduction.....	38
4.2 Materials and methods	41
4.3 Results and discussion.....	41
4.4 Implications	46
4.5 Conclusion.....	46
4.6 Acknowledgments	47
5 Clarithromycin does not affect the stability of a lung surfactant monolayer at the air-water interface	48
5.1 Introduction.....	49
5.2 Materials and methods	52
5.3 Results and discussion.....	52
5.3.3 The interaction between Clarithromycin and Curosurf monolayers .	52
5.3.4 Bactericide activity of Clarithromycin incorporated in the lung surfactant.....	60

5.4 Implications	62
5.4 Conclusion.....	63
5.4 Declaration of Interest	63
5.4 Acknowledgments	63
6 Influence of Levofloxacin and Clarithromycin on the Structure of DPPC Monolayers.....	65
6.1 Introduction.....	66
6.2 Materials and methods	68
6.3 Results and discussion.....	69
6.4 Conclusions.....	80
6.5 Conflicts of interest.....	81
6.6 Acknowledgments	81
7 Conclusions and perspectives.....	82
References	84
A Published papers	100
B Submitted papers.....	101
C Supplementary material -1	102
D Supplementary material -2.....	104
E Supplementary material -3.....	105

List of figures

Figure 1. Structure of the main lipid constituents of lung surfactant.	18
Figure 2. Three-dimensional models of surfactant proteins and natural lung surfactant structures. Adapted from Casals and Cañadas, 2012(CASALS; CAÑADAS, 2012) and Perez-Gil, 2008(PÉREZ-GIL, 2008).	20
Figure 3. Naphthyridone ring, nucleus structure of fluoroquinolones (Left). Levofloxacin structure (Right).	24
Figure 4. 6-O-methylerythromycin A structure.	26
Figure 5. Chemical structure of the amphoteric Levofloxacin.	41
Figure 6. (A) Surface pressure-Area isotherms for pure Curosurf (black), Levofloxacin-Curosurf 0.1% w/w (red), and Levofloxacin-Curosurf 10% w/w (blue). (B) Experimental compressional modulus CS^{-1} as a function of surface pressure in Langmuir films of pure Curosurf (black), Levofloxacin-Curosurf 0.1% w/w (red), and Levofloxacin-Curosurf 10% w/w (blue).	42
Figure 7. Experimental PM-IRRAS spectra of Langmuir films of pure Curosurf (A), Levofloxacin-Curosurf 0.1% w/w (B), and Levofloxacin-Curosurf 10% w/w (C) at surface pressures 0 (black) and 30 (red for (A), blue for (B), and green for (C)) mNm^{-1} in the C H region (2800–3000 cm^{-1}), C O region (1400–1800 cm^{-1}), and C O region (1000–1300 cm^{-1}).	43
Figure 8. Brewster angle microscopy images of pure Curosurf, Levofloxacin-Curosurf 0.1% w/w, and Levofloxacin-Curosurf 10% w/w at $\pi = 0, 10, 20, 30, \text{ ad } 40 \text{ mN m}^{-1}$. All BAM images have a 25 μm scale bar at the left-hand corner.	45
Figure 9. (A) Experimental surface pressure as a function of the trough area for pure Curosurf (black), and Clarithromycin-Curosurf 0.1% w/w (red), 1% w/w (green), and 10% w/w (blue). (B) Experimental compressional modulus CS^{-1} as a function of surface pressure in Langmuir films of pure Curosurf (black), Clarithromycin-Curosurf 0.1% w/w (red), 1% w/w (green), and 10% w/w (blue).	53

- Figure 10. Experimental PM-IRRAS spectra of Langmuir films of Clarithromycin-Curosurf 0%, 0.1%, and 10% w/w at surface pressures 30 mNm⁻¹ in the (A) C–H region (2800–3000 cm⁻¹), and (B) C–O region (1000–1250 cm⁻¹).56
- Figure 11. Compression-expansion isotherms of pure Curosurf (black diamonds) and its mixtures with Clarithromycin 0.1 (red dashed line), 1 (green dotted line), and 10 % w/w (blue dashed-dotted line). Isotherms were obtained at a compression rate of 10 mm/min under one cyclic regime (compression-expansion) showing a complete hysteresis loop....56
- Figure 12. Brewster angle microscopy images of pure Curosurf, and Clarithromycin- Curosurf 0.1% and 10% w/w at $\pi = 0, 10, 20, 30$, and 40 mN m⁻¹. All BAM images have a 25 μm scale bar at the left-hand corner.59
- Figure 13. Antibacterial activity of Clarithromycin, Curosurf and Clarithromycin/Curosurf mixtures on *B. cereus* and *E. coli* strains. A) Clarithromycin resistance profile of each bacterial strain on LB plates. Tested strains, *B. cereus* Iso AC4 and *E. coli* DH5 α , and antibiotic concentration are indicated. Bacterial growth was marked as “-” for fully sensitive strains, “+++” for full growth as in antibiotic-free plates and “++” for weaker bacterial growth on the LB clarithromycin plates. B-D) Bacterial viability determined by the MTT conversion test of *B. cereus* (B-C) or *E. coli* (D) suspensions, treated for 3h (B) or 5h (C-D). Viability presented as the percentage relative to the MTT conversion quantified in control treatments with DMSO/water. Clarithromycin and Curosurf final concentrations are indicated. All antibacterial assays were performed using clarithromycin/Curosurf 1:9 mixtures (10% mass ratio). See Methods for details. Statistically significant viability inhibition is indicated for t-tests with $p \leq 0.0001$ (***), $p=0.0002$ to 0.0006 (**) and $p=0.001$ to 0.009 (*). Top brackets indicate the significance of specific comparisons and asterisks on the bars indicate the significance of the inhibitory effect of the specified treatment relative to the DMSO/water control treatment.....61
- Figure 14. (A) Surface pressure-area (π -A) isotherms of pure (black) and mixed DPPC/Clarithromycin monolayers at 10 % w/w (blue); 1 %

(green) and 0.1 % (red). (B) Surface compressional modulus at the air-water interface calculated from the isotherms in (A). (C) Surface pressure-area (π -A) isotherms of pure DPPC (black) and mixed DPPC/Levofloxacin at 10 % w/w (blue); 1 % (green) and 0.1 % (red). (D) Surface compressional modulus at the air-water interface from the isotherms in (B)70

Figure 15. Brewster angle microscopy images of pure DPPC (1 g.L⁻¹) (A) 0 mNm⁻¹ and (B) 30 mNm⁻¹. Mixed DPPC/Clarithromycin at 0 mNm⁻¹ (C 0.1% w/w; D 1%; E 10%) and 30 mNm⁻¹ (F 0.1% w/w; G 1%; H 10%). Mixed DPPC/Levofloxacin at 0 mNm⁻¹ (I 0.1% w/w; J 1%; K 10%) and 30 mNm⁻¹ (L 0.1% w/w; M 1%; N 10%).....72

Figure 16. Upper graph: PM-IRRAS spectra of pure DPPC with increasing surface pressure. Lower graph: PM-IRRAS spectra of pure DPPC (black solid line), DPPC/Levofloxacin 0.1% w/w (green dot-dashed line), DPPC/levofloxacin 10% w/w (brown double-dashed-dot line), DPPC/ Clarithromycin 0.1% w/w (red dashed line) and DPPC/ Clarithromycin 10% w/w (blue dot line) at the head groups region (1450–1800 cm⁻¹) 30 mNm⁻¹.74

Figure 17. Neutron Reflectometry data and the best two-layer fittings from simultaneously fitted d-DPPC on ACMW (green) and h-DPPC on D₂O (blue) monolayers at the air-water interface and a surface pressure of 30 mNm⁻¹. Upper figure: Reflectivity vs Q (Å⁻¹), Lower figure: The scattering length density plot of all contrasts vs the distance from the interface.76

Figure 18. Neutron Reflectometry data and the best two-layer fittings obtained from simultaneous fitted: h-DPPC/antibiotic on D₂O (orange); d-DPPC/antibiotic on D₂O (blue) and d-DPPC/antibiotic on ACMW (green) at 10% w/w and a surface pressure of 30 mNm⁻¹ Upper Figure: Reflectivity vs Q (Å⁻¹). Lower Figure: The scattering length density plot of all contrasts vs the distance from the interface. Left images correspond to DPP/Clarithromycin. Right images correspond to DPPC/Levofloxacin.78

Figure A.1. Published paper: Chapter 4.100

Figure B.1. Submitted paper 1: Chapter 5.101

Figure C.1. The IR powder spectrum of pure Levofloxacin.	102
Figure C.2. PM-IRRAS spectra of Langmuir films of pure Curosurf (A, B, and C), Levofloxacin-Curosurf 0.1% w/w (D, E, and F), and Levofloxacin-Curosurf 10% w/w (G, H, and I) at surface pressures 0, 10, 20, 30 and 40 mN m ⁻¹ in the C–H region (2800–3000 cm ⁻¹), C–C region (1400–1800 cm ⁻¹), and C–O region (1000–1300 cm ⁻¹).....	103
Figure D.1. Consecutive compression-expansion isotherms for pure Curosurf (black dashed line) and mixed Curosurf/Clarithromycin at 10% w/w. (blue dashed-dot line)	104
Figure E.1. Amplitude sweep of pure DPPC and mixed DPPC/antibiotics at 25°C using a DWR geometry at a strain amplitude of 1%. The full symbols represent the storage modulus G' and the empty symbols represent the loss modulus G'', respectively.....	105
Figure E.2. PM-IRRAS spectra of DPPC at surface pressures of 0, 30 and 40 mNm ⁻¹ for 1450 to 1800 cm ⁻¹ region (A) and 2800 to 3000 cm ⁻¹ (B) region. DPPC + 0.1% (w/w) Clarithromycin at surface pressures of 0, 30 and 40 mNm ⁻¹ for 1450 to 1800 cm ⁻¹ region (C) and 2800 to 3000 cm ⁻¹ (D) region. DPPC + 10 % (w/w) Clarithromycin at surface pressures of 0, 30 and 40 mNm ⁻¹ for 1450 to 1800 cm ⁻¹ region (E) and 2800 to 3000 cm ⁻¹ (F) region. DPPC + 0.1% (w/w) Levofloxacin at surface pressures of 0, 30 and 40 mNm ⁻¹ for 1450 to 1800 cm ⁻¹ region (G) and 2800 to 3000 cm ⁻¹ (H) region. DPPC + 10 % (w/w) Levofloxacin at surface pressures of 0, 30 and 40 mNm ⁻¹ for 1450 to 1800 cm ⁻¹ region (I) and 2800 to 3000 cm ⁻¹ (J) region.	109

List of tables

Table 1. Lipid and protein compositions of mostly used clinical surfactants7.....	22
Table 2. Summary of the scattering lengths densities used in the reflectivity calculations.....	74
Table 3. Summary of the parameters used for the best obtained NR fits using a two-layer model on pure DPPC (1mgmL^{-1}) and mixed DPPC/antibiotic monolayers at 10% w/w and 30 mNm^{-1}	77
Table E.1. BAM images for pure DPPC and mixed DPPC/Levofloxacin monolayers at 0.1, 1 and 10 % w/w under different surface pressures. All BAM images have a $25\text{ }\mu\text{m}$ scale bar at the left hand corner.	106
Table E.2. BAM images for pure DPPC and mixed DPPC/Clarithromycin monolayers at 0.1, 1 and 10 % w/w under different surface pressures. All BAM images have a $25\text{ }\mu\text{m}$ scale bar at the left hand corner.	107
Table E.3. Fitting parameters for a DPPC monolayer using two isotopic contrasts at surface pressures of 5, 20 and 30 mNm^{-1}	110
Table E.4. Fitting parameters for a DPPC/Clarithromycin (CLA) monolayer using three isotopic contrasts at surface pressures of 5, 20 and 30mN m^{-1} . θ is the alkyl tail tilt angle relative to the surface normal.	111
Table E.5. Fitting parameters for a DPPC/Levofloxacin (LEV) monolayer using different isotopic contrasts at surface pressures of 5, 20 and 30mN m^{-1} . θ is the alkyl tail tilt angle relative to the surface normal.	112

List of abbreviations

AFM – Atomic force microscopy
ACMW – Air-contrast matched water
AMPs – Antimicrobial peptides
ARDS – Acute respiratory distress syndrome
ATR-FTIR – Attenuated total reflection- Fourier transform infrared spectroscopy
BAM – Brewster angle microscopy
BDP – Beclomethasone dipropionate
BLES – Bovine lipid extract surfactant
DMSO – Dimethyl sulfoxide
DPPC – 1,2-dipalmitoyl-sn-glycero-3-phosphocholine
DPPG – 1,2-dipalmitoyl-sn-glycero-3-phospho-(1'-rac-glycerol)
DPPS – 1,2-Dipalmitoyl-sn-glycero-3-phosphoserine
FDA – Food and drug administration
GUV's – Giant unilamellar vesicles
LB – Lysogeny broth
LC – Liquid condensed
LE – Liquid expanded
LS – Lung surfactant
MD – Molecular dynamics
MTT – Methylthiazolyldiphenyl-tetrazolium bromide
NMR- Nuclear magnetic resonance
NR – Neutron reflectometry
OD – Optical density
PG – Phosphatidylglycerol
POPC – 1-palmitoyl-2-oleoyl-glycero-3-phosphocholine
POPG – 1-Palmitoyl-2-oleoyl-sn-glycero-3-(phospho-rac-(1-glycerol))
PM-IRRAS – Polarization modulation-infrared reflection-adsorption spectroscopy
SLD – Scattering length density
SM – N-palmitoyl-D-erythro-sphingosylphosphorylcholine

1

Introduction

What is the importance of interface science? Interface science is a branch of study that involves the chemical/physical interactions that take place at the level of the boundaries edges –between phases– that constitute a system; as dominant aspects on the behavior of a whole system. This sets the foundation for the development of applied and interdisciplinary science.

At this point, the surfactant-based drug delivery systems research has allowed the appearing of more effective and less-invasive strategies for controlled release of drugs. In addition, biomimetic membrane systems investigations give new insights to understand the relationship between structure and function of mixed systems carrying therapeutical agents. Nevertheless, smart delivery systems demand a deep understanding of the interactions with target molecules, as well as, the biophysical properties at the nano-scale to overcome remaining physicochemical and biological barriers.

Natural lung surfactant is a lipoproteic fluid produced in the alveolar epithelium with a dual function: to lower the surface tension of the thin liquid film that lines the respiratory epithelium, as well as to act as a host defense against inhaled pathogens and particles(LOPEZ-RODRIGUEZ; PÉREZ-GIL, 2014). In this way, natural lung surfactant constitutes an essential lipid-protein complex that guarantees the gas exchange and consequently the organism gets the necessary energy to keep normal cell functions.

Exogenous lung surfactant is a lipoproteic extract from mammals lungs (bovine/porcine) that have been used to replace the natural lung surfactant when there is a lack or dysfunction of it (HAITSMA; LACHMANN; LACHMANN, 2001; HIDALGO; CRUZ; PÉREZ-GIL, 2015). Frequently, disorders in natural lung surfactant function have been related to the presence of pathogens agents

conducting inflammatory processes. Accordingly, exogenous lung surfactant replacement therapy carrying therapeutic drugs directly to lungs have been used as a synergistic methodology to treat surfactant function impairments, at the same time that minimizes side effects.

However, the introduction of a drug substance in the lung surfactant membrane could eventually compromise its structure, organization, stability, and interfacial properties as well as impairs the efficiency of the therapeutical agent. Due to this, a deep assessment of the interactions between the drug and the components of the lung surfactant extract can contribute to design a constructive interplay in respiratory formulations. Owing to this, the present doctorate thesis shows an overall and interdisciplinary study about the structure and the interactions between a porcine lung surfactant extract (Curosurf) with two different types of antibiotics (Levofloxacin and Clarithromycin) used for pneumonia treatment as well as with DPPC monolayers, mimicking the lung surfactant function at the air-water interface.

We believe that the aim of this work will help to promote the development of a new treatment for pneumonia with a low dose and fewer side effects. Our results firmly suggest that Levofloxacin and Clarithromycin incorporation, at least up to the fractions used in this work, will not interfere in the normal physiology of the lung surfactant system.

2 Theoretical foundation

In this chapter, a succinct background about the main concepts related to this doctorate thesis is provided. In section 2.2 and 2.3, an overlook on the state of the art in the context of this thesis is presented and discussed.

2.1 Lung surfactant: Composition, structure, and function

Natural lung surfactant is the essential surface-active agent that lines the pulmonary alveoli to lower the surface tension and prevent the alveolar collapse – as the alveoli become smaller during expiration– (PEREZ-GIL, 2010) during the respiratory process. The surface-active agent, produced by type II pneumocytic cells secreted in the form of multilamellar structures, consists of 90% lipids and 5-10% proteins. In the lipid content, 80-90% are phospholipids (PL), 70-80% of which are phosphatidylcholines (PC), approximately half of which is

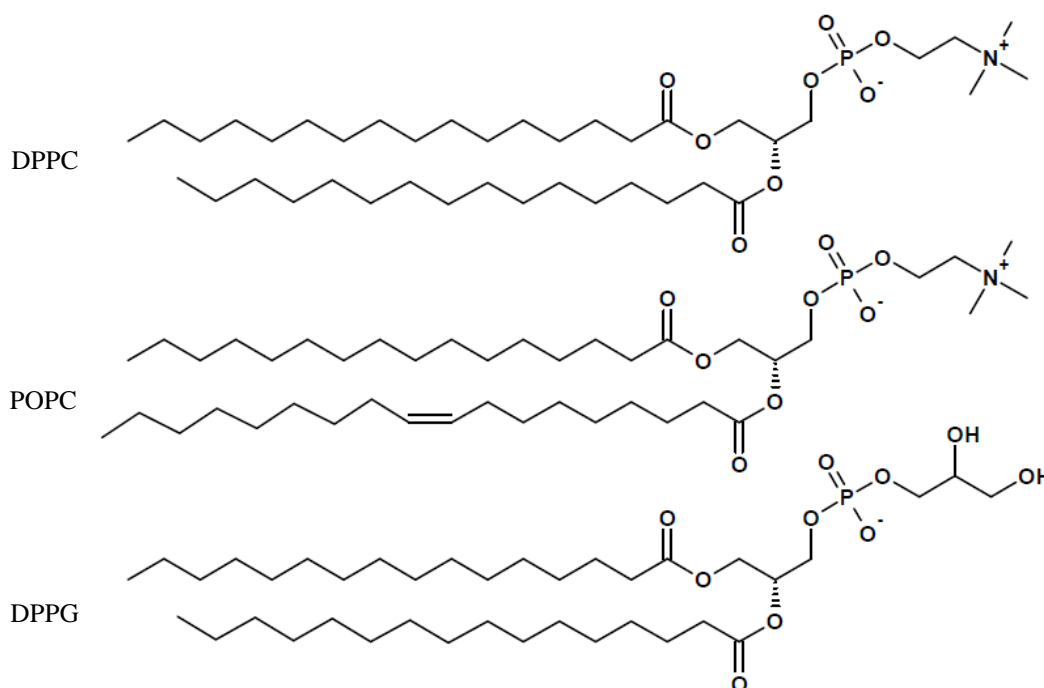


Figure 1. Structure of the main lipid constituents of lung surfactant.

dipalmitoylphosphatidylcholine (DPPC)(DUNCAN; LARSON, 2008) (Fig.1). Phosphatidylglycerol (PG) comprises approximately 10% of the lipid pool and small amounts of neutral lipids (~5-10 wt.%), primarily cholesterol, and α -tocopherol along with remaining PC molecular species mainly unsaturated as palmitoyl-oleoyl phosphatidylcholine (POPC)(CASALS; CAÑADAS, 2012) are also found. For a detailed description of most constituents, the readers are referred to Zhang et al. (2011)(ZHANG et al., 2011b).

The main function of this surfactant complex is to facilitate the respiratory mechanics, minimizing the energy that the lung tissue must provide to keep the gaseous exchange surface open and exposed during the successive inspiration-expiration cycles(PEREZ-GIL, 2010); which increases the pulmonary compliance. In physical chemistry, pulmonary alveoli can be considered as a balloon filled with air and surrounded by a thin liquid film. In consequence, the pressure difference sustained across the alveoli capillary membrane, i.e. the interface between two static fluids can be described through the Young–Laplace equation(BERNHARD, 2016) (1):

$$\Delta\rho = \frac{2\gamma}{r} \quad (1)$$

where $\Delta\rho$ is the pressure difference across the fluid interface, γ is the surface tension and r the radius of the alveolus. During the respiration process, specifically, at the end of expiration, the lung surfactant concentrate at the air-water interface of the alveoli membrane to act against the collapsing force that tends to reduce the surface area, thus reducing the pressure difference inside the alveoli and preventing the lung collapse. Besides, the natural lung surfactant has a second essential function: to act as the first barrier against inhaled pathogens and toxins, and indeed a defense system which also depends on its protein composition.

Although natural lung surfactant is mainly composed of lipids, and DPPC – which is responsible for the reduction of surface tension in the lungs to near-zero – (DUNCAN; LARSON, 2008) is the primary component of lung surfactant;

proteins make up 10% of lung surfactant, which can be divided into two groups; the hydrophilic proteins SP-A and SP-D, and the hydrophobic proteins SP-B and SP-C (HAITSMA; LACHMANN; LACHMANN, 2001) (Fig.2). According to the literature, the biophysical properties of natural lung surfactant largely depend on the presence of the SP-B and SP-C hydrophobic proteins. These proteins are crucial for surfactant activity inside the alveoli and their incorporation into lipid mixtures promotes proper interfacial adsorption, film stability, and re-spreading abilities (ALONSO et al., 2004). When the surfactant film, at the alveolar spaces, reaches surface tensions lower than 25 mNm^{-1} (surface pressures higher than 45 mNm^{-1}) during compression, it folds through three-dimensional transitions, creating multilamellar reservoirs excluded from the interface, which maintains minimal tensions (or maximal pressures). At this stage, the SP-C protein appears to facilitate the folding of the interfacial films, the exclusion of certain fluid lipids and lipid/protein complexes from the interface and the formation of three-dimensional phases (ZHANG et al., 2011b). SP-B, on the other hand, stabilizes the interfacial film and supports the formation of membrane-membrane contacts, providing mechanical stability to the compressed multi-layered films. Upon

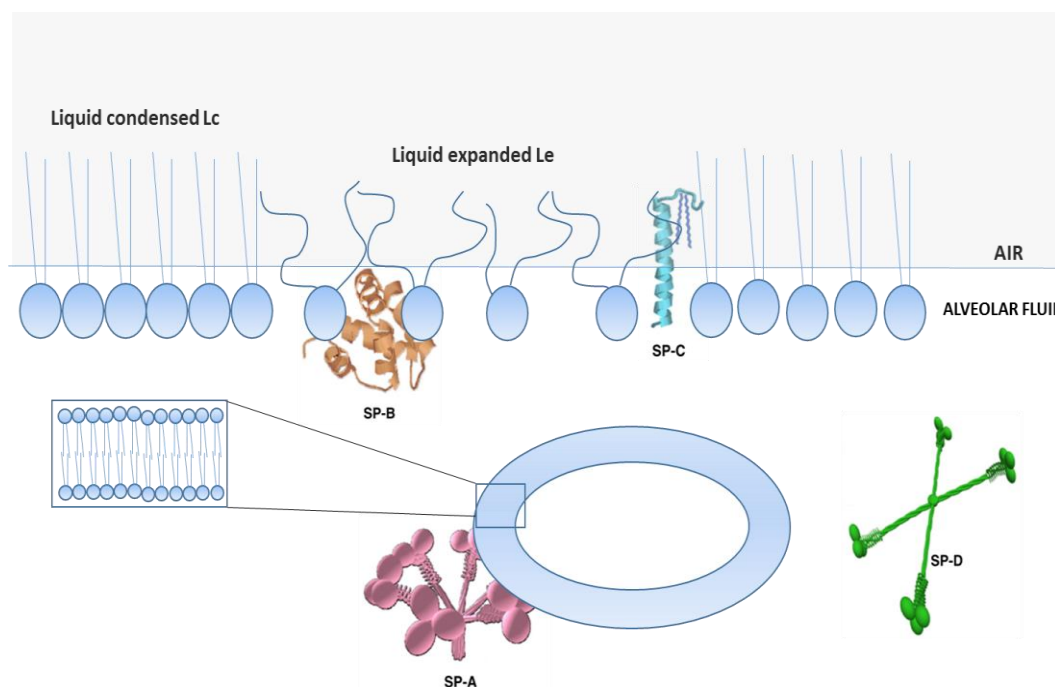


Figure 2. Three-dimensional models of surfactant proteins and natural lung surfactant structures. Adapted from Casals and Cañadas, 2012(CASALS; CAÑADAS, 2012) and Perez-Gil, 2008(PÉREZ-GIL, 2008).

expansion, SP-B and SP-C are thought to promote insertion and re-spreading of the phospholipids from the reservoirs back into the interface(HIDALGO; CRUZ; PÉREZ-GIL, 2015; ZHANG et al., 2011a). On the other hand, the hydrophilic proteins SP-A and SP-D have the ability to bind with carbohydrates and lipids to function as antimicrobial agents against a range of viruses, bacteria, fungi, etc(HIDALGO; CRUZ; PÉREZ-GIL, 2015; LOPEZ-RODRIGUEZ; PÉREZ-GIL, 2014; MUKHERJEE et al., 2008; PARRA; PÉREZ-GIL, 2015; VELDHUIZEN; HAAGSMAN, 2000).

As seen so far, lung surfactant has a vital function in air-breathing organisms. The pathological consequences of lack, deficiency or dysfunction of lung surfactant in mammals are severe. Acute respiratory distress syndrome (ARDS) is a serious pulmonary condition in which fluid collects in pulmonary alveoli, depriving organs of oxygen. This condition occurs when there is a significant trauma as sepsis (a blood infection), severe pneumonia, aspiration or shock from any cause, which led to lung surfactant inhibition or inactivation. ARDS is also a common cause of death in premature infants due to lung immaturity; however, it can affect adult patients with severe lung injury(ISKANDER, 2011).

Due to the overall similarities in lung surfactant composition among mammals, organic solvent extracts of natural lung surfactant are used as exogenous formulations in preventing ARDS to significant extents(MUKHERJEE et al., 2008). Clinical formulations like Survanta[®], Infasurf[®], and Curosurf[®], etc., are animal-derived surfactants FDA-approved in the USA, and widely used in the Western countries(RAGHAVENDRAN; WILLSON; NOTTER, 2012). A list of mostly used clinical substitutes of natural lung surfactant can be found in Table 1.

Table 1. Lipid and protein compositions of mostly used clinical surfactants(ZHANG et al., 2011b).

Animal derived surfactants		Composition in percentage			
Generic/Trade name	Source	PC/DPPC	Cholesterol	SP-B	SP-C
Beractant (Survanta)	Bovine lung mince	71/50	<0.2	0.04	0.9
Calfactant (Infasurf)	Calf lung lavage	79/43	5-8	0.9	0.7-1.3
Poractant alfa (Curosurf)	Porcine lung mince	69/47	0	0.4	0.7
BLES	Bovine lung lavage	77/41	2-3	0.5	1.5

2.2

Exogenous lung surfactant as a drug delivery system

The respiratory system possesses important advantages that facilitate to address drugs release and absorption. The lungs have a large surface area (approximately 100 m² for a human adult), and typical features of the thin alveolar epithelium coating their inner surface include high permeability and significant vascularisation. In addition, the low alveolar enzymatic activity results in a very slow clearance of drugs, compared to other ways of administration. Therefore, the bioavailability of different types of molecules is considerably better than when they are delivered through conventional methods (oral, topical or injected), especially for poorly water-soluble drugs(HIDALGO; CRUZ; PÉREZ-GIL, 2015). Thus, the idea of using lung surfactant as a drug transporter started to be developed in the late 1990s, when it was hypothesized that delivering drugs in combination with the pulmonary proteolipidic material could increase the local effectiveness while minimizing systemic side effects(HAITSMA; LACHMANN; LACHMANN, 2001; HIDALGO; CRUZ; PÉREZ-GIL, 2015; KHARASCH et al., 1991; VAN 'T VEEN et al., 1996). Currently, many authors have explored the incorporation of both drugs and nanoparticles in lung surfactant replacement therapies for the treatment of pneumonia and others pulmonary pathologies. In this regard, Wang *et al.*,(WANG et al., 2012) has carried out a study to characterize the biophysical interaction between a natural surfactant preparation (Infasurf) and two commonly used inhaled corticosteroids, budesonide and beclomethasone dipropionate (BDP). Based on surface activity measurements by the Langmuir balance and lateral film structure studies by atomic force

microscopy (AFM), their findings suggest that when Infasurf is used as a carrier, a budesonide concentration less than 1 wt % of surfactant or a BDP concentration up to 10 wt % should not significantly affect the biophysical properties of Infasurf, thus being feasible for pulmonary delivery. This study further suggests that different affinities to the surfactant films are responsible for the different behavior of budesonide and BDP. Later, Banaschewski *et al.*, (BANASCHEWSKI *et al.*, 2015) have tested and compared various antimicrobial peptides (AMPs) suspended in a bovine lipid-extract surfactant (BLES) by assessing surfactant-AMP mixture biophysical and antimicrobial functions by AFM and surface tension measurements (sessile drop technique). They observed that all AMP/surfactant mixtures exhibited an increase of spreading compared to a BLES control, but their bactericidal activities are highly reduced in the presence of BLES due to the charged phospholipids present in the lung surfactant. Solving this issue, the results support the proof of concept that AMP-based surfactant can be utilized for the therapy of bacterial infections.

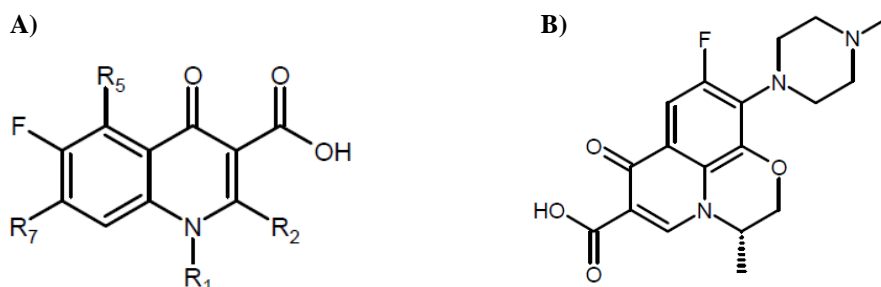
Thus far, many of the scientific studies in this area are limited to several preclinical assays and just a few of them have applied in deep morphological/structural assessments. This is due in part to the complex composition and organization of the lung surfactant system (BASABE-BURGOS *et al.*, 2018). Such complexity makes the task of unraveling the influence of therapeutical agents on the biophysical properties of the surfactant system difficult, and vice-versa. Therefore, DPPC is often used to represent the saturated lipid component and POPC or POPG the unsaturated lipid components in Langmuir monolayers, which are frequently used as model membranes (BRINGEZU *et al.*, 2001; PICARDI *et al.*, 2011).

2.3

Antibiotics and model lung surfactant monolayers

Since the presence of pathogens agents in the airways has been related with disruption of the pulmonary surfactant system and inflammation processes, one of the main concerns related to the treatment of patients with pulmonary infection is to address antibiotics directly to the pulmonary tissue to minimize systemic side

effects and impairment of the surfactant function(HAITSMA; LACHMANN; LACHMANN, 2001; WRIGHT et al., 2001).



**Figure 3. Naphthyridone ring, nucleus structure of fluoroquinolones (Left).
Levofloxacin structure (Right).**

One of the most spread and commonly used antibiotics for the treatment of lower respiratory tract infections are fluoroquinolones. The fluoroquinolones are synthetic fluorinated analogs of nalidixic acid, a 1,8-naphthyridine that possess a 4-quinolone nucleus –a naphthyridone– (see Fig.3a). These compounds are potent broad-spectrum bactericidal, offering excellent activity against Gram-negative, Gram-positive, and atypical pathogens (e.g. against *Streptococcus pneumoniae* and *Staphylococcus aureus*)(TORRES; LIAPIKOU, 2012). Thus, fluoroquinolones remain as the most common antibiotics used globally by intravenous and oral administration(LODE; ALLEWELT, 2002; VARDAKAS et al., 2008). Among fluoroquinolones, Levofloxacin is a third-generation fluoroquinolone which has been emerged as one of the most prominent members of the quinolone class and is extensively used in the treatment of community-acquired respiratory infections. Levofloxacin –a soluble 1,8-cyclo compound– (SHARMA; JAIN; JAIN, 2009; TORRES; LIAPIKOU, 2012; ZHANEL et al., 2002) (Fig.3b) has been considered a valuable respiratory therapeutic agent included on the World Health Organization's list of essential medicines, as one of the most effective and safe medicines needed in a health system(WORLD HEALTH ORGANIZATION, 2015) due to its high and proved safety and tolerability.

On the other hand, a second class of antibiotic molecules useful in treating respiratory infections are the macrolides. Macrolides are a large class of complex

antibiotics molecules with a high molecular weight (greater than 500 g mol⁻¹), consisting of, at least, 12- to 16-membered macrolactone ring. The ring is commonly substituted by hydroxyl groups and one or more deoxy sugars, usually cladinose and desosamine(STEPANIĆ et al., 2012). Like drugs, they have been in widespread clinical use for over 50 years and are effective against Gram-positive and certain Gram-negative microorganisms. Besides, macrolide antibiotics are considered to be one of the safest antibiotic treatments available, with a drug hypersensitivity reaction prevalence of 0.4% to 3% of all treatments(CHIRIAC; DEMOLY, 2015). In addition, their relative safety makes macrolides the drugs of choice for many respiratory infections in pediatric patients(KANEKO; DOUGHERTY; MAGEE, 2007). Recently, macrolides have been reported to possess wider biological activities such as anti-inflammatory, antitumor, and antimalarial properties. They are also used against respiratory tract infections by *Streptococcus pneumoniae*, *Haemophilus influenzae*, and *Moraxella catarrhalis*(KOSOL et al., 2012). A reason for the success of macrolides as drug molecules is their favorable pharmacological/physicochemical properties, besides its high accumulation in cells and tissues as well as high binding to lipids(MUNIĆ et al., 2011). Clarithromycin is a second-generation broad-spectrum macrolide antibiotic (Fig.4) developed in 1980, which has been widely administrated for the treatment of lower respiratory tract infectious bacteria such as *Chlamydophila pneumoniae*, *Klebsiella pneumonia*, *Pseudomonas aeruginosa*, and *Mycoplasma pneumonia*(DIMER et al., 2015; MOGHADDAM et al., 2013). Clarithromycin – 6-O-methylerythromycin A–, also included on the World Health Organization's List of Essential Medicines, emerged through efforts to improve the predecessor antibiotic erythromycin that experience acid instability in the digestive tract, causing side effects, such as nausea and stomachache(GREENWOOD; IRVING, 2012).

Traditionally, the treatment of respiratory infections consists on high doses of single or combined antibiotics administered by oral or intravenous route, which induce undesirable side effects mainly due to high systemic bioavailability. Drug association to an effective transportation system offers a targeted route of administration with several advantages over conventional dosage forms (SALEM; FLASHER; DÜZGÜNEŞ, 2005). The local route of drug administration allows one order of magnitude-lower drug doses to be delivered, compared to systemic administration by the oral route or by injection. The low dosing locally reduces systemic exposure to the drug, and thereby systemic side effects, and increases the drug therapeutic index (LOIRA-PASTORIZA; TODOROFF; VANBEVER, 2014). Hence, the design of innovative strategies for drug delivery to the alveoli membrane is getting more attention as a non-invasive route of drug release for the most pharmaceuticals. In this context, drug delivery systems directly to airways are a promising route of administration for active agents such as Levofloxacin and Clarithromycin (ALHAJLAN; ALHARIRI; OMRI, 2013; CHEOW; CHANG; HADINOTO, 2010; CHEOW; HADINOTO, 2011; DIMER et al., 2015; FORIER et al., 2014; JESÚS VALLE; GONZÁLEZ LÓPEZ; SÁNCHEZ NAVARRO, 2008; MOGHADDAM et al., 2013; PARK et al., 2013; TOGAMI; CHONO; MORIMOTO, 2012; YE et al., 2017).

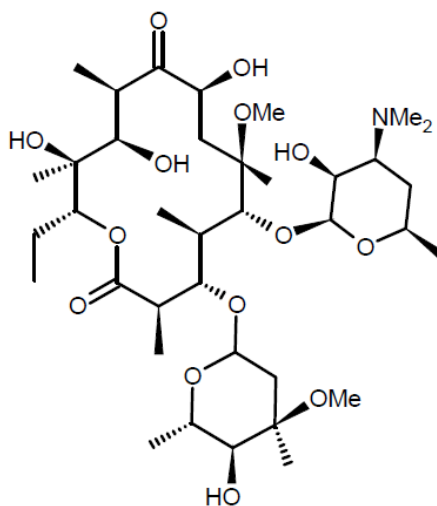


Figure 4. 6-O-methylerythromycin A structure.

As many of these strategies involve the encapsulation of drugs inside lipid nanocarriers or its merge with exogenous pulmonary surfactant preparations, the specific role of individual components as well as the physicochemical impact of

the lipid/drug interactions on the biophysical structure of the targeted membrane, must be fully deciphered and understood (MORENO-SASTRE et al., 2015). Thereby, Langmuir monolayers at the air-water interface provide accessible models for studies of lung surfactants and other amphiphilic molecules at the air-alveolus interface. Langmuir studies on lipid monolayers can be achieved over the surface of water/buffer using a surface Langmuir balance. This technique allows for various parameters such as lipid composition, subphase, and temperature to be controlled to mimic biological conditions. Changes in the lipid monolayer morphology at the air-water interface can be studied by *in situ* Brewster angle microscopy to the 2D Langmuir monolayers (C. PEETLA, A. STINE, 2009). Besides, many other techniques such as Infrared reflection-absorption spectroscopy (IRRAS) can be used to investigate the effects of the interaction of drugs or drug delivery systems on lipids. An advantageous and well-proven approach in monolayer biophysics termed polarization modulation-infrared reflection-adsorption spectroscopy (PM-IRRAS), applied over lipid monolayers *in situ*, provides unique molecular structure and orientation information from the Langmuir films constituents, without interfering effect of water vapor and carbon dioxide on the modulated reflectivity (MENDELSON; MAO; FLACH, 2010).

In this context, Bensikaddour, *et al.*, (BENSIKADDOUR et al., 2008a) have been investigated the interactions of two fluoroquinolone antibiotics (Ciprofloxacin and Moxifloxacin) with lipid monolayers/bilayers composed of DPPC/DOPC, using an array of complementary techniques. To gain further information at the molecular level on the interaction between Ciprofloxacin and lipids they studied the effect of increasing amounts of antibiotics on surface pressure-area isotherms (π -A) coupled with ATR-FTIR. Their studies indicate that there is a relationship between the lipid chain conformation and orientation with changes in membrane properties and the ability of drugs to diffuse through membranes determined by the drug lipophilicity. AFM imaging of supported lipid bilayers showed that Moxifloxacin induced, to a greater extent than Ciprofloxacin, an erosion of the DPPC domains in the DOPC fluid phase, while Langmuir studies show a condensing effect of the monolayer in the presence of both drugs. Additionally, the same authors published studies using Ciprofloxacin on [DOPC:DPPC] and [DOPC:DPPG] liposomes demonstrating that the interactions of this antibiotic

with lipids depend markedly on the nature of their phosphate head groups and that Ciprofloxacin interacts preferentially with anionic lipid compounds, like phosphatidylglycerol (BENSIKADDOUR *et al.*, 2008b). Further, Montero *et al.*, (MONTERO; MERINO-MONTERO; VINUESA, 2006) have discussed the interaction of Ciprofloxacin and two methyl derivative isomers of the drug with liposomes and supported planar bilayers composed of lipids from microbial membranes of *Escherichia coli* (i.e. phosphatidylethanolamine, phosphatidylglycerol, cardiolipin, etc). The experiments have shown that the three fluoroquinolones interact electrostatically with the bilayer, however, inducing different changes in height, roughness, and area covered by the supported planar bilayers. This result provides evidence for a different interaction of each antibiotic at the membrane-water interface. Previous studies from the same authors related to the interaction between, Ciprofloxacin and its pentyl derivative, with membranes models such as liposomes and monolayers using calorimetric and surface balance techniques (MONTERO; HERNÁNDEZ-BORRELL; KEOUGH, 1998), demonstrated that hydrophobicity of the drug had a role in determining the nature of drug-membrane interaction as seen in greater perturbations of the lipid packing by pentyl Ciprofloxacin. Their overall observations led to conclude that drug membrane solubility might have some effect on the pharmacokinetics of the drugs in the cells. Moreover, Grancelli *et al.*, (GRANCELLI *et al.*, 2002) reported studies of the interaction between Ciprofloxacin and its N-4-butylpiperazinyl derivative with DPPC (vesicles/monolayers) as a model membrane. Their work described that both fluoroquinolones might be surface active drugs that interact at the lipid-bilayer interface where the headgroups are located. Their experiments provide evidence that fluoroquinolones have an effect on the headgroup ordering and/or average orientation of the DPPC headgroups, which appears to depend on the phospholipid gel/fluid phase. Monolayer experiments point to the possibility that Ciprofloxacin could be segregated or 'squeezed-out' from the phospholipid environment which could have an influence on a slower efflux activity for some bacteria.

Regarding lipid/drug studies with macrolides, Azithromycin is another antibiotic drug that has been widely investigated for its interactions with phospholipids. Tyteka *et al.*, (TYTECA *et al.*, 2003) have studied the effect of

Azithromycin/phospholipid interactions on membrane organization and fluidity using Langmuir-Blodgett monolayers, liposomes, and J774 macrophages as cell membrane models. Equilibrium dialysis and ^{31}P NMR revealed that Azithromycin binds to lipidic model membranes and decreases the mobility of phospholipid phosphate heads. In contrast, Azithromycin had no effect deeper in the bilayer, based on fluorescence polarization measurements. AFM showed that Azithromycin perturbed lateral phase separation in Langmuir-Blodgett monolayers, indicating a perturbation of membrane organization in lateral domains. They conclude that Azithromycin directly interacts with phospholipids, modifies biophysical properties of the membrane and affects membrane dynamics in living cells, which it is likely to be related with perturbation of endocytosis. On the other hand, Berquand *et al.*, (BERQUAND *et al.*, 2005) have investigated the effect of this macrolide antibiotic on the molecular organization, fluidity, and permeability of DPPC:DOPC, DPPE:DOPC, SM:DOPC, and SM:Chol:DOPC lipid vesicles. Their studies demonstrated that the influence of the drug on lipidic domains strongly depends on the lipid nature. Azithromycin was able to erode gel domains of DPPC and DPPE domains embedded in a fluid DOPC matrix, but had no effect on SM or SM:cholesterol domains. Fa *et al.*, (FA *et al.*, 2007) have studied the effect of Azithromycin on the elastic properties of DOPC giant unilamellar vesicles (GUVs). Microcinematographic and morphometric analyses revealed that the addition of azithromycin increases lipid membrane fluctuations, leading to the eventual disruption of the largest GUVs. Azithromycin decreased both the bending modulus and the apparent area compressibility modulus of the lipid membrane. Thus, the data shows that azithromycin can alter the elastic properties of DOPC lipid bilayers by decreasing the coercive energy between DOPC molecules (C. PEETLA, A. STINE, 2009). In addition, Ceccarelli *et al.*, (CECCARELLI *et al.*, 2015) investigated the insertion of Azithromycin into preformed Langmuir monolayers of pure DPPC and mixed DPPC/DPPS (dipalmitoylphosphatidylserine), using adsorption experiments. Their results reveal that the antibiotic did not show any surface activity nor induce an increase of the surface pressure, indicating none or very limited interaction with the DPPC monolayer. Moreover, in the presence of DPPS, azithromycin induced an appreciable increase $\Delta\pi$ probably due to the possible electrostatic interactions between DPPS and the protonated amino-groups of the drug. This is in agreement

with the previous investigations from Berquand *et al.*, (BERQUAND *et al.*, 2005) where they show that the interaction of the lipid membranes with the antibiotic is strongly dependent on the lipid nature. Further studies from Dynarowicz-Łątka *et al.*, (DYNAROWICZ-ŁĄTKA *et al.*, 2005; HAC-WYDRO *et al.*, 2005a, 2005b) have explored the influence of Amphotericin B (AmB) –an antifungal medication subgroup of the macrolide antibiotics which exhibits similar structural elements– into Langmuir monolayers formed by sterol/DPPC lipids, showing that AmB strongly interacts with sterols in monolayers. The interactions with cholesterol are preferred as compared to ergosterol. On the other hand, the interactions between AmB and DPPC are not significant, and therefore larger amount of “free” AmB molecules can interact with both cholesterol and ergosterol. Instead, some AmB derivatives of the second generation seem that, in the presence of phospholipids, turns immobilized by its interactions with DPPC.

As seen so far, the molecular properties of lipids and its interactions with drugs can modulate membrane processes. Since the molecular interactions between them are highly dependent on their own physical-chemistry nature, it is necessary to study any membrane model as independent and aims to unveil the molecular mechanisms involved. Molecular arrangement changes have been inferred from morphological studies, but have not been shown via direct measurements of the phase structure.

2.3

About the layout of this manuscript

This doctorate thesis is an article-based one, which means that the section "Results and discussion" is an adaptation of journal papers already published/submitted. For the sake of simplicity, the material and methods (Section 3) are introduced in the traditional way. When the reader reaches the papers section (Section 4 to Section 6), it is just referred backward in Section 3 in order to understand the methodology.

3

Materials and methods

Since this thesis is based on an article layout, the methodology will be presented here and omitted in the respective articles. The papers will only focus on the presentation of the results and discussion.

3.1

Langmuir monolayers

3.1.1

Curosurf experiments

Spectroscopic chloroform grade (greater than 99.99%) used to prepare spreading solutions for the Langmuir monolayers was purchased from Sigma-Aldrich, Brazil, while the natural lung surfactant (Curosurf) was obtained from Chiesi Farmacêutica Ltda. Curosurf is an animal-derived surfactant extract, prepared from porcine lungs, containing almost exclusively polar lipids, in particular, phosphatidylcholine (about 70% of total phospholipid content), PG and other lipids (about 30% of total phospholipid content), and about 1% of hydrophobic proteins SP-B and SP-C. Levofloxacin and Clarithromycin were donated by Aché Laboratórios Farmacêuticos. The solvents chloroform and acetone used for cleaning were of ACS grade, purchased from Vetec, Brazil. The water used throughout the experiments was supplied by a Milli-Q Integral 10 purification system from Millipore USA (resistivity 18.2 MΩ·cm). For the Langmuir experiments, 20 µL chloroform solutions ($\sim 0.4 \text{ g L}^{-1}$) of natural lung surfactant were spread, in some cases containing Levofloxacin. The PTFE Langmuir trough (dimensions $300 \times 75 \text{ mm}^2$) housed in a class 10,000 clean room, was provided with two mechanical barriers symmetrically controlled by a KSV-Nima computer interface (Biolin Scientific, Finland). A waiting time of 10 min was allowed for chloroform evaporation and monolayer equilibration, before the surface pressure - area (π -A) isotherms were recorded at a compression rate of 10 mm min^{-1} . The isotherms are reported as an average of at least three measurements.

The surface compressional modulus (C_S^{-1}), also known as the in-plane elasticity, was calculated from the surface pressure isotherms using the expression:

$$C_S^{-1} = -A \left(\frac{\partial \pi}{\partial A} \right) \quad (2)$$

where π is surface pressure and A is the trough area (DAVIES; RIDEAL, 1963; DYNAROWICZ-LATKA et al., 2001)

3.1.2 DPPC experiments

Fully hydrogenated (h-) and tail deuterated (d_{62} -) DPPC were purchased from Avanti Polar Lipids. Stock solutions of DPPC, with and without antibiotics, were prepared in HPLC grade chloroform (Sigma-Aldrich). Monolayers of pure lipid DPPC and mixed with the drugs were prepared by spreading 30 μ L solution (1 g.L⁻¹ in chloroform) over a Milli-Q water subphase in the Langmuir trough, under the same conditions mentioned before. Mixed DPPC/antibiotic systems for each drug were prepared at three concentrations relative to DPPC stock solution (i.e., 0.1, 1 and 10%). Compressional modulus values were obtained by numerical calculation of the first derivative from the isotherm data according to the expression (2) (TOIMIL et al., 2012). Isotherms were carried out both independent of, and in conjunction with, NR, BAM and PM-IRRAS measurements individually, at different surface pressures.

3.2 Brewster angle microscopy

Lipid monolayers in the BAM experiments were prepared under the same conditions as described before. During the imaging procedure, BAM images were recorded periodically throughout continuous compression, using a Nima trough coupled with an ultra-objective BAM 2 Plus microscope (Nano Film EP4 Technology, Germany) connected to a high-quality GigE CCD camera and appropriate 480 nm laser. The monolayer morphology was evaluated by inspecting the image: darker regions with no light reflection, result from a clean

water surface or lower density lipid coverage, while the brighter spots correspond to dense monolayer domains (GERALDO et al., 2013; PINHEIRO et al., 2013b).

3.3

Polarization-modulation infrared reflection absorption spectroscopy

PM-IRRAS measurements were taken with a KSV PMI 550 instrument (KSV instruments Ltd., Helsinki, Finland). The Langmuir trough is placed in a way that the light beam reaches the monolayer at a fixed incidence angle of 80° , at which the intensity is maximum with a low level of noise. The incoming light is continuously modulated between *s*- and *p*-polarization at a high frequency, which allows for the simultaneous measurement of the spectra for the two polarizations. The reflectivities for *s*- and *p*- polarizations, R_s and R_p , are acquired in the 800-4000 cm^{-1} range with 8 cm^{-1} resolution, and the differential spectrum is obtained by calculating the $(R_p - R_s)/(R_p + R_s)$ ratio (PINHEIRO et al., 2013b) (SANDRINO et al., 2014).

3.4

Neutron reflectometry experiments in DPPC monolayers

NR measurements were performed using the SURF reflectometer (PENFOLD et al., 1997) on Target Station 1 at the ISIS Spallation Neutron Source at Rutherford Appleton Laboratory, Didcot, UK. Specular neutron reflectivity is largely determined by the variation in the scattering length density (SLD) along the surface normal. A reflectivity profile was recorded at two glancing angles of incidence, *viz.* 0.5° and 1.5° . Since neutron scattering is a nuclear effect, the scattering length varies for different isotopes, and therefore isotopic substitution can be used to obtain reflectivity profiles, corresponding to a single molecular density profile. This provides a means of determining the composition of multi-component systems, thus yielding detailed structural information of an adsorbed layer (CLIFTON et al., 2011; HAZELL et al., 2016). Pure DPPC and mixed DPPC/antibiotic monolayers were prepared and surface pressure measurements were used to monitor film compression. NR experiments were carried out at surface pressures of 5, 20, and 30 mNm^{-1} over an air-contrast matched water (ACMW) subphase (8% D_2O , 92% H_2O) on which the reflectivity profile is only

sensitive to the interfacial monolayer, and with a D₂O subphase on which reflection is sensitive to the hydrogenous material.(CLIFTON et al., 2012) The beam intensity was calibrated with respect to a clean D₂O surface.

Reflectivity data were fitted simultaneously using MOTOFIT(NELSON, 2006), written for IGOR Pro, which uses the Abeles optical matrix method to calculate the reflectivity of thin layers, each with a thickness, t ; its corresponding SLD, ρ ; a percentage hydration (% volume fraction of water) and a term for the roughness between layers, σ . It enables the global fitting of data sets of different isotopic compositions(NELSON, 2006). A two-layer model was used to fit the data, where the upper layer (from the air to the subphase) represents the lipid tails and the lower layer corresponds to the polar headgroups. SLD values used in this work for h-/d₆₂- DPPC and both antibiotics are summarized in Table 2. The SLD values were calculated using the total neutron scattering lengths for each component as well as the molecular volume data obtained for the antibiotics using the Molinspiration molecular properties calculator (<http://www.molinspiration.com/cgi-bin/properties>). For the mixed lipid-drug systems, the SLD of each layer was allowed to change under the constraint of a proper lipid/drug ratio (*i.e.*, 9:1 at 10% w/w of a drug) either in the headgroup layer or the acyl tail layer, as follows:

$$\rho_{Layer} = \rho_{DPPCtails} * 0.9 + \rho_{antibiotic} * 0.1 \quad (3)$$

This provides information related to the co-localization of the antibiotics within the DPPC monolayer.

3.5 Molecular dynamics simulations¹

Levofloxacin and Clarithromycin MD simulations were performed as a collaboration from Pimentel's group using the Gromacs 5.0.6. computer program(HESS et al., 2008) and a mixture of saturated/unsaturated phospholipids in good approximation to Curosurf composition applying atomistic/coarse-grained

¹ MD simulations were executed in collaboration with Evelina D. Estrada-López, Alline A. Pedreira, Lucas M. P. Souza, and Felipe R. Souza.

molecular dynamics (MD) approach. Since the simulations were obtained in collaboration and these are complementary information to the experimental data, some results from MD could be mentioned, however, details of it will be not discussed in this doctorate thesis.

3.6

Antibacterial activity quantification²

Gram-positive and Gram-negative bacteria were utilized to assess the antibacterial activity of Clarithromycin at various concentrations, combined or not with Curosurf. The tested bacterial strains included the environmental strain *Bacillus cereus* Iso AC4/CS262 and *Escherichia coli* DH5 α . *B. cereus* were grown at 30 °C while *E. coli* were grown at 37 °C (MACHADO-FERREIRA et al., 2015). The assessment of bacterial sensitivity/resistance profile to Clarithromycin was performed by streaking each strain on LB agar plates with Clarithromycin at 40, 20, 15, 10 $\mu\text{g mL}^{-1}$ or on Clarithromycin-free LB agar. Plates were incubated at a proper temperature for 24h.

Antibacterial activity was quantified through viability tests based on the 3-(4,5-dimethylthiazol-2-yl)-2,5-diphenyltetrazolium bromide (MTT) conversion. (GABRIELSON et al., 2002; MOSMANN, 1983; STEVENS; OLSEN, 1993) The overnight LB growth of each tested strain was inoculated 1/100 v.v. in fresh LB medium, incubated at an adequate temperature/100 rpm/4h for log phase growth and 50 μL of OD₆₀₀ = 0.125 LB bacterial suspensions placed in each well of 96-well plates. Serial dilutions of Clarithromycin (20 mg mL^{-1} in DMSO) were prepared in DMSO, and Curosurf (80 mg mL^{-1}) was serially diluted in Milli-Q water. Each dilution of Clarithromycin and Curosurf was combined in a 1:2.25 volume ratio to generate Clarithromycin/Curosurf 1:9 mass ratio mixtures. Control mixtures combining each Clarithromycin/DMSO dilution with water, each Curosurf dilution with DMSO and DMSO/water were similarly prepared at 1:2.25 volume ratio. Mixed volumes were added to 500 μL of LB and 50 μL of each solution merged with the bacterial suspension in each well of the 96-well test plates. The volumes 20 μL , 10 μL and 4 μL of each mixture were

² *In vitro* tests were executed in collaboration with Nathally B. Oliveira, Jéssica Cavaleiro and Carlos Augusto Gomes Soares.

tested, leading to different DMSO ratios in the final medium as specified. The 96-well plates were incubated at room temperature for 1h or 3h, followed by an extra 2h incubation with 10 μL MTT 5 mg mL^{-1} solution, completing a total of 3h or 5h incubations. Plates were spun at 3500 rpm/2 min, the liquid phase discarded and the formazan solubilized in 100 μL of DMSO for OD_{490} reads in a SpectraMax[®] M2e multi-detection microplate reader (Molecular Devices Corp.). All tests were performed in quadruplicate for each sample and controls. Data are presented as the percentage related to the readings for DMSO/water control treatments. Where calculated, the significant differences in quantification averages were determined by the student's t-test.

4

Interaction of Levofloxacin with lung surfactant at the air-water interface

Stephanie Ortiz-Collazos,¹ Evelina D. Estrada-López,¹ Alline A. Pedreira,¹ Paulo H. S. Picciani,² Osvaldo N. Oliveira Jr.,³ and Andre S. Pimentel^{1,*}

1. Departamento de Química, Pontifícia Universidade Católica do Rio de Janeiro, Rio de Janeiro, RJ 22453-900 Brazil
2. Instituto de Macromoléculas Professora Eloisa Mano, Universidade Federal do Rio de Janeiro, Rio de Janeiro, RJ 21941-598, Brazil
3. Instituto de Física de São Carlos, Universidade de São Paulo, São Carlos, SP 13566-590, Brazil

*Corresponding author: Andre Silva Pimentel – E-mail: a_pimentel@puc-rio.br

Published: *Colloids and Surfaces B: Biointerfaces* 158 (2017) 689–696

Abstract

The molecular-level interaction of Levofloxacin with lung surfactant was investigated using Langmuir monolayers and atomistic molecular dynamics (MD) simulations. In the simulation, the DPPC/POPC mixed monolayer was used as a lung surfactant model and the molecules of Levofloxacin were placed at the air-lipid interface to mimic the adsorption process on the lung surfactant model. The simulation results indicate that amphoteric Levofloxacin expands the lung surfactant, also stabilizing the film for Levofloxacin fractions until 10% w/w at least. The Langmuir monolayers made with the lung surfactant Curosurf had expanded isotherms upon incorporation of Levofloxacin, without changes in monolayer elasticity. In fact, Levofloxacin induced film stability with increased collapse pressures in the Curosurf isotherms and delayed the phase transition,

according to Brewster angle microscopy (BAM) imaging. Using polarization-modulated infrared reflection-absorption spectroscopy (PM-IRRAS), we found that Levofloxacin is preferentially located in the head group region, inducing an increased organization of the Curosurf film. This location of Levofloxacin was confirmed with MD simulations. The stability inferred demonstrates that the lung surfactant can be used as a drug delivery system for the administration via inhalation or intratracheal instillation of Levofloxacin to treat lung diseases such as pneumonia and respiratory distress syndrome.

Keywords: Langmuir films, pulmonary system, antibiotic fluoroquinolone, respiratory distress syndrome, pneumonia

4.1 Introduction

Levofloxacin is a broad spectrum antibiotic of the fluoroquinolone class used to treat many bacterial infections, including gastroenteritis, pelvic inflammatory disease, chronic prostatitis, urinary tract infections, acute bacterial sinusitis, meningitis, anthrax, tuberculosis, and pneumonia. Its possible side effects include tendon inflammation and rupture, psychosis, seizures, peripheral nerve damage, trouble sleeping, diarrhea, and nausea (DAVIS; BRYSON, 1994; ZHANEL et al., 2002). It is commercially available as a generic medication to be used orally or intravenously (WORLD HEALTH ORGANIZATION, 2015). Because Levofloxacin is one of the most important drugs essential to any national health system, considerable benefits would be obtained if the drug administration could be made in a less invasive local or topical use. This can in principle be achieved using lung surfactant as drug carrier and spreading agent, which could be used to treat premature infants with neonatal respiratory distress syndrome that usually have also pneumonia (GRIESE, 1999; HIDALGO; CRUZ; PÉREZ-GIL, 2015). Lung surfactant has actually been used in vivo as a drug carrier (BANASCHEWSKI et al., 2015; FAJARDO et al., 1998; HERTING et al., 1999; KHARASCH et al., 1991; NATARAJAN et al., 2016; VAN'T VEEN et al., 1996; VAN 'T VEEN et al., 1996; YEH et al., 2008), including for the transport

of antibiotics to the lung(DALLOW et al., 2014; GEORGIEV; GEORGIEV; LALCHEV, 2010; KOTECKA; KRYSINSKI, 2015).

A successful use of lung surfactant as drug carrier is only possible if the surfactant is not destabilized by the drug. Hence, before attempts are made to employ the lung surfactant with a specific drug in in vivo tests, it makes sense to verify whether the surfactant will remain stable upon interacting with the drug. Such a study can be made with Langmuir monolayers representing the lung surfactant(BANASCHEWSKI et al., 2015; BENSIKADDOUR et al., 2008b; BERQUAND et al., 2005; CHIMOTE; BANERJEE, 2005a, 2005b, 2005c, PINHEIRO et al., 2013a, 2013b), which allows for determining the molecular-level interactions between the surfactant constituents and the drug. For instance, Chimote and Banerjee studied the interaction of a triple antituberculosis cocktail (isoniazid, rifampicin, and ethambutol) mixed with 1,2-dipalmitoyl-sn-glycero-3-phosphocholine (DPPC) monolayers, and found that interfacial adsorption of DPPC was greatly improved when the drug was mixed (CHIMOTE; BANERJEE, 2005b). They also studied mixed monolayers of DPPC and phosphatidylglycerol (PG)(CHIMOTE; BANERJEE, 2005c), and natural lung surfactant monolayers(CHIMOTE; BANERJEE, 2005a), where mycolic acid and trehalose dimycolate were used to mimic the cell wall of *Mycobacterium tuberculosis*. They showed that the active lipid components on the mycobacterium inhibit the function of the phospholipids in the lung surfactant, fluidizing and collapsing the film. Atomic force microscopy (AFM) images revealed aggregation when the mycolic acid and trehalose dimycolate were added to the natural lung surfactant(CHIMOTE; BANERJEE, 2005c).

Pinheiro et al.(PINHEIRO et al., 2013a, 2013b) investigated the interactions of a new analog of rifabutin with DPPC monolayers and vesicles. They showed strong interactions of rifabutin with the polar heads of DPPC, indicating bioaccumulation of the drug in the lung. The results confirm that rifabutin changes the phospholipid packing and decreases the phase transition temperature of the phospholipid, which may affect its adsorption capacity at the air-water interface and fluidize the DPPC film. Banaschewski et al.(BANASCHEWSKI et al., 2015) found that the presence of microbiotic peptides accelerated the formation of

natural lung surfactant films and affected little its biophysical function under high concentrations. However, the antimicrobial activity of most tested peptides was inhibited in the presence of natural lung surfactant due to electrostatic interactions between the polar groups of phospholipids and peptides. AFM images suggested that the peptides are possibly incorporated in the film, modifying film structure. The interaction of DPPC and 1,2-dipalmitoyl-sn-3-glycero[phospho-rac-(1-glycerol)] (DPPG) with the antibiotics azithromycin and ciprofloxacin was studied to characterize molecular organization, fluidity, and permeability of model membranes (BENSIKADDOUR et al., 2008b; BERQUAND et al., 2005). *In situ* AFM images showed that azithromycin destroys the gel phase of DPPC domains and increases the fluidity of lipid vesicles at the air-water interface. On the other hand, the antibiotic ciprofloxacin does not affect the transition temperature of DPPC, but it increases the order of hydrocarbon chains of the liposomes. Further, ciprofloxacin dramatically changes the transition temperature of DPPG vesicles and reduces the order of hydrocarbon chains. Ciprofloxacin preferentially interacts with the polar head of anionic lipids such as DPPG. The aim of this study is to understand the molecular interaction of Levofloxacin with the lung surfactant at the air-water interface using the Curosurf lung surfactant and molecular dynamics (MD) simulations. The lung surfactant model used in the MD study is a binary lipid monolayer (DPPC and POPC, 1-palmitoyl-2-oleoyl-sn-glycero-3-phosphocholine) in order to simplify the simulation by eliminating surfactant proteins. The Langmuir film technique provides a way to investigate the surface pressure-area isotherm (π -Area), compressional modulus, stability, conformational and structural order, and film morphology. Molecular dynamics simulations are a powerful technique to determine the order parameter, organization, stability, and formation of aggregates at the molecular level (PADILLA-CHAVARRÍA; GUIZADO; PIMENTEL, 2015a). A full review of the MD simulation of lung surfactant models is given in the literature and will not be repeated here. The techniques we used are complementary, and suitable to establish if Levofloxacin can be mixed with lung surfactant without loss of its mechanical properties, which are important for the lung function. It is not our intention at this point to verify if the lung surfactant inactivates the antibiotic properties of Levofloxacin.

4.2

Materials and methods

The reader is referred to the description in section 3.1, page 31.

4.3

Results and discussion

Levofloxacin, whose amphoteric structure is shown in Fig. 5, behaves as an amphoteric molecule in a polarizable medium such as in a Langmuir monolayer since it contains a negatively charged acidic group at one side and a positively charged group at the other side. This was confirmed with molecular dynamics simulations in which we compared the amphoteric and uncharged forms of Levofloxacin, and found that the simulation results match the experimental data for the amphoteric form, but not for the uncharged one. The surface pressure isotherms in Fig. 6A point to a concentration-dependent effect of Levofloxacin on the Curosurf monolayer. The addition of Levofloxacin shifts the isotherm to larger areas, i.e., causing monolayer expansion, with all π -A isotherms behaving similarly with collapse at ca. 40 mNm⁻¹. With 10% of Levofloxacin, the monolayer-to-multilayer phase transition appears at higher surface pressures than for pure Curosurf monolayers, which means an increased stability. Fig. 6B presents the compressional modulus for pure Curosurf, 0.1% Levofloxacin-Curosurf monolayer, and 10% Levofloxacin-Curosurf monolayer.

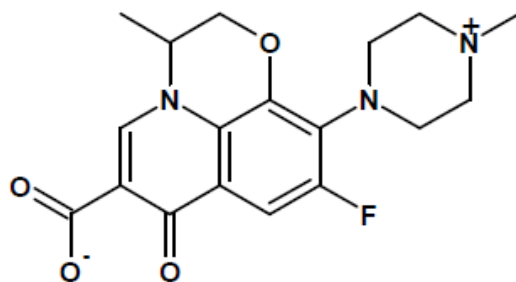


Figure 5. Chemical structure of the amphoteric Levofloxacin.

Below 40 mNm⁻¹, the compressional modulus (C_S^{-1}) is indistinguishable for all of the Levofloxacin fractions investigated, and therefore the only difference appears at the monolayer-to-multilayer phase transition. The maximum value of C_S^{-1}

reached $\sim 110 \text{ mNm}^{-1}$, corresponding to the liquid-condensed (LC) state, while the phase transition of monolayer-to-multilayer is observed as an abrupt C_s^{-1} decrease to $\sim 45 \text{ mNm}^{-1}$. The mixed 10% Levofloxacin-Curosurf monolayer seems to have a large phase transition followed by a wide “kink” that is not present in pure Curosurf monolayer. It is known that quinolones exhibit amphoteric character and marked hydrophilicity (STERGIOPOULOU et al., 2009). Some electrostatic interaction may occur between polar head groups in the lung surfactant, and amine and carboxyl groups in Levofloxacin, contributing to the monolayer shift and retarding the phase transition. On the other hand, the Levofloxacin molecules may interact with the hydrocarbon chains because they are flexible. In summary, Levofloxacin causes an expansion in the surface pressure isotherms of Curosurf, probably because it is inserted between the polar heads, with practically no change

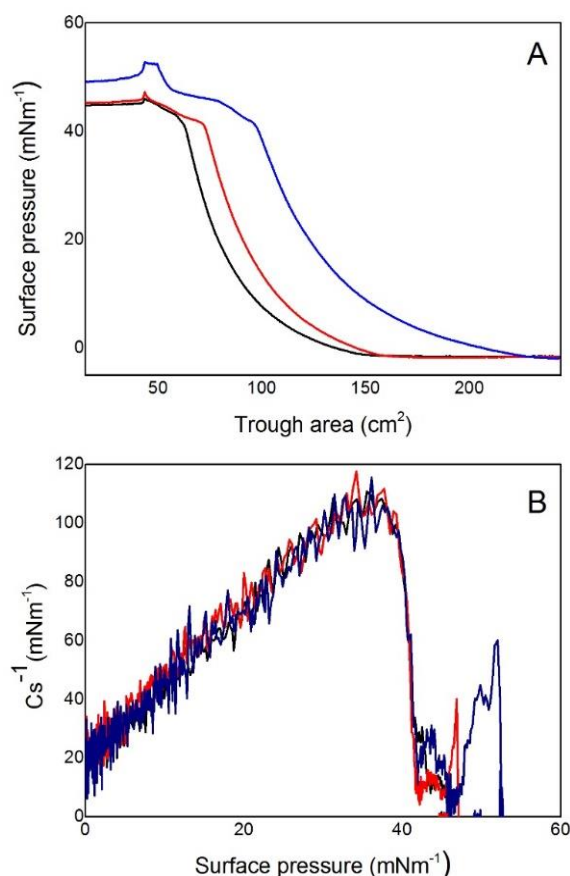


Figure 6. (A) Surface pressure-Area isotherms for pure Curosurf (black), Levofloxacin-Curosurf 0.1% w/w (red), and Levofloxacin-Curosurf 10% w/w (blue). (B) Experimental compressional modulus C_s^{-1} as a function of surface pressure in Langmuir films of pure Curosurf (black), Levofloxacin-Curosurf 0.1% w/w (red), and Levofloxacin-Curosurf 10% w/w (blue).

in elasticity. This means that Levofloxacin does not affect the membrane stability neither the appearance of the isotherms profile, though it is inserted in a way that it contributes to the area per lipid occupied at the interface. The monolayer expansion observed experimentally for the incorporation of Levofloxacin in Curosurf in Fig. 6A was consistent with the increased area per molecule in the simulated DPPC-POPC monolayer models. The PM-IRRAS spectra of Curosurf and Curosurf/Levofloxacin monolayers are shown in Fig. 7A-C. The bands in Fig. 7A assigned to CH_2 stretching at 2850 cm^{-1} (symmetrical) and 2917 cm^{-1} (asymmetrical) have increased intensity as the Curosurf film is compressed, as a result of both condensing and orientation of nonpolar alkyl tails. A weak CH_3 symmetric stretching band at 2965 cm^{-1} is also observed, whose position varies with increasing surface pressures. The region between 1100 and 1800 cm^{-1} provides information on head group conformation. The bands at 1095 cm^{-1} (PO_2^- sym. str.), 1150 cm^{-1} (C-O-C) and 1195 cm^{-1} (HO-CR_2) have no significant

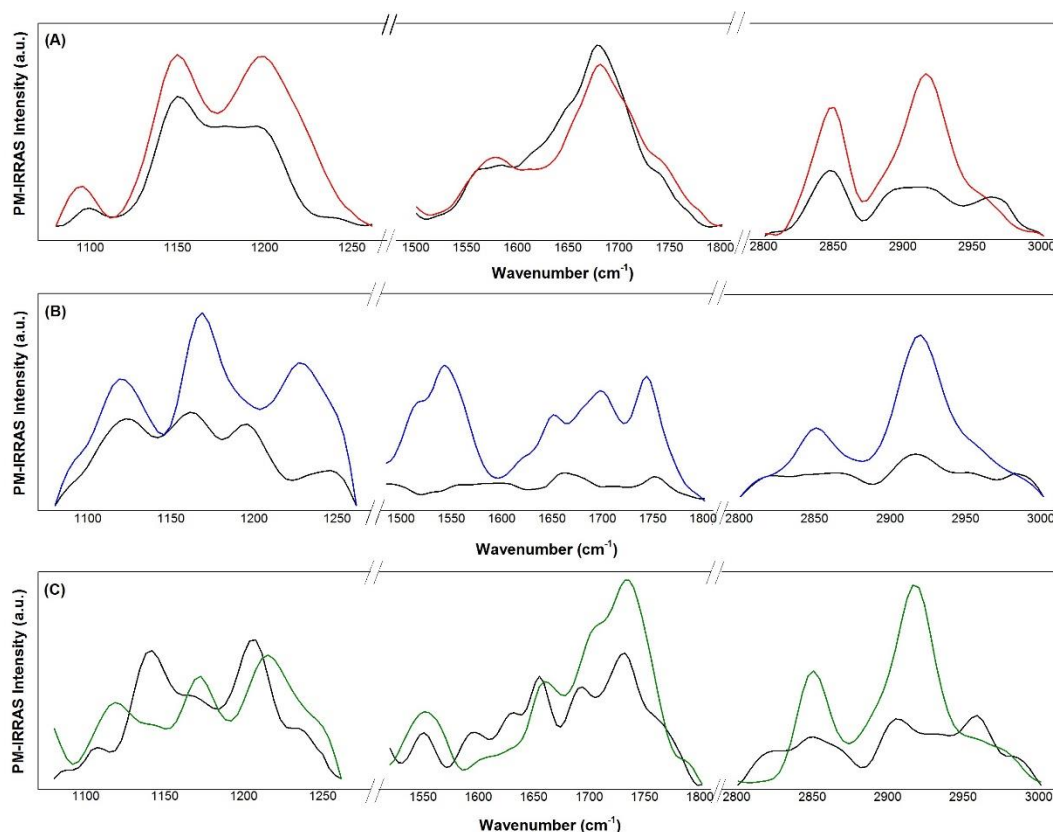


Figure 7. Experimental PM-IRRAS spectra of Langmuir films of pure Curosurf (A), Levofloxacin-Curosurf 0.1% w/w (B), and Levofloxacin-Curosurf 10% w/w (C) at surface pressures 0 (black) and 30 (red for (A), blue for (B), and green for (C)) mNm^{-1} in the C H region ($2800\text{--}3000\text{ cm}^{-1}$), C O region ($1400\text{--}1800\text{ cm}^{-1}$), and C O region ($1000\text{--}1300\text{ cm}^{-1}$).

change in spectra intensity after compression of the pure monolayer. On the other hand, incorporation of Levofloxacin at 0.1% and 10% clearly affects the infrared bands, as shown in Fig. 7B and C. CH₂ stretching bands of Curosurf are not significantly affected by the addition of Levofloxacin; instead, a new band at 2960 cm⁻¹ (CH₃ stretching of Levofloxacin) appears especially at low surface pressures, indicating the presence of Levofloxacin at the air-water interface (Fig. 7C). Also, the presence of new bands at 1520, 1543 and 1743 cm⁻¹ after addition of Levofloxacin could suggest a preferential molecular interaction between Levofloxacin and phospholipids head groups. As shown in Fig. C.1 in the Supplementary material-1, the IR powder spectra of pure Levofloxacin exhibit peaks at 1515, 1536, and 1718 cm⁻¹, which confirms that there is levofloxacin on the film. The PM-IRRAS spectra in Fig. C.2 in the Supplementary material-1 for Langmuir monolayers of pure Curosurf and Levofloxacin-containing monolayers, at surface pressures 0, 10, 20, 30, and 40 mNm⁻¹, indeed confirm that at high pressures Levofloxacin molecules are mostly placed among polar phospholipids headgroups while the CH region is largely unaffected. These findings suggest that Levofloxacin molecules shift to the polar heads with increasing surface pressure.

BAM images of pure Curosurf and mixed Levofloxacin-Curosurf monolayers are shown in Fig. 8. They compare the two-dimensional molecular organization of Curosurf monolayers with and without Levofloxacin (0.1 and 10%) recorded as a function of surface pressure ($\pi \sim 0, 10, 20, 30$ and 40 mNm^{-1}). The pure monolayer displays the beginning of starry condensed domains of Curosurf at very low surface pressures ($\sim 5\text{-}10 \text{ mNm}^{-1}$) in the LE state. As the lateral compression is increased, the fractal domains grow in number, slightly in size and get closer, thus forming a continuous phase near 30 mNm^{-1} , without coalescing though. Very bright regions appear as the surface pressure increased. Pinheiro et al. attributed these bright spots to lose fluidic material from the interface (PINHEIRO et al., 2013a, 2013b). At 40 mNm^{-1} , fractal domains of the pure Curosurf monolayer are again visible with a decrease of the bright regions. This may be explained with the phase transition process (squeezing-out) and the enrichment of DPPC molecules in the monolayer.

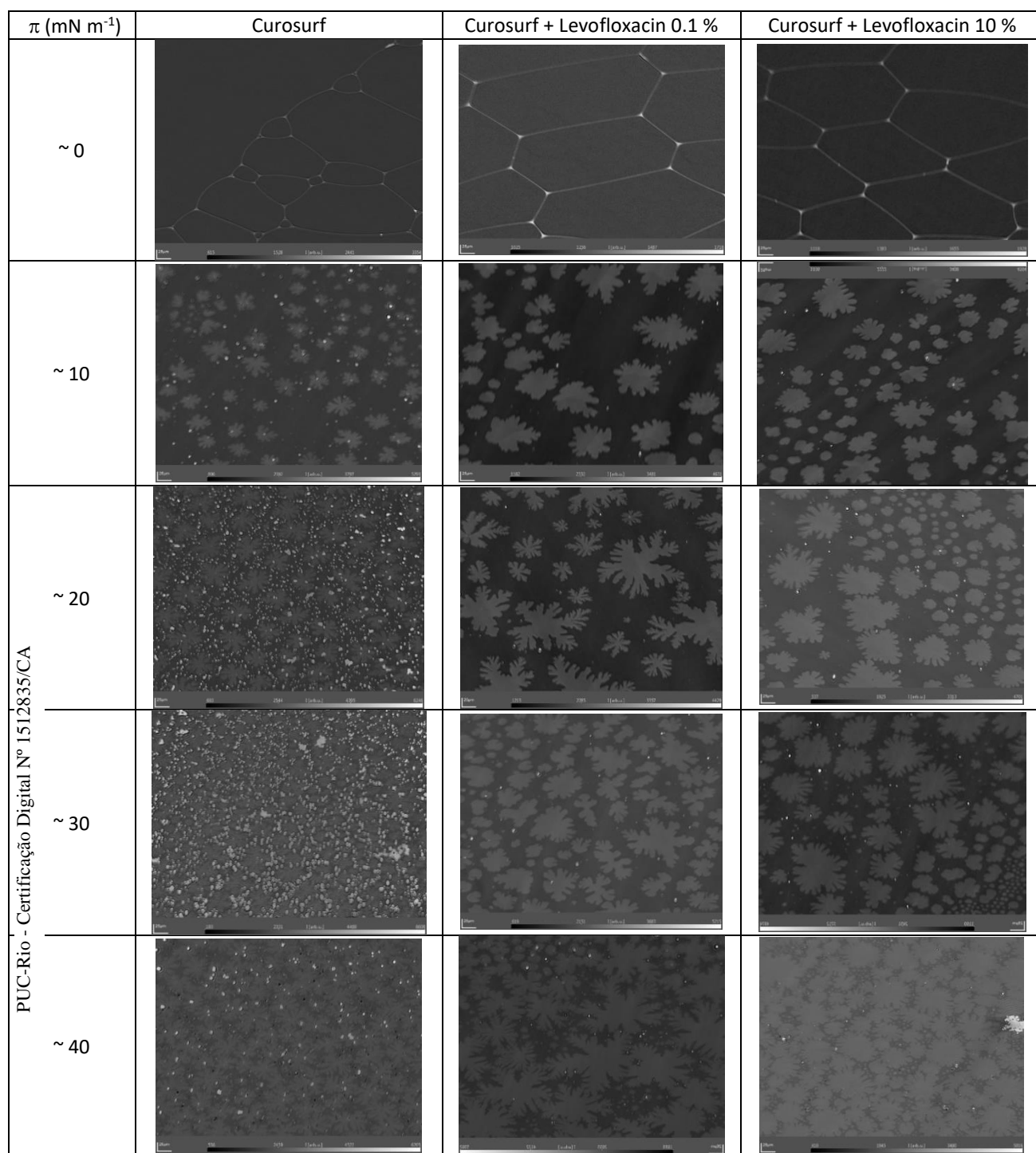


Figure 8. Brewster angle microscopy images of pure Curosurf, Levofloxacin-Curosurf 0.1% w/w, and Levofloxacin-Curosurf 10% w/w at $\pi = 0, 10, 20, 30$, and 40 mN m⁻¹. All BAM images have a 25 μ m scale bar at the left-hand corner.

The addition of Levofloxacin in the Curosurf monolayer seems to delay its collapse and increase the size of fractal domains. Also, the very bright regions do not appear as Levofloxacin is added, which indicates significant changes in the

Curosurf monolayer. Even at a low fraction of Levofloxacin (0.1%) one observes larger, more ramified fractal domains than for the pure monolayer. Besides, differences are noted in the refractivity index of fractal domains owing to distinct orientations of the lipids in the monolayer at surface pressures below $\sim 20 \text{ mNm}^{-1}$. Higher fractions of Levofloxacin (10%) result in similar effects, though at low surface pressures (below $\sim 20 \text{ mNm}^{-1}$) the fractal domains are more circularly shaped and numerous. Further monolayer compression (up to $\sim 30 \text{ mNm}^{-1}$) allows the Curosurf domains to grow and become a more condensed and ordered phase (LC). It is worth mentioning that bright spots at pure Curosurf monolayer were significantly depleted in the presence of Levofloxacin at low (0.1%) and high (10%) fractions. It may be an indication that Levofloxacin effectively improves monolayer stability.

4.4 Implications

Levofloxacin is nowadays administered in large doses with possible adverse effects in patients. The dynamics of Levofloxacin interacting with the lung surfactant seems to be promising because Levofloxacin appears to stabilize the lung surfactant monolayer. It is also worth mentioning that the interaction of Levofloxacin is sufficiently strong to keep it for long times in the polar head groups region of the lung surfactant. The chemical structure and properties of Levofloxacin cause the formation of few aggregates in the lung surfactant when the Levofloxacin fraction is around 10% w/w. Furthermore, Levofloxacin may also form aggregates, not resulting in the collapse of the lung surfactant. Therefore, high fractions ($\sim 10\%$ w/w) of Levofloxacin may not induce collapse of the lung surfactant and inactivate it. From these results, it seems possible that Levofloxacin may be administered locally using lung surfactant as a carrier.

4.5 Conclusion

Data from three experimental methods in Langmuir monolayers representing a cell membrane model and atomistic molecular dynamics simulation were obtained to understand the stability of Levofloxacin interacting with the lung surfactant.

Incorporation of Levofloxacin induced an expansion in the surface pressure isotherms of Curosurf monolayers, with no significant changes in the compressional modulus. With the PM-IRRAS technique, we observed an increased monolayer organization during compression. BAM images showed that the film collapse is delayed by adding 10% Levofloxacin in the monolayer. According to the simulations, Levofloxacin molecules are located between the polar heads, stabilizing the film and forming only a few aggregates. Relevant implications could be inferred from the properties of Levofloxacin interacting with the monolayer. In particular, one may envisage administration of Levofloxacin via inhalation or intratracheal instillation using lung surfactant as a drug delivery system, in order to possibly treat lung diseases such as pneumonia and respiratory distress syndrome.

4.6

Acknowledgments

The authors thank the Brazilian funding agencies CNPq (GrantNo. 465259/2014-6), FAPERJ (Grant No. 210.558/2015, and E-26/010.001241/2016), and FAPESP (Grant No. 2013/14262-7 and 2015/21055-8) for financial support. S.O.C. acknowledges CNPq for a graduate fellowship. E.D.E.L. thanks FAPERJ for a graduate fellowship. A.A.P. acknowledges CNPq for an undergraduate research fellowship. We thank Dr. Adriano M. Alencar (IF/USP) who supplied the lung surfactant samples. The Levofloxacin active sample was provided by Dr. Cristiano R. W. Magalhães (Aché Laboratórios Farmacêuticos).

Clarithromycin does not affect the stability of a lung surfactant monolayer at the air-water interface

Stephanie Ortiz-Collazos,¹ Lucas M. P. Souza,¹ Felipe R. Souza,¹ Nathally B. Oliveira,² Jéssica Cavaleiro,² Carlos Augusto G. Soares,² Paulo H. S. Picciani,³ Osvaldo N. Oliveira Jr.,⁴ and Andre S. Pimentel^{1,*}

1. Departamento de Química, Pontifícia Universidade Católica do Rio de Janeiro, Rio de Janeiro, RJ 22453-900 Brazil
2. Departamento de Genética, Instituto de Biologia, Universidade Federal do Rio de Janeiro, Rio de Janeiro, RJ 21944-970, Brazil
3. Instituto de Macromoléculas Professora Eloisa Mano, Universidade Federal do Rio de Janeiro, Rio de Janeiro, RJ 21941-598, Brazil
4. Instituto de Física de São Carlos, Universidade de São Paulo, São Carlos, SP 13566-590, Brazil

*Corresponding author: Andre Silva Pimentel – E-mail: a_pimentel@puc-rio.br

Submitted paper: *Journal of Biomolecular Structure & Dynamics*

Abstract

Clarithromycin is one of the most employed drugs to treat pneumonia and other diseases of the respiratory tract, but it causes side effects and undesirable interference with other drugs, mostly associated with the mode of administration. In this paper, we provide evidence that Clarithromycin may be incorporated into the lung surfactant with preserved antibacterial activity, which could then allow for drug delivery. Using Langmuir monolayers of an exogenous lung surfactant as the model for the lung surfactant monolayer, we show that Clarithromycin

integrated into the lung surfactant monolayer does not cause any collapse, as determined by surface pressure isotherms, polarization-modulated infrared reflection absorption spectroscopy (PM-IRRAS), and Brewster angle microscopy (BAM) analyses. The integrity of the lung surfactant in the presence of 10% w/w Clarithromycin was corroborated with coarse-grained molecular dynamics simulations in which the membrane was represented by a lung surfactant monolayer model, consisting of a mixed phospholipid monolayer with the surfactant protein B model. Significantly, Clarithromycin has kept its antibacterial activity using MTT assays when incorporated in the lung surfactant. Mixtures of an exogenous lung surfactant and Clarithromycin were capable of killing both Gram-positive and Gram-negative bacteria when tested *in vitro*, with some tested combinations leading to improved antibiotic activities when compared to Clarithromycin alone. Clarithromycin delivery with a lung surfactant carrier may thus represent a new way to combat pneumonia and persistent pulmonary infections with less (or no) side effects.

Keywords: Langmuir film, pulmonary system, Antibiotic, Macrolide, Respiratory distress syndrome, Pneumonia.

5.1 Introduction

Clarithromycin is a broad-spectrum macrolide antibiotic usually administered as an alternative to penicillin to treat bacterial infections caused by *Helicobacter pylori* and pneumonia, being effective against lower and upper respiratory tract infections (GREENWOOD, 2008). This antibiotic was developed in 1980 from Erythromycin through efforts to avoid acid instability in the digestive tract, which causes undesirable side effects, such as stomach ache and nausea (GREENWOOD, 2008). There are still a number of remaining side effects from Clarithromycin, including vomiting, abdominal pain, nausea, diarrhea, in addition to suspicion of cardiac death (WINKEL et al., 2011) and liver disease (TIETZ et al., 2003) outcomes. Clarithromycin also inhibits the cytochrome P450 3A4 involved in the metabolism of many drugs, thus leading to unexpected alterations in drug levels (FERRERO et al., 1990; GANDHI et al., 2013; GÉLISSE et al., 2007;

PATEL et al., 2013; POLIS et al., 1997; SEKAR et al., 2008). In spite of these possible problems, Clarithromycin is on the list of the most effective (at moderate cost), essential medicines in the health systems of many countries. Hence, the effort to develop alternative ways to administer Clarithromycin apart from the usual oral and intravenous forms represents a public health priority. As it has been done with corticoid drugs(KUO et al., 2010), we propose here the use of lung surfactant as a carrier for the direct delivery of Clarithromycin through the respiratory tract. For this, it is crucial that the drug does not induce collapse of the lung surfactant monolayer and preserve its biological activity and function.

Pulmonary surfactant model membranes offer an opportunity to simulate and predict whether a target antibiotic drug can be stably incorporated into the lung surfactant, preserving its antibacterial activity when incorporated into the lipoproteic mixture. Due to its multiple advantages, such as the precise control of the monolayer packing density, Langmuir film method is a potent tool commonly used for studying specific aspects of physical-chemistry phenomena at lipid membrane interface(KORCHOWIEC et al., 2006, 2011; MAGET-DANA, 1999). Thus, lung surfactant monolayers approaches can lead to a better understanding of the interaction between the membrane components. Many studies in the literature deal with the interaction of drugs with lung surfactant, though as we shall exemplify next, the results are normally dependent on the drug and the lipid composition in the monolayer model. Therefore, it is not possible to predict from data in the literature whether a particular drug will preserve the lung surfactant structure, as well as keep its activity. For example, Chimote and Banerjee(CHIMOTE; BANERJEE, 2005b) observed that rifampicin, isoniazide, and ethambutol interact with 1,2-dipalmitoyl-sn-glycero-3-phosphocholine (DPPC) monolayers, even increasing the monolayer surface activity in some cases, which may imply that these antibiotics could be administered mixed in the pulmonary surfactant. Levofloxacin was observed to expand the lung surfactant film, stabilizing it without changing its elasticity(ORTIZ-COLLAZOS et al., 2017a). In contrast, Chimote and Banerjee(CHIMOTE; BANERJEE, 2005c) reported that the mycobacterial lipids (mycolic acid and cord factor) affect Curosurf surface properties, which could explain the hindering of surfactant activity that may justify the alveolar atelectasis effect of the bacteria(CHIMOTE;

BANERJEE, 2005a). The macrolide antibiotic azithromycin was found to destroy the gel phase of DPPC bilayers, with an increase in fluidity (BERQUAND et al., 2005) and ciprofloxacin disorganized the acyl chains of DPPC and 1,2-dipalmitoyl-sn-glycero-3-phospho-(1'-racglycerol) (DPPG) (BENSIKADDOUR et al., 2008b). The antimicrobial peptides LL-37, CATH-1, CATH-2, and CRAMP affected little the biophysical function of lung surfactant, but they lost most of their antimicrobial activity (BANASCHEWSKI et al., 2015; NEVILLE et al., 2010; SEVCSIK et al., 2008) owing to a deactivation mechanism (SOUZA et al., 2018). Other works in the literature are worth mentioning with regard to drug interaction with lung surfactant models. These include antitubercular drug-loaded surfactants, used as inhalable drug delivery systems for pulmonary tuberculosis (CHIMOTE; BANERJEE, 2009), the interaction of Rifabutin and N'-acetyl-Rifabutin with model lung surfactant monolayers (PINHEIRO et al., 2012, 2013a), and vesicles (PINHEIRO et al., 2013b).

The scope of the present work was to address the interactions of Clarithromycin with Curosurf monolayers –an exogenous lung surfactant prepared from porcine lungs– implementing an experimental-theoretical study to verify if the drug could be incorporated into the pulmonary surfactant preparation. The molecular-level interactions of Clarithromycin were investigated by combining three different types of techniques in a complementary manner. Pure and mixed Clarithromycin/Curosurf Langmuir monolayers were characterized using surface pressure isotherms, polarization-modulation infrared reflection absorption spectroscopy (PM-IRRAS) and Brewster angle microscopy (BAM). This study was supplemented with coarse-grained molecular dynamics (MD) simulations where the Curosurf monolayer model was made to consist of a mixture of DPPC, 1-palmitoyl-2-oleoyl-sn-glycero-3-phosphocholine (POPC), 1-palmitoyl-2-oleoyl-sn-glycero-3-phospho-(1'-rac-glycerol) (POPG), 1-palmitoyl-2-oleoyl-sn-glycero-3-phosphoethanolamine (POPE), 1,2-dipalmitoyl-sn-glycero-3-phospho-L-serine (DPPS), 1,2-dipalmitoyl-sn-glycero-3-phospho-(1'-myo-inositol) (DPPI), 1-myristoyl-2-hydroxy-snglycero-3-phosphocholine (LPC), N-stearoyl-D-erythro-sphingosylphosphorylcholine (DPSM), and a model of surfactant protein B (SP-B). MD simulations have already been used in lung surfactant models and the readers are referred to ref. (PADILLA-CHAVARRÍA; GUIZADO; PIMENTEL,

2015b) for an overview. These simulations are useful to determine order parameter, organization, and stability at the molecular level, being complementary to the Langmuir monolayer experimental studies to establish the mechanical properties and decide if Clarithromycin and lung surfactant can be mixed without loss of lung function. In order to check the possible inactivation of Clarithromycin by the lung surfactant, cell viability assays were performed with a Gram-positive and a Gram-negative bacteria. The impact and novelty of this study are related to the incorporation of Clarithromycin in the lung surfactant monolayer, preserving the film stability and keeping its antimicrobial activity.

5.2

Materials and methods

The reader is referred to the description in section 3, page 31.

5.3

Results and discussion

5.3.3

The interaction between Clarithromycin and Curosurf monolayers

Figure 9A shows that Clarithromycin presence induces a slight condensation in the π -A isotherm of the Curosurf monolayer, which depends on concentration. Clarithromycin at a 0.1%, 1%, and 10% fractions shifts the isotherm to a slightly lower area. The condensation effect in π -A monolayers is usually related in literature to the stabilization of the lateral repulsion between the acyl chains (HUSSEIN et al., 2013). The effect appears to be common especially when there are charged lipids with ions (EBARA et al., 1994). Since the observed effect in our case was scarce, it could be more likely attributed to the electrostatic interactions between the Curosurf components and the hydrophobic Clarithromycin, than the loss of material from the interface. Nevertheless, it is worth to mention that under high compression (over 50 mNm⁻¹) some fluid components are normally ‘squeezed-out’ from the pulmonary surfactant monolayer (See Fig. D.1 Supplementary material-2). The isotherm was very reproducible as the experiment was repeated at least 3 times. Fig 9A only shows the isotherms until it reaches the monolayer-to-multilayer transition plateau

occurring in surfactant films around $40\text{--}50\text{ mNm}^{-1}$, (ZHANG et al., 2011a) aiming to study the effects of the antibiotic in the lipoproteic monolayer. In literature, it has been reported that, during adsorption at the alveolar interface, physiologically effective surfactant films can decrease the surface tension of the air-water interface from $\sim 70\text{ mNm}^{-1}$ to $\sim 20\text{--}25\text{ mNm}^{-1}$ at $37\text{ }^{\circ}\text{C}$, but no further. At this final surface tension range (which corresponds a surface pressure around $\sim 45\text{--}50\text{ mNm}^{-1}$), the phospholipid molecules at the air-water interface are in thermodynamic equilibrium with the molecules in the bulk phase. This equilibrium surface tension (γ_{eq}) corresponds to the equilibrium spreading pressure (π_e) of phospholipids, which is the highest surface pressure obtained by spreading the excess phospholipids with chloroform at the air-water

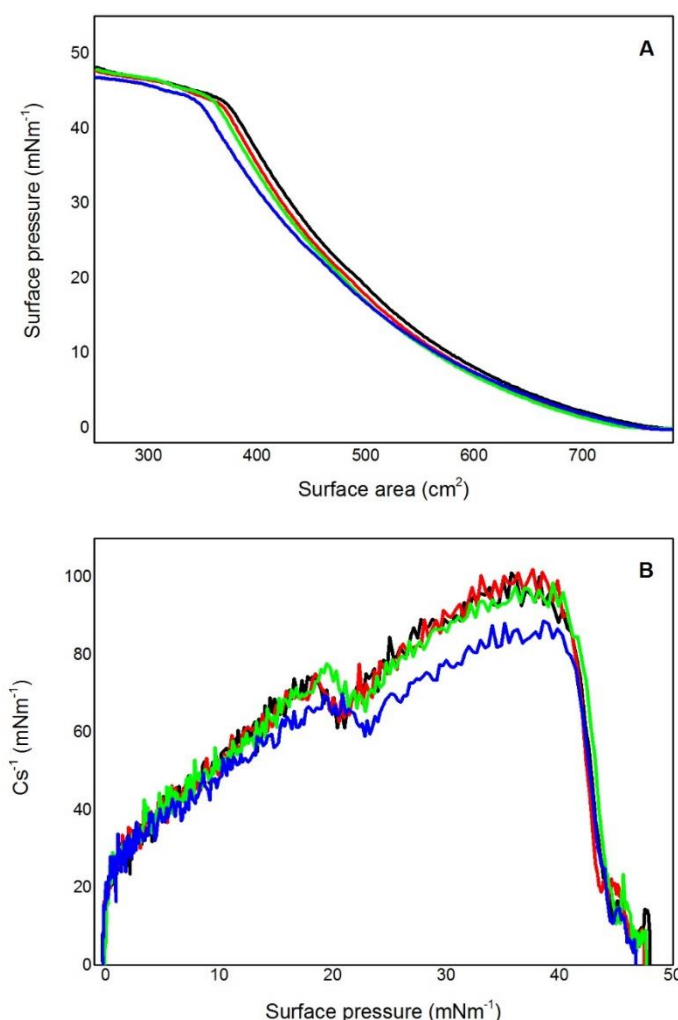


Figure 9. (A) Experimental surface pressure as a function of the trough area for pure Curosurf (black), and Clarithromycin-Curosurf 0.1% w/w (red), 1% w/w (green), and 10% w/w (blue). (B) Experimental compressional modulus C_s^{-1} as a function of surface pressure in Langmuir films of pure Curosurf (black), Clarithromycin-Curosurf 0.1% w/w (red), 1% w/w (green), and 10% w/w (blue).

interface(ZUO et al., 2008). Incorporation of Clarithromycin did not substantially affect this transition at ca. 44 mNm^{-1} , which is unusual because the collapse pressure normally changes when guest molecules are added at high fractions(GRIFFITH et al., 2013).

Regarding to the surface elasticity C_s^{-1} , figure 9B shows that 10% w/w of Clarithromycin induces a slight decrease in the compressional modulus (C_s^{-1}) of Curosurf monolayer, particularly in the pressure region comprising the value believed to correspond to the lateral pressure of a biological membrane ($\sim 30\text{-}35 \text{ mNm}^{-1}$)(SCHÜRCH; BACHOFEN; POSSMAYER, 2001; SCHURCH; LEE; GEHR, 1992; VELDHUIZEN et al., 1998). The maximum of C_s^{-1} reached for pure Curosurf monolayers was around 100 mNm^{-1} at a surface pressure of 35 mNm^{-1} , which means that the monolayer is in a liquid-condensed (LC) state. At the same surface pressure, the mixed monolayer at 10% of the drug reaches its maximum C_s^{-1} value around 86 mNm^{-1} , still remaining at the LC state. For 0.1% and 1% of antibiotic additions, the C_s^{-1} values were almost overlapping the pure Curosurf values. Although the differences in C_s^{-1} values in overall are small, the influence of the drug can be seen on it. Lower values of C_s^{-1} with a high addition of drug can be ascribed to a slight increase of the elasticity/fluidity of the lipid monolayer, which means less rigid, hence, more compressible monolayers(BROWN; BROCKMAN, 2007; TSANOVA; GEORGIEV; LALCHEV, 2014). Thus, low additions of drug (0.1 and 1% w/w) seems to maintain the monolayer order/packing of molecules in contrary to the highest addition (10% w/w) that increases its compressibility, as a result of a high content of new molecules which prevents the lipids from attaining a highly-packed structure(HUSSEIN et al., 2013). Also, two minima were observed in C_s^{-1} curves. The first one is at $\sim 20 \text{ mNm}^{-1}$ representing the LE-LC phase transition and the second one is at $\sim 40 \text{ mNm}^{-1}$ corresponding to the monolayer-to-multilayer process. At this point, C_s^{-1} values for all monolayers decreased sharply at high surface pressures owing to the formation of multilayer structures(HIDALGO et al., 2006). Besides, it can be seen that, as drug concentration increases, the minima at $\sim 20 \text{ mNm}^{-1}$ is gradually shifted to higher surface pressures. It proves that the antibiotic is interacting with Curosurf monolayers in low surface

pressures and it is in fact inserted in the monolayer. These results are in agreement with the literature (ZHANG et al., 2011a).

The preserved stability of the Curosurf monolayer in the presence of Clarithromycin was confirmed in subsidiary experiments using monolayer compression-expansion experiments, mimicking the expiration/inspiration movements, as well as using PM-IRRAS and BAM. Fig. 10 shows a surface pressure-area hysteresis loop measured during oscillation of interfacial area to test the effectiveness of spreading and stability of the ‘collapse’ pressure of Curosurf monolayers in the presence of the drug. As it can be seen, pure Curosurf monolayer exhibits a large but limited hysteresis which is related to its surface viscoelasticity, the ‘squeeze-out’ of Curosurf unsaturated lipid components, and mainly to the collapse and re-spreading of phospholipid molecules. Since the drop in surface pressure during the monolayer expansion was not abrupt, and the surface pressure at full trough expansion returns to the same value of the starting point of the cycle, one can conclude that there is an effective re-incorporation of lipid material from the interface. This behavior reflects minimized film collapse and efficient film replenishment (PANAIOTOV et al., 2015; ZUO et al., 2008). The presence of Clarithromycin does not increase the hysteresis profile of pure Curosurf monolayers neither produces significant changes at the surface pressure related to monolayer-multilayer transition. The surface pressures of the compression-expansion isotherm in the presence of the drug is about 13% smaller than those for the pure Curosurf monolayer. This finding is consistent with an improvement caused by the antibiotic facilitating the interfacial work of breathing.

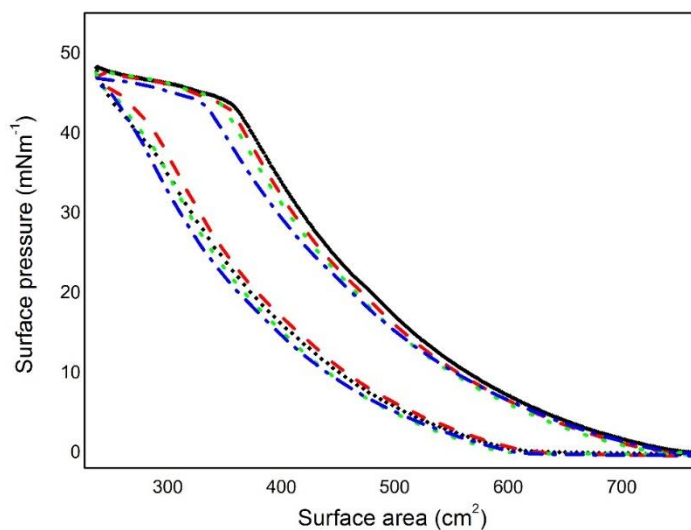


Figure 11. Compression-expansion isotherms of pure Curosurf (black diamonds) and its mixtures with Clarithromycin 0.1 (red dashed line), 1 (green dotted line), and 10 % w/w (blue dashed-dotted line). Isotherms were obtained at a compression rate of 10 mm/min under one cyclic regime (compression-expansion) showing a complete hysteresis loop.

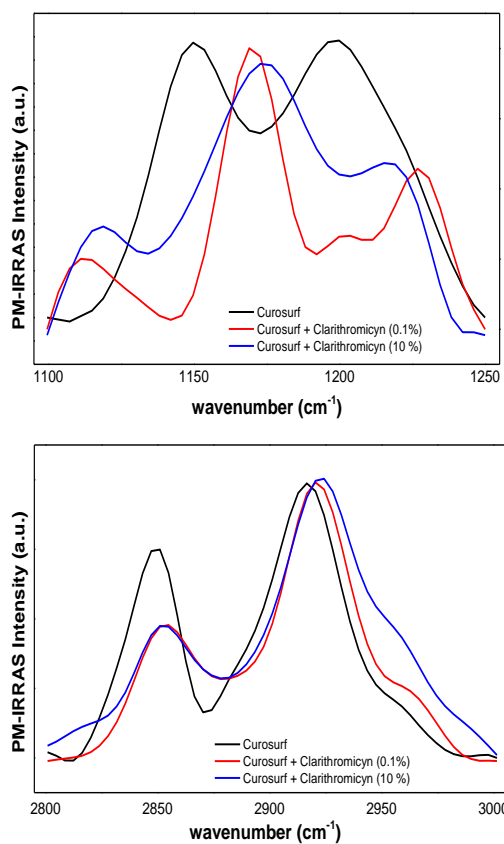


Figure 10. Experimental PM-IRRAS spectra of Langmuir films of Clarithromycin-Curosurf 0%, 0.1%, and 10% w/w at surface pressures 30 mNm⁻¹ in the (A) C–H region (2800–3000 cm⁻¹), and (B) C–O region (1000–1250 cm⁻¹).

Figure 11 compares PM-IRRAS spectra of Curosurf with increasing quantities of Clarithromycin (0.1 and 10% wt). In the region between 1100-1250 cm^{-1} the bands assigned to Curosurf appear at 1150 cm^{-1} (C-O-C) and 1200 cm^{-1} (PO_2^-). Considerable changes occur by adding Clarithromycin, with the band at 1150 cm^{-1} shifting to 1168 cm^{-1} and 1174 cm^{-1} as the Clarithromycin fraction increased from 0.1 to 10% (wt). The band at 1200 cm^{-1} shifted to 1227 and 1217 cm^{-1} with 0.1 to 10% (wt) Clarithromycin, respectively. Two main bands at 2849 cm^{-1} and 2916 cm^{-1} are assigned to symmetric and anti-symmetric CH stretching, respectively, and the shoulder at 2960 cm^{-1} is ascribed to CH_3 symmetric stretching. With the increase in Clarithromycin concentration, the bands associated with the hydrophobic tails are shifted, from 2849 to 2852 and 2854 cm^{-1} .

A similar behavior is observed for the band at 2916 shifted to 2920 and 2924 cm^{-1} , respectively. Variations in the vibration frequency of a band in the PM-IRRAS spectra are related in literature with changes in the electronegativity of the surrounding chemical medium and the ordering of the molecules on the surface (VIEIRA; SCHENNACH; GOLLAS, 2015). Shifts to higher wavenumbers suggest a strengthening of the chemical bond. Our results with Clarithromycin can be probably due to the electrostatic interaction between the positive charges of the amino group on the desosamine ring of the macrolide structure with the negative phosphate/ester groups from lipid polar heads. Further, as seen from the surface pressure-area isotherms the drug causes a condensation effect affecting the lipid packing organization and, in consequence, the absorption bands shifts to higher wavenumber. Accordingly, both the head groups and the hydrocarbon chains are affected by Clarithromycin, with the effect being more significant in the head group. As the interaction with polar heads is electrostatic, the effect on it may be more noticeable than the hydrocarbon chain interaction, as also found in the literature (CHIMOTE; BANERJEE, 2009; SCHWEDE et al., 2003). Significantly, the PM-IRRAS spectra in Figure 11 are consistent with the MD simulations, which showed that bulky Clarithromycin molecules interact with the head groups but penetrate to some small extent into the hydrocarbon chains.

Figure 12 shows BAM images of Curosurf and Curosurf-Clarithromycin monolayers (0.1% and 10% wt). Images from pure Curosurf monolayers shows

the beginning of starry condensed domains at very low surface pressures (~ 5 - 10 mNm^{-1}) in the LE state. Around 20 mNm^{-1} fractal 2D structures are closer and larger with the increase in surface pressure. Also, it can be seen the appearance of very bright spots on the fluid phase. The brighter spots reflect more light than the uniform condensed phase film, and hence are likely thicker than the film. These structures are attributed to the fluid phase material being pushed out of the interface, i.e. the loss of the less stable fluid non-DPPC interfacial material when the ‘squeeze-out’ process is occurring (ALONSO et al., 2004; ZHANG et al., 2011a). When Clarithromycin is added at least until 40 mNm^{-1} , the appearance of these spots is significantly reduced. It means that the drug stabilizes the monolayer. At 0.1% w/w of Clarithromycin and a surface pressure of ~ 20 mNm^{-1} , the domains appear bigger, much more ramified, but conserve the starry-like shape. Instead, at 10% w/w of the drug, the 2D structures started to be formed in quasi-circular geometry at 5 mNm^{-1} , indicating a different nucleation process for the highest addition of Clarithromycin. From 10 to 20 mNm^{-1} a round nucleus can be observed in fractal structures. The different behavior at 10% due to the appearance of small rather circular domains, with a narrower size distribution, could be expected as the favorable domain shape of lipid mixtures in the presence of a high content of guest molecules –as concluded from the surface compressibility (C_s^{-1}) analysis–, which affects to some extent their domains border line tension and the electrostatic interaction between the molecules within each domain. Overall, from the BAM images in Figure 12 one infers that incorporation of Clarithromycin causes the Curosurf monolayer to be more stable.

In summary, our data show that Clarithromycin molecules may interact with both the hydrocarbon chains and head groups because they are flexible, without disrupting the monolayer stability neither the interfacial spreading abilities. The experimental results from Curosurf/Clarithromycin mixed monolayers can be rationalized in terms of a slight condensation in the surface pressure isotherms as drug concentration is gradually increased. The antibiotic is incorporated into the lipid tails region of the monolayer but close to the polar head groups, i.e., interacting with both hydrophobic and polar head groups. There is a small change in elasticity at 10% w/w of the drug, without affecting the monolayer stability and structure.

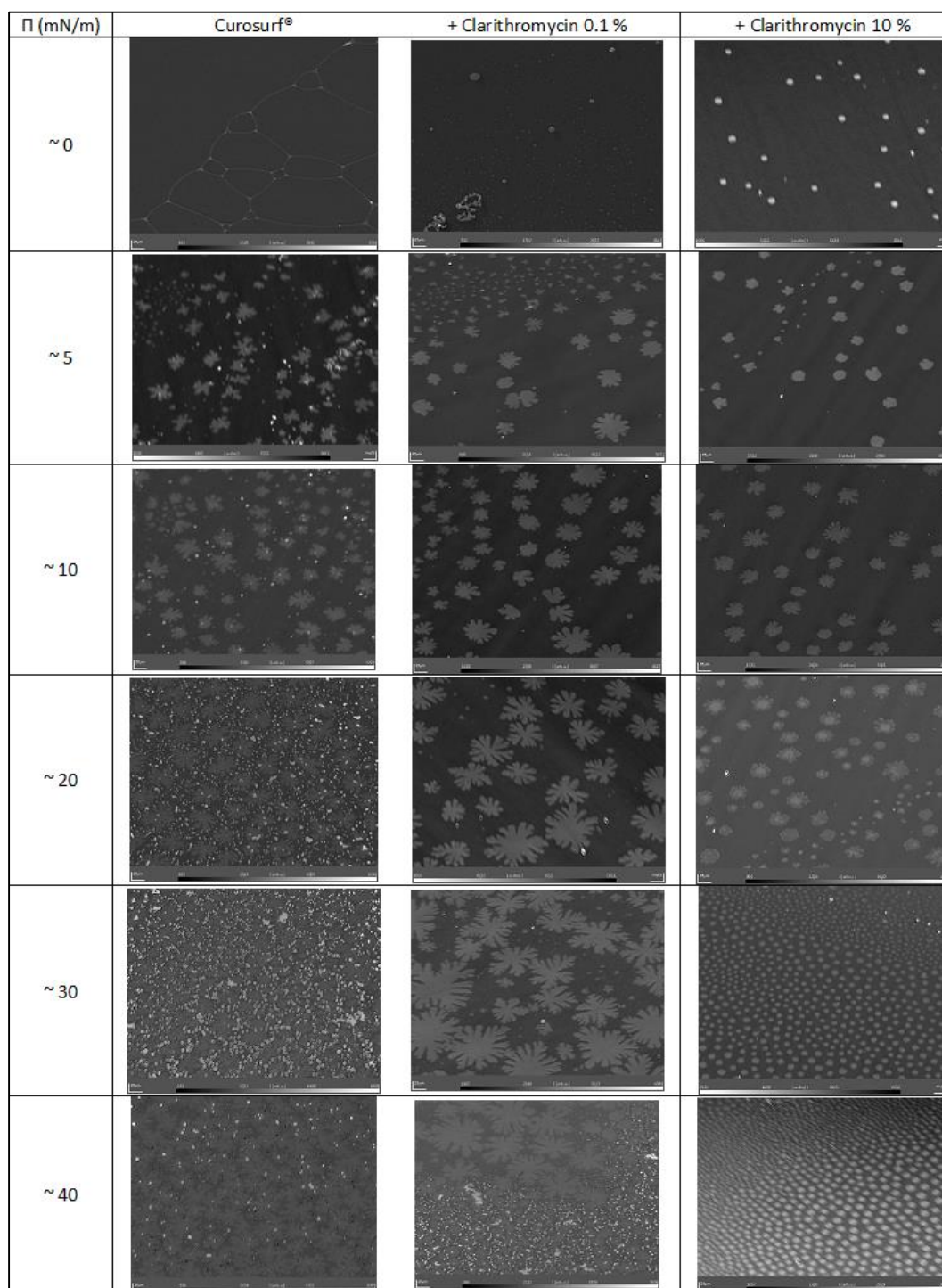


Figure 12. Brewster angle microscopy images of pure Curosurf, and Clarithromycin-Curosurf 0.1% and 10% w/w at $\pi = 0, 10, 20, 30$, and 40 mN m⁻¹. All BAM images have a 25 μ m scale bar at the left-hand corner.

5.3.4

Bactericide activity of Clarithromycin incorporated in the lung surfactant

The effect of Curosurf combination with Clarithromycin and its effect on the antibiotic activity were assessed using a sensitive Clarithromycin (Clr^s) Gram-positive strain of *B. cereus* and a Clarithromycin-resistant (Clr^r) Gram-negative strain of *E. coli* (Figure 13A). Curosurf itself reduced the viability of *B. cereus*, but this activity was abolished in the presence of DMSO 6.15 $\mu\text{L mL}^{-1}$ (Figure 13B). The use with such DMSO concentration indicated that Clarithromycin keeps its inhibitory activity on *B. cereus* even in the presence of Curosurf. To assess the dose-dependent effect of Curosurf on Clarithromycin activity, lower amounts of DMSO were used, thus leading to a reduced concentration of antibiotic and tested under longer incubation times (Figure 13C). Although Curosurf presents significant inhibitory activity on *B. cereus* under high concentration (222 $\mu\text{L mL}^{-1}$), the reduction of bacterial viability was significantly more intense when Clarithromycin was added at the tested 1:9 ratio. This is more evident when using lower concentrations of Clarithromycin ($\leq 12.3 \mu\text{L mL}^{-1}$) /Curosurf ($\leq 111 \mu\text{L mL}^{-1}$), as indicated. Curosurf at 111 $\mu\text{L mL}^{-1}$ was still inhibitory to *B. cereus* but at this concentration, 1.2 μL of DMSO in 1 mL of the medium is able to block such an effect. The antibiotic combination with Curosurf clearly potentiates the activity on this Gram-positive strain, causing significant activity in usually sub-inhibitory concentrations of Clarithromycin, when tested alone. The increase in antibiotic activity of Clarithromycin when incorporated in Curosurf was notable for Clr^r *E. coli*, which tolerates Curosurf with no background inhibitory activity, with or without DMSO (Figure 13D). The activity of Clarithromycin at 61.5-30.8 $\mu\text{L mL}^{-1}$ increased significantly, from an average inhibitory effect of 16-19% on the *E. coli* viability, to 42-46% when combined with Curosurf at 1:9 mass ratio. Combined as Clarithromycin/Curosurf mixtures, such low concentrations of Clarithromycin as 15.4-7.7 $\mu\text{L mL}^{-1}$ were also able to significantly reduce ($\sim 21\%$ inhibition) the *E. coli* viability, when compared to control treatments with DMSO/water mixture. The effect of Clarithromycin/Curosurf combination on plate tests could not be properly determined (data not shown), possibly due to the use of solid media constraining the interaction of these compounds with the target cells.

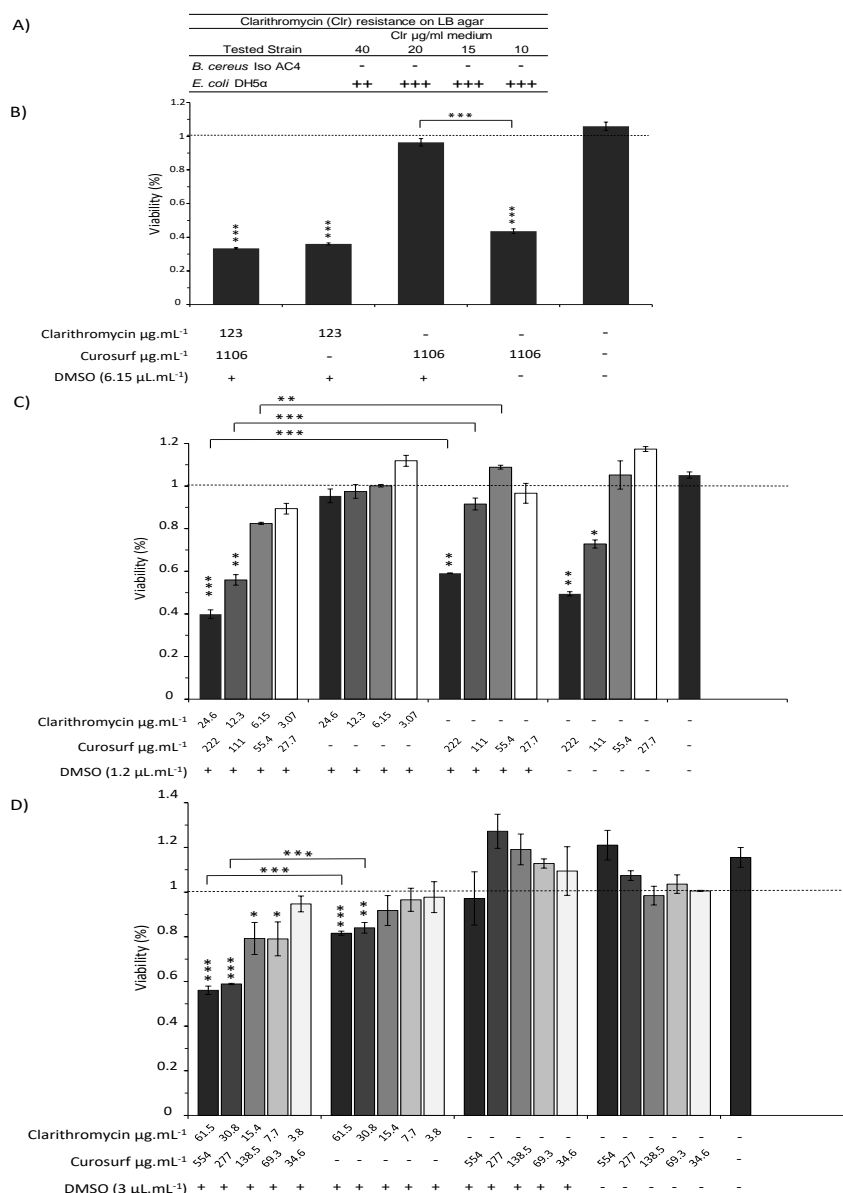


Figure 13. Antibacterial activity of Clarithromycin, Curosurf and Clarithromycin/Curosurf mixtures on *B. cereus* and *E. coli* strains. A) Clarithromycin resistance profile of each bacterial strain on LB plates. Tested strains, *B. cereus* Iso AC4 and *E. coli* DH5a, and antibiotic concentration are indicated. Bacterial growth was marked as “-” for fully sensitive strains, “+++” for full growth as in antibiotic-free plates and “++” for weaker bacterial growth on the LB clarithromycin plates. B-D) Bacterial viability determined by the MTT conversion test of *B. cereus* (B-C) or *E. coli* (D) suspensions, treated for 3h (B) or 5h (C-D). Viability presented as the percentage relative to the MTT conversion quantified in control treatments with DMSO/water. Clarithromycin and Curosurf final concentrations are indicated. All antibacterial assays were performed using clarithromycin/Curosurf 1:9 mixtures (10% mass ratio). See Methods for details. Statistically significant viability inhibition is indicated for t-tests with $p \leq 0.0001$ (***), $p=0.0002$ to 0.0006 (**) and $p=0.001$ to 0.009 (*). Top brackets indicate the significance of specific comparisons and asterisks on the bars indicate the significance of the inhibitory effect of the specified treatment relative to the DMSO/water control treatment.

5.4 Implications

One of the most important goals in the research on Clarithromycin is to try and reduce its gastrointestinal side effects and undesired interaction with other drugs, which could in principle be done with new delivery strategies. Today Clarithromycin is available as immediate and extended-release tablets, and in powder form for oral suspension. Since Clarithromycin is widely used to treat pneumonia and persistent respiratory tract infections, such as those committing patients of cystic fibrosis or infection in chronic obstructive pulmonary diseases, we propose that it could be delivered via inhalation or intratracheal instillation by incorporation into the lung surfactant. For this delivery strategy to be successful, Clarithromycin should not collapse the lung surfactant monolayer. The results presented here clearly show that Clarithromycin may be incorporated into such a monolayer without causing instabilities. Obviously, the data were obtained with simplified monolayer models, but the evidence from distinct experimental and simulation techniques gives us confidence that these models are realistic. Also significant concentrations as high as 10% w/w could be incorporated, which is useful for administering the drug locally.

The other issue to consider is whether incorporation in the lung surfactant would not hinder Clarithromycin activity, and to test this hypothesis we performed the viability assays with two types of bacteria. This is a major concern since phospholipids exerted a weak antagonistic interaction in some situations (FERRARA; DOS SANTOS; LUPI, 2001). The lack of information about the interaction of surfactant proteins and/or real lung surfactants with antibiotics (in special, Clarithromycin) indicates the importance of getting further information on this subject. Clarithromycin at physiological pH or in neutral aqueous solution is positively charged so that it may interact with any negatively charged component in the lung surfactant, decreasing its normal rate of killing bacteria. At least in these *in vitro* tests performed in our experiments, the combination with Curosurf not only kept Clarithromycin activity, but also increased it in some cases. This surfactant possibly improves the interaction/availability of this hydrophobic macrolide onto bacterial cells and/or

synergistically acts on cellular membranes or other targets, increasing the inhibitory activity of the antibiotic. The explanation for this increased antimicrobial activity may come from destabilization in the lipid ordering of the bacterial membrane due to the phospholipid composition of Curosurf.

5.4 Conclusion

Langmuir monolayers of Curosurf have been used here as simplified models for the lung surfactant monolayer, whose experimental results with varied techniques indicated that the monolayer stability is not affected by Clarithromycin, at least up to 10% w/w. Clarithromycin was found to interact with the polar head groups and the lower part of the hydrocarbon tails of phospholipid molecules according to PM-IRRAS data. These results were consistent with MD simulations on a Curosurf monolayer model, which were particularly useful to demonstrate monolayer integrity at the surface pressure typical of a biological membrane. The main conclusion drawn from these monolayer studies is that Clarithromycin can indeed be incorporated into a lung surfactant monolayer without collapsing it. Furthermore, in *in vitro* assays, we showed that Clarithromycin combined with Curosurf can kill Gram-positive as well as Gram-negative bacteria, which brings the hope of employing lung surfactant as a drug delivery system to treat pneumonia and respiratory distress syndrome.

5.4 Declaration of Interest

All authors listed have contributed sufficiently to the project to be included as authors, and all those who are qualified to be authors are listed in the author byline. No conflict of interest, financial and personal relationships with other people or organizations that could inappropriately influence (bias) their work.

5.4 Acknowledgments

The authors are thankful to the National Council for Scientific and Technological Development (CNPq-465259/2014-6), the National Institute of Science and

Technology Complex Fluids (INCT-FCx), the São Paulo Research Foundation (FAPESP, Grant No. 2014/50983-3, 2013/14262-7, and 2015/21055-8), and the Rio de Janeiro Research Foundation (FAPERJ, Grant No. 210.558/2015, and E-26/010.001241/2016) for financial support. This study was financed in part by the Coordenação de Aperfeiçoamento de Pessoal de Nível Superior - Brasil (CAPES) - Finance Code 001. S.O.C. thanks CNPq for a graduate fellowship. E.D.E.L. acknowledges FAPERJ for a graduate fellowship. A.A.P. thanks CNPq for an undergraduate research fellowship. We thank Dr. Cristiano R. W. Magalhães (Aché Laboratórios Farmacêuticos) for providing the Clarithromycin active sample and Dr. Adriano M. Alencar (IF/USP) for supplying the lung surfactant samples.

Influence of Levofloxacin and Clarithromycin on the Structure of DPPC Monolayers

Stephanie Ortiz-Collazos,¹ Paulo H. S. Picciani,² Osvaldo N. Oliveira Jr.,³ Andre S. Pimentel¹ and Karen J. Edler^{4,*}

1. Departamento de Química, Pontifícia Universidade Católica do Rio de Janeiro, Rio de Janeiro, RJ 22453-900 Brazil
2. Instituto de Macromoléculas Professora Eloisa Mano, Universidade Federal do Rio de Janeiro, Rio de Janeiro, RJ 21941-598, Brazil
3. Instituto de Física de São Carlos, Universidade de São Paulo, São Carlos, SP 13566-590, Brazil
4. Department of Chemistry, University of Bath, Claverton Down, Bath BA2 7AY, UK

*Corresponding author: Karen J. Edler – E-mail: K.Edler@bath.ac.uk

Working paper: *Langmuir* (Aimed journal)

Abstract

Research on lipid/drug interactions at the nanoscale underpins the emergence of synergistic mechanisms for topical drug administration. The structural understanding of bio-mimetic systems employing 1,2-dipalmitoyl-sn-glycero-3-phosphocholine (DPPC) as a membrane model mixed with antibiotics, as well as their biophysical properties, is of critical importance to modulate the effectiveness of therapeutic agents released directly to the airways. In this paper, we investigate the structural details of the interaction between Levofloxacin, 'a respiratory quinolone', and the macrolide Clarithromycin, with DPPC monolayers

at the air-water interface, using a combination of Brewster angle microscopy, polarization modulation-infrared reflection-adsorption spectroscopy (PM-IRRAS), surface pressure isotherms and neutron reflectometry (NR) to describe the structural details of this interaction. The results allowed association of changes in the π -A isotherm profile with changes in the molecular organization and the co-localization of the antibiotics within the lipid monolayer by NR measurements. Overall, both antibiotics are able to increase the thickness of the acyl tails in DPPC monolayers with a corresponding reduction in tail tilt as well as to interact with the phospholipid headgroups as shown by PM-IRRAS experiments. The effects on the DPPC monolayers are correlated with the physical-chemical properties of each antibiotic and dependent on its concentration.

Keywords: membrane, lung surfactant, macrolide, fluoroquinolone, phospholipids, neutron reflectometry.

6.1 Introduction

The biological membrane is a complex two-dimensional structure which contains a mosaic of proteins, lipids, glycolipids, and carbohydrates embedded in a fluid bilayer of phospholipids (NICOLSON, 2014; SINGER; NICOLSON, 1972). It is responsible for protecting the cell from its surroundings, controlling the movement of substances in and out of the cell, which determines proper functioning of a cell and the entire organism. It is also involved in cell adhesion, cell signaling, and ion exchange. It is also a barrier for the entrance of any toxic substance which could eventually interact with the membrane proteins or embed into the phospholipid bilayer, changing the membrane properties (BREZESINSKI; MÖHWALD, 2003; NICOLSON, 2014; SINGER; NICOLSON, 1972).

The Langmuir technique allows the formation of phospholipid monolayers at the air-water interface which may be used as the simplest model of a biological membrane to investigate the interactions with species such as drugs, toxins or pollutants (BREZESINSKI; MÖHWALD, 2003; DELEU; PAQUOT;

NYLANDER, 2005; GRIFFITH et al., 2013; ORTIZ-COLLAZOS et al., 2017b). This approach is especially convenient since the monolayer stability may be investigated (GRIFFITH et al., 2013; ORTIZ-COLLAZOS et al., 2016, 2017b; PANTOJA-ROMERO et al., 2016) and the compounds can be purposefully added to the subphase at a controlled concentration (GRIFFITH et al., 2013; HAC-WYDRO; DYNAROWICZ-ŁATKA, 2006; JABŁONOWSKA; BILEWICZ, 2007) or mixed with the lipid monolayer (ORTIZ-COLLAZOS et al., 2017b). 1,2-dipalmitoyl-sn-glycero-3-phosphocholine (DPPC) is the most important and abundant phospholipid occurring in natural membranes. Its monolayer at the air-water interface is well characterized (JYOTI et al., 1996; WEIDEMANN; VOLLHARDT, 1995). Therefore, this phospholipid is often used as a model of the outer cell membrane leaflet (DELEU; PAQUOT; NYLANDER, 2005; HIDALGO et al., 2006; PÉREZ et al., 2005), lung surfactant bilayers (PADILLA-CHAVARRÍA; GUIZADO; PIMENTEL, 2015a) and monolayers (ESTRADA-LÓPEZ et al., 2017; SOUZA et al., 2018).

Neutron reflectometry (NR) is a powerful technique to examine the structure of amphiphiles normal to the interface and provides valuable contrast variation measurements for the structural description and characterization of mixed systems such as lipid membrane models (DI COLA; GRILLO; RISTORI, 2016; KISELEV, 2011). Indeed, DPPC is a phospholipid widely used to mimic the interfacial properties of lung surfactant (LS) at the air-water interface because it is the main LS constituent (BENSIKADDOUR et al., 2008a; DUAN et al., 2013; FOLLOWS et al., 2007; FULLAGAR; HOLT; GENTLE, 2008; PINHEIRO et al., 2013a), thus it can reveal key information related to interactions with target molecules. For example, Fullagar et al applied NR on surfactant protein B (SP-B)/DPPC mixed films at the air-water interface to identify SP-B localization in the film as a function of surface pressure, as well as the squeeze-out process of the protein from the lipid monolayer (FULLAGAR; HOLT; GENTLE, 2008). In the same line of reasoning, Follows et al, studied the organization and dynamics of LS preparations of bovine and porcine origin at the air-water interface by NR. These results showed that a multilayer structure can be formed in exogenous surfactant even at very low concentrations and suggested that

multilayer models need to be incorporated into the current interpretations of *in vitro* studies (FOLLOWS et al., 2007). On the other hand, some studies have used NR to examine the structure of asymmetric outer membrane models of Gram-negative bacteria *P. aeruginosa* as a mixed DPPC bilayer (CLIFTON et al., 2013; MICHEL et al., 2017); also its interaction with cyclic antibiotic lipopeptides has been further investigated by Han *et al* (HAN et al., 2017). However, as far as we know, the structural organization, stability, co-localization and packing density of the lipids in an LS membrane model interacting with fluoroquinolones and macrolides at the air-water interface have not been studied using the NR technique.

In this work, the structural details of the interaction between Levofloxacin (a third-generation fluoroquinolone), as well as the semisynthetic macrolide Clarithromycin, with DPPC monolayers (acting as an LS membrane model) are studied at the air-water interface. Levofloxacin is cataloged as a “respiratory quinolone” due to the enhanced activity against the important respiratory pathogen *Streptococcus pneumonia*. Clarithromycin is a broad-spectrum antibiotic and one of the safest antibiotics available mostly used to treat infections of the upper and lower respiratory tract, including pneumonia and bronchitis (ORTIZ-COLLAZOS et al., 2017b). Some studies also suggest that aerosol formulation of Clarithromycin is an effective pulmonary drug delivery system for the treatment of respiratory infections (TOGAMI; CHONO; MORIMOTO, 2012). We have used NR, Brewster angle microscopy (BAM), polarization-modulation infrared reflection-absorption spectroscopy (PM-IRRAS) and Langmuir trough techniques to obtain new structural information about these mixed systems that can contribute to the design of new strategies in respiratory medicine.

6.2

Materials and methods

The reader is referred to the description in section 3, page 31.

6.3 Results and discussion

The antibiotics Clarithromycin and Levofloxacin are not surface active and do not form Langmuir monolayers on their own. They do interact with DPPC monolayers at the air/water interface, as shown in the π -A isotherms in Fig 14A and 14C. The isotherms were repeated several times and were shown to be reproducible. As expected for DPPC, the isotherm displays a plateau around ~ 8 mNm⁻¹ characteristics of an LE (liquid expanded) - LC (liquid condensed) phase transition. Upon further compression, there was a steep change in slope of the isotherm reaching the LC phase with an area per molecule of ~ 46.2 Å² (at a surface pressure of 30 mNm⁻¹) also consistent with the literature (DUNCAN; LARSON, 2008) (JAGALSKI et al., 2016). For mixed DPPC/Clarithromycin systems, there is a concentration-dependent effect, since the addition of the drug shifts the isotherm to lower areas, i.e., causes monolayer condensation. The shift to lower areas is probably due to the change in surface compressibility induced by Clarithromycin penetration into the monolayer, as seen in the change in slope of the isotherm in the LC region. Fig 14B and 14D show the surface compressional modulus, C_s^{-1} , as a function of the surface pressure for the pure and mixed lipid-drug monolayers. Typical experimental values in the literature of surface compressional modulus for DPPC monolayers are 10–50 mNm⁻¹ for LE films, 100–250 mNm⁻¹ for LC films, and >250 mNm⁻¹ for solid films (HAZELL et al., 2016) (DUNCAN; LARSON, 2008). For the pure DPPC monolayer, the C_s^{-1} plot shows that above ca. 17 mNm⁻¹ the lipid film is in a LC phase. However, for mixed DPPC/Clarithromycin systems, there is a slight depletion of C_s^{-1} values at the same surface pressure, and LC phases are reached only upon further lateral compression of the monolayer. It means that mixed DPPC/Clarithromycin monolayers became more compressible than the pure DPPC one. These results suggest a lipophilic interaction between Clarithromycin and the phospholipid tails, in addition to drug insertion into the film, which appears to be homogeneous according to the BAM images to be shown later on (FA et al., 2007).

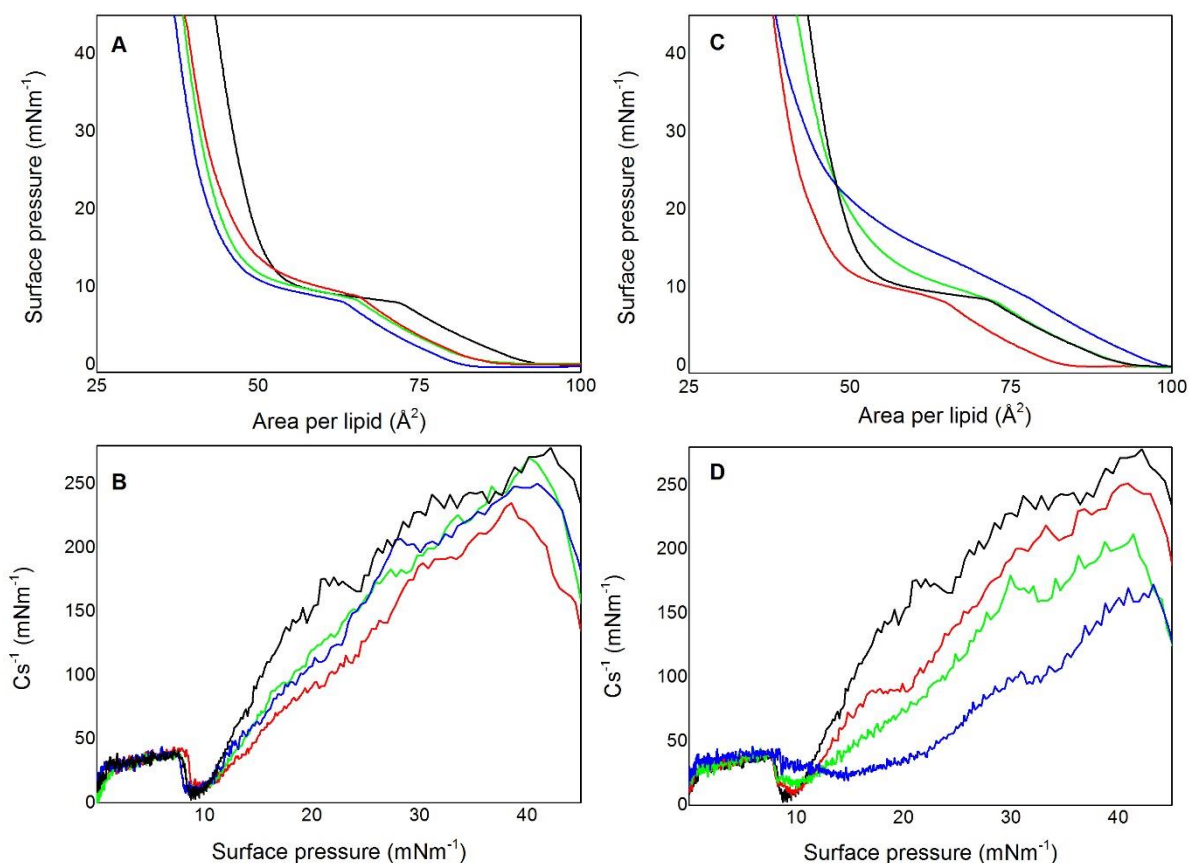


Figure 14. (A) Surface pressure-area (π -A) isotherms of pure (black) and mixed DPPC/Clarithromycin monolayers at 10 % w/w (blue); 1 % (green) and 0.1 % (red). (B) Surface compressional modulus at the air-water interface calculated from the isotherms in (A). (C) Surface pressure-area (π -A) isotherms of pure DPPC (black) and mixed DPPC/Levofloxacin at 10 % w/w (blue); 1 % (green) and 0.1 % (red). (D) Surface compressional modulus at the air-water interface from the isotherms in (B).

For mixed DPPC/Levofloxacin monolayer systems in Fig 14C, upon 0.1 % w/w Levofloxacin addition, a shift to lower areas in the isotherm was also observed. As the Levofloxacin concentration is increased (10% w/w), the isotherm profile displays a second-order phase transition as well as changes in the slope of the isotherm at high surface pressures. It indicates changes in the packing of lipid molecules represented as a ‘delay’ in the lateral monolayer organization. Regarding the monolayer elasticity in Fig 14D, there is a progressive increase of monolayer compressibility as C_s^{-1} values dramatically decrease to values below those for pure DPPC. Also, the delay in the LC phase formation is evident in C_s^{-1} plots, especially at high Levofloxacin concentration (10% w/w), since the monolayer remains at the LE state until high surface pressures ($\sim 30 \text{ mNm}^{-1}$)

where it passes to the LC phase. The latter may be related to a different organization of the lipid molecules in the presence of a high drug concentration, which hinders the formation of the LC phase. Overall, these results could indicate that Levofloxacin interacts with phosphatidylcholine mainly through electrostatic interactions with the hydrophilic groups (GRANCELLI et al., 2002) and induces more elastic states, hence more compressible monolayers (WÜSTNECK et al., 2005) than pure DPPC and DPPC/Clarithromycin mixtures. The collapse pressure of pure DPPC was around 68.7 mNm^{-1} , and this was not reduced with the addition of both drugs. Therefore, incorporation of both antibiotics does not affect or anticipate the collapse process of DPPC monolayers.

Interfacial rheology experiments (see Fig. E.1 Supplementary material-3) on pure DPPC and mixed DPPC/antibiotics monolayers were also carried out using a double wall ring (DWR) geometry accessory in combination with a magnetic bearing stress rheometer (Discovery HR-3, TA Instruments, USA) on the dispersed films into the rheometer trough. As described in the previous Langmuir trough studies, the same stock solutions have been used here over an ultrapure water subphase. An oscillatory strain experiment showed that the surface shear modulus G' and G'' of pure DPPC were indistinguishable from a clean water surface. However, an amplitude sweep test of the DPPC/antibiotic mixtures at the higher concentrations (Levofloxacin and Clarithromycin at 10% w/w) showed that the viscous modulus G'' rose above noise level (Fig E.1). The effect was more pronounced in the Clarithromycin mixture than in the Levofloxacin one. Nevertheless, the flow curve and the frequency sweep tests just display noise. These results indicate that the addition of antibiotics affects the mechanical properties of the DPPC monolayer but they are not strong enough effects to be measured with the DWR geometry. The fact that the viscous/loss moduli G'' in the DPPC/Clarithromycin mixtures was higher than in the DPPC/Levofloxacin mixed monolayer demonstrates that the first one is a more viscous and ordered monolayer. Those results are in agreement with the surface compressional modulus C_s^{-1} results calculated from the π -A isotherms.

Figure 15 shows a summary of the BAM images recorded from π -A isotherms at 0 and 30 mNm^{-1} where the existence of lateral structural changes on the DPPC monolayer in the presence of both antibiotics is confirmed. Tables E.1 and E.2 in Supplementary material-3 present the full images of pure and mixed DPPC/Levofloxacin and DPPC/Clarithromycin monolayers recorded as a function of surface pressure. Ordered condensed domains of pure DPPC are formed at very low surface pressure in the form of small patches ($\sim 5 \text{ mNm}^{-1}$) that grow in size and gain a lobulated shape under lateral compression (typical for the enantiomeric DPPC molecule (KLOPFER; VANDERLICK, 1996)). These DPPC domains achieve high molecular packing and become an LC phase at surface pressures between 20 and 30 mNm^{-1} . With the increase of Levofloxacin and Clarithromycin

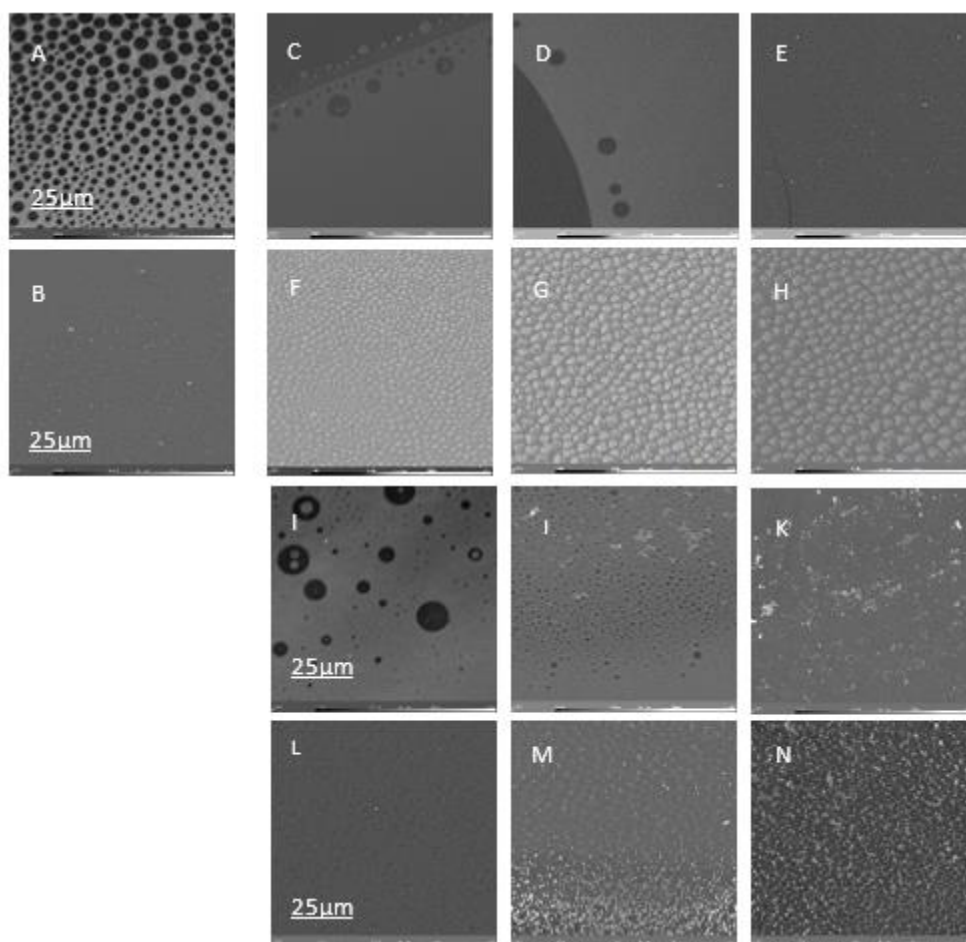


Figure 15. Brewster angle microscopy images of pure DPPC (1 g.L^{-1}) (A) 0 mNm^{-1} and (B) 30 mNm^{-1} . Mixed DPPC/Clarithromycin at 0 mNm^{-1} (C 0.1% w/w; D 1%; E 10%) and 30 mNm^{-1} (F 0.1% w/w; G 1%; H 10%). Mixed DPPC/Levofloxacin at 0 mNm^{-1} (I 0.1% w/w; J 1%; K 10%) and 30 mNm^{-1} (L 0.1% w/w; M 1%; N 10%).

concentrations, the lipid domains adopt a more star-like shape due to their interaction with antibiotic molecules. Previous reports (STEFANIU; BREZESINSKI; MÖHWALD, 2012; WIELAND et al., 2016) attribute changes in the shape of DPPC domains to the presence of particles that modify the line tension between domains, which affect their appearance. Moreover, the LC phase is reached at smaller surface areas (for the same pressure), indicating the loss of molecular arrangement, as reflected by the black holes (defects) at surface pressures $> 30 \text{ mNm}^{-1}$. When the antibiotic content is higher than 1%, bright circular domains are observed, which may indicate the existence of lipid/drug aggregates which have a lower line tension than pure DPPC domains. These aggregates affect the DPPC molecular organization, thus changing the isotherms as in Fig. 14.

Figure 16 compares the PM-IRRAS spectra of pure DPPC with the addition of Clarithromycin and Levofloxacin at 0.1 and 10% (w/w) in a surface pressure of 30 mNm^{-1} at the head groups region. Pure DPPC bands (Upper graph) at 1698 cm^{-1} (C=O stretching, fatty acid) and 1742 cm^{-1} (C=O stretching, ester) change their orientation (downwards to upwards) with increasing surface pressure, indicating that phospholipids headgroups change their orientation from perpendicular to parallel to the air-water interface upon compression. With the addition of Clarithromycin and Levofloxacin (Lower graph) at any studied quantity, the polar phospholipid headgroups are no longer sensitive to surface pressure, remaining with the same orientation (parallel) (see full PM-IRRAS spectra in Fig. E.2 A-J in Supplementary material-3). This is an indication that both antibiotics have interaction with the phospholipid headgroups. Furthermore, no significant changes were observed for alkyl tail bands at 2850 cm^{-1} (CH_2 symmetric) and 2925 cm^{-1} (CH_2 antisymmetric). The PM-IRRAS spectra indicate that Clarithromycin and Levofloxacin interact with the headgroups of DPPC. Also, they affect the organization of DPPC upon compression. The bands centered at 1650 and 1547 cm^{-1} represents the effect of interfacial water molecules, and are usually attributed to the difference of reflectivities of the air-water interface covered and uncovered by the monolayer. (GOTO et al., 2016; SORIANO et al., 2017)

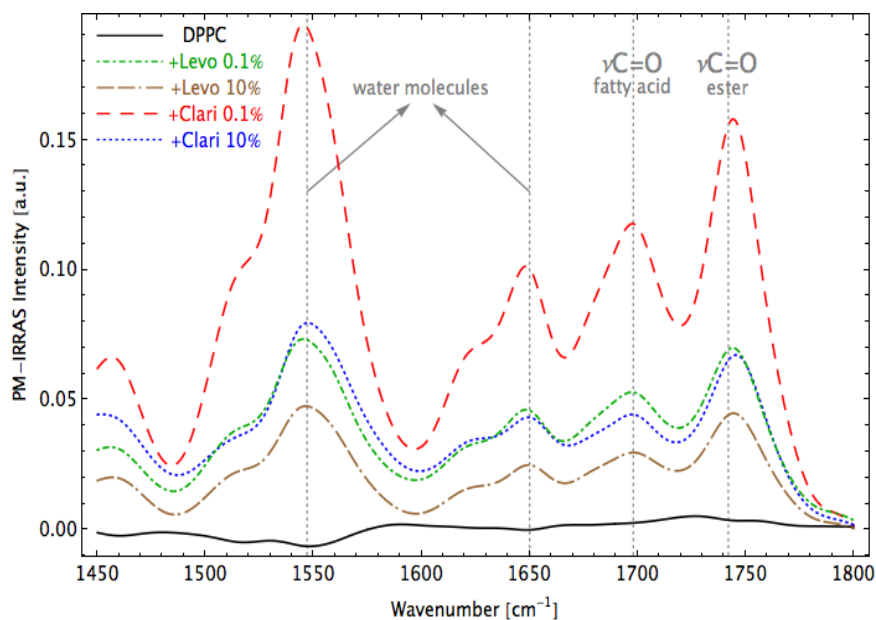
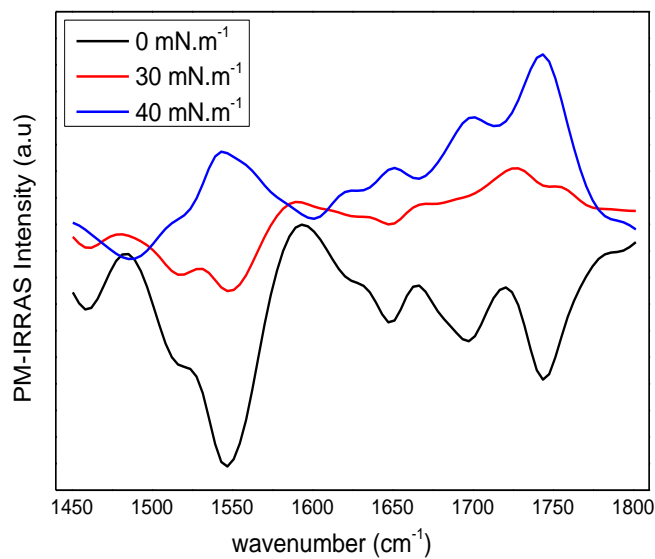


Figure 16. Upper graph: PM-IRRAS spectra of pure DPPC with increasing surface pressure. Lower graph: PM-IRRAS spectra of pure DPPC (black solid line), DPPC/Levofloxacin 0.1% w/w (green dot-dashed line), DPPC/levofloxacin 10% w/w (brown double-dashed-dot line), DPPC/ Clarithromycin 0.1% w/w (red dashed line) and DPPC/ Clarithromycin 10% w/w (blue dot line) at the head groups region (1450–1800 cm⁻¹) 30 mNm⁻¹.

Before NR studies, the stability of the mixed monolayers was checked by holding the target surface pressures using a feedback loop. All the systems were left undisturbed for a lapse of time of 90 min with little loss of material from the interface (less than ~5% in area). Two reflectometry profiles for a pure DPPC monolayer over different subphases: D₂O and ACMW, along with their corresponding SLD profile at 30 mNm⁻¹ are presented in Fig 17. Simultaneous two-layer model fitting of the experimental reflectometry data revealed that our results are consistent with published results.(JAGALSKI et al., 2016) Table 2 summarizes the scattering length densities used in the fitting procedure for pure and mixed DPPC (-h/-d₆₂) and table 3 summarizes the structural parameters obtained in fittings at 30 mNm⁻¹ and 10 % w/w of the drug.

Table 2. Summary of the scattering lengths densities used in the reflectivity calculations.

Lipid/antibiotic/subphas e	$\rho/10^{-6} \text{ \AA}^{-2}$	$\rho/10^{-6} \text{ \AA}^{-2}$ with 10% w/w of Levofloxacin	$\rho/10^{-6} \text{ \AA}^{-2}$ with 10% w/w of Clarithro.
DPPC headgroup	1.67	1.67	1.67
h-DPPC tail	-0.38	-0.36	-0.35
d-DPPC tail	7.24	6.69	6.59
Clarithromycin	0.66	-	-
Levofloxacin	1.7	-	-
D ₂ O	6.35	-	-
ACMW	0	-	-

In the fitting of the different contrast data sets, the layer thicknesses were constrained between each data set, because it is assumed that the physical dimensions of the films are unaffected by changes in deuteration of the components(FULLAGAR; HOLT; GENTLE, 2008). From the data sets for pure DPPC (see Supplementary material-3 Table E.3 for full fitting parameters) it is possible to see the interfacial film emerging as the surface pressure increases and the reflectivity profiles display higher intensity. At a surface pressure of 30 mNm⁻¹ these fittings provide an area per lipid molecule of 53.2 Å² (from the lipid tails) and a thickness of the hydrocarbon layer of 16.0 Å, resulting in a tilt angle (relative to the surface normal) of 33.3° calculated as follows: $\beta = \arccos(t_{\text{tails}}/l_{\text{palmitoyl}})$. The length (l) of the DPPC tails used was 19.15 Å as reported by Vaknin *et al*(DIETRICH et al., 2009; VAKNIN et al., 1991), compatible with

previous DPPC tilt angles reported (BREZESINSKI et al., 1995; ESTRELA-LOPIS; BREZESINSKI; MÖHWALD, 2004; GERICKE; FLACH; MENDELSON, 1997; GULER et al., 2009; MOHAMMAD-AGHAIE et al., 2010; POCIVAVSEK et al., 2011; TAKESHITA; OKUNO; ISHIBASHI, 2017; TOIMIL et al., 2012)

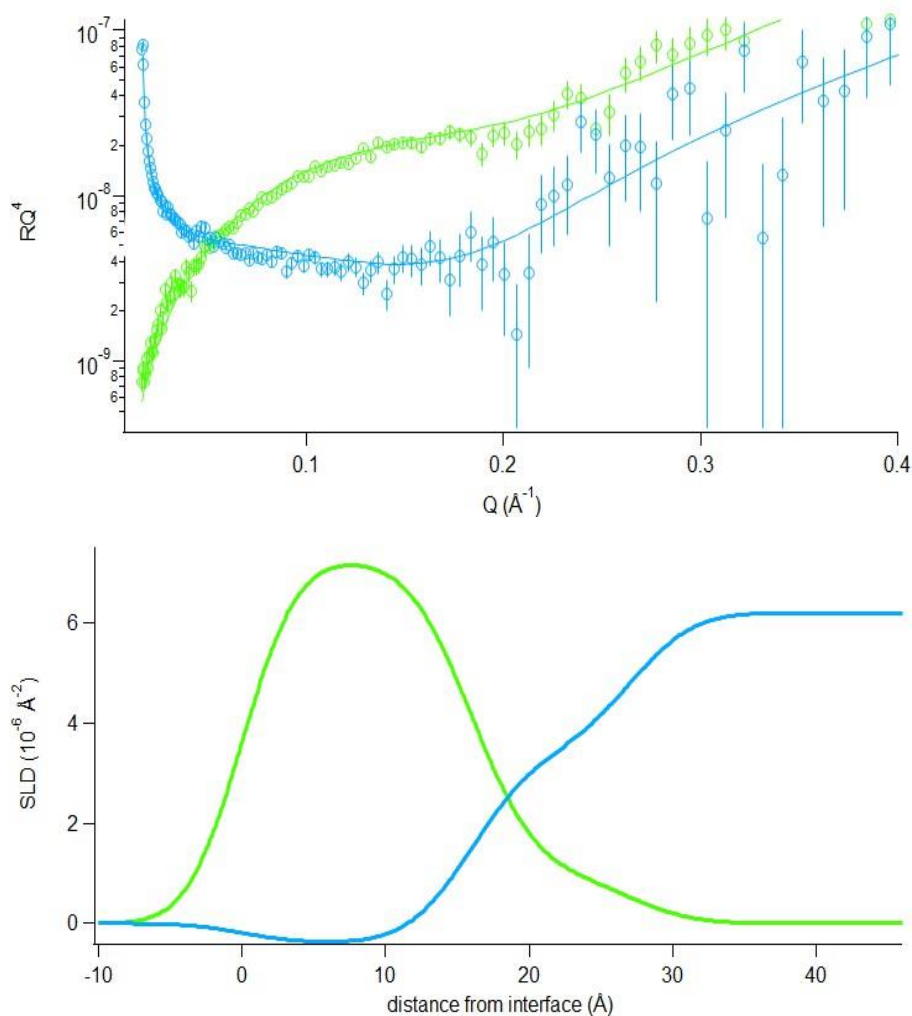


Figure 17. Neutron Reflectometry data and the best two-layer fittings from simultaneously fitted d-DPPC on ACMW (green) and h-DPPC on D_2O (blue) monolayers at the air-water interface and a surface pressure of 30 mNm^{-1} . Upper figure: Reflectivity vs Q (\AA^{-1}), Lower figure: The scattering length density plot of all contrasts vs the distance from the interface.

Table 3. Summary of the parameters used for the best obtained NR fits using a two-layer model on pure DPPC (1mgmL⁻¹) and mixed DPPC/antibiotic monolayers at 10% w/w and 30 mNm⁻¹.

	Tail layer thickness t/Å	Headgroup layer thickness t/Å	Roughness (head-to-tail interface) σ/Å	Solvent penetration (headgroup) %	Tail tilt angle (relative to the surface normal)
DPPC	16 ± 0.7	11 ± 2	3.5 ± 1	38 ± 9	33.3°
DPPC/Levo 10%	18 ± 0.3	13 ± 0.7	3.9 ± 1	45 ± 4	20.0°
DPPC/Clari 10%	19 ± 0.3	9.1 ± 0.4	4.5 ± 0.5	19 ± 3	7.17°

Figure 18 shows the NR profiles and the best data fitting for the mixed lipid-drug curves at 30 mNm⁻¹; as well as their corresponding SLD profiles for a concentration of 10 % w/w. The influence from both antibiotics on the interfacial structure of DPPC monolayers is seen in the structural parameters in Tables E.4 and E.5 in the Supplementary material-3. The best fit for mixed DPPC/Clarithromycin monolayers was obtained considering that the molecule is located within the hydrocarbon tails. As can be seen in table 3, the introduction of Clarithromycin showed a thickness increase of the tail groups from ~ 16.0 to ~ 19.0 Å (at 30 mNm⁻¹ and 10% of drug) and increased roughness from ~ 3.5 to ~ 4.5 Å at the top of the tails. These effects are in agreement with the Clarithromycin compressional effect in the monolayer, in consequence, the tilt angle of the tail decreases as the concentration of drug increases(FULLAGAR; HOLT; GENTLE, 2008)(ISKANDER, 2011). On the other hand, there was also a gradual decrease in the solvent penetration of the headgroups, from ~ 38% in pure DPPC monolayers to 19% at the highest addition of drug; as well as a reduction in the headgroup thickness (from ~ 11 to 9.1 Å). From Kosol *et al*(KOSOL et al., 2012), it is known that macrolides are able to bind to membrane models through electrostatic interaction between the amino groups of the macrolides with the phospholipid headgroup. Clarithromycin, chemically known as 6-O-methylerythromycin A, contains in its structure a desosamine ring (deoxy sugar), permitting it to exist in both protonated (>96%) and neutral (<4%) forms at physiological pH due to the pKa of the dimethylamino group (~8.6-8.9)(GOLDMAN et al., 1990; SCHLÜNZEN et al., 2001). These results indicate that Clarithromycin, owing to its hydrophobic nature, co-localizes mainly within the acyl tails of DPPC through van der Waals forces(C. PEETLA, A. STINE,

2009). Furthermore, Clarithromycin probably guides its deoxy sugar units close to the polar headgroups allowing the positively charged amino group to interact with the polarizable PC headgroups.

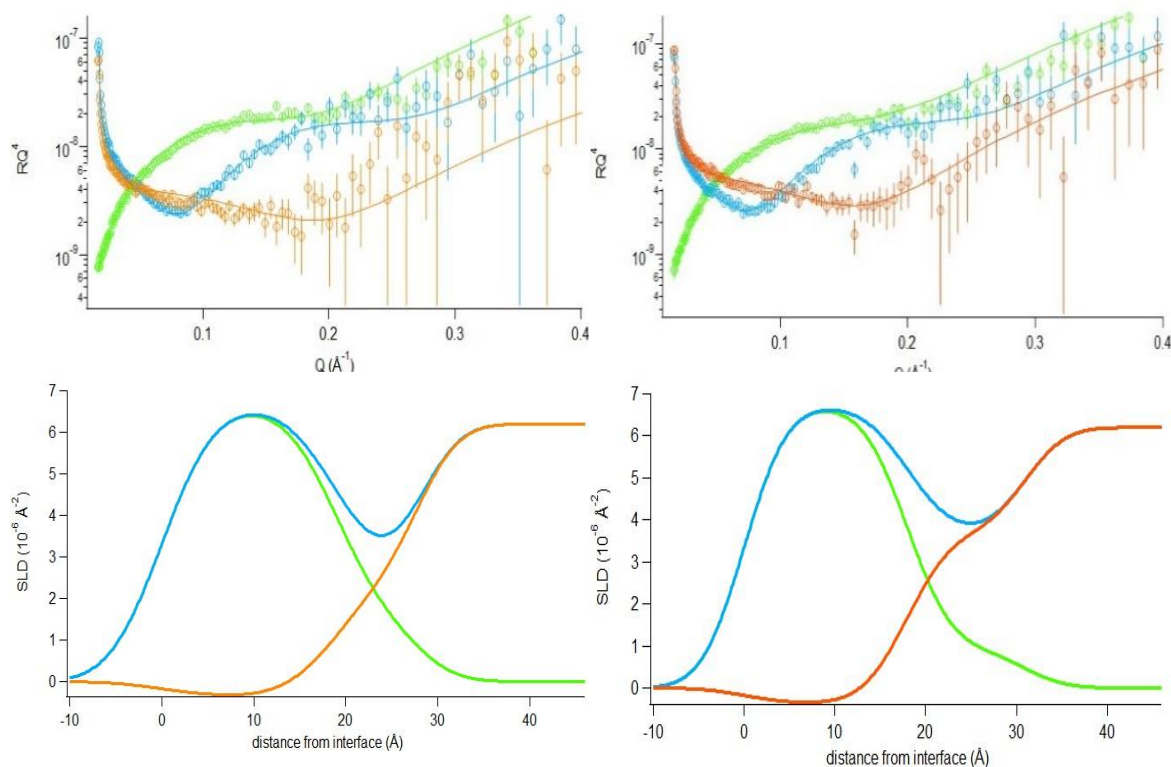


Figure 18. Neutron Reflectometry data and the best two-layer fittings obtained from simultaneous fitted: h-DPPC/antibiotic on D₂O (orange); d-DPPC/antibiotic on D₂O (blue) and d-DPPC/antibiotic on ACMW (green) at 10% w/w and a surface pressure of 30 mNm⁻¹. Upper Figure: Reflectivity vs Q (Å⁻¹). Lower Figure: The scattering length density plot of all contrasts vs the distance from the interface. Left images correspond to DPP/Clarithromycin. Right images correspond to DPPC/Levofloxacin.

From the best data fits of Levofloxacin mixtures, (which differs from Clarithromycin due to its hydrophilic character and its smaller volume), it was possible to observe a less remarkable increase in the tail thickness along with a reduction in its tilt angle (from ~ 16 to 18 Å and $\sim 33^\circ$ to 20° respectively). Earlier studies have indicated the ability of a fluoroquinolone antibiotic (Ciprofloxacin) to alter the tilt angle of the acyl chain of DPPC monolayers (BENSIKADDOUR et al., 2008a, 2008b). In addition, it was noticed that Levofloxacin induces an increase in the headgroups thickness from ~ 11 to 13 Å. Also, the hydration percentage of the headgroups was reduced at low Levofloxacin concentration but

it increases from 38% to 45 % at the highest addition of drug. These results suggest that Levofloxacin, as a zwitterionic molecule at pH ~ 7 (HIRANO et al., 2006; LAMBERT; REGNOUF-DE-VAINS; RUIZ-LÓPEZ, 2007; MITSCHER, 2005), penetrates the monolayer and co-localizes mainly at the head to tail interfacial region. Since fluoroquinolones enable attractive interplays between the positively charged piperazine ring at the C-7 position of the quinolone and the negatively charged phosphate groups of the phospholipid heads, (FRESTA et al., 2002; GRANCELLI et al., 2002; MONTERO; MERINO-MONTERO; VINUESA, 2006) Levofloxacin could replace water molecules surrounding the headgroup region through electrostatic dipole-dipole interactions (hydrogen-bond interactions). This could explain the differences found in the SLD profile format in the headgroup region at 30 mNm^{-1} , compared with the pure DPPC SLD profile. These observed effects are consistent with a decreased area per lipid molecule seen in the surface pressure isotherms. In the paper Ortiz-Collazos, *et al* (ORTIZ-COLLAZOS et al., 2017b), have been shown by MD simulations that Levofloxacin molecules are located preferentially between the polar head groups phospholipids at surface pressures of 43 mNm^{-1} which is in agreement with the results presented here. Besides, according to the compressional effect of the drug in the monolayer, it was observed that the tilt angle of the tail decreases especially upon 0.1 % w/w of Levofloxacin addition.

Our results show that the effects of introducing both drugs on DPPC monolayers are related with the particularities of its interplay with the lipid membrane model. The lower compressibility values found in Levofloxacin mixtures, especially at 10% w/w and 30 mNm^{-1} , indicates a high fluidity of the model membrane at this point. This fact may directly affect the drug release at the surface packing pressure found in biological membranes. Further, as mentioned before, Levofloxacin is able to form hydrogen bonds with the lipid head groups, which probably facilitate its permeability through the lipid layer. Instead, Clarithromycin due to its high lipophilicity is more homogeneously inserted in the monolayer and induces slight perturbations on the monolayer organization. Changes in the acyl chain thickness are due to the hydrophobic attraction between the lipid tails and the inserted antibiotic. This could result in a slower release of Clarithromycin from the hydrophobic tails to the aqueous medium. However, its strong interaction with the

lipid headgroups could be a key factor which mediates its membrane diffusion and binding to the bacterial proteins. The structural information obtained about the orientation and localization of the antibiotics in the lung surfactant membrane-mimetic system facilitates the understanding of the interaction of such compounds with lipid membranes to predict the biophysical behavior of future smart drug-delivery formulations.

6.4 Conclusions

From this information, we have determined the structural details of the interaction between Levofloxacin and Clarithromycin antibiotics, each interacting with DPPC monolayers respectively. Langmuir studies shown that the introduction of both antibiotics induces changes in packing and lipid organization, as evidenced by a shifting in the isotherm to lower areas i.e., causing the monolayers to be more compressible. BAM experiments confirmed changes in the DPPC domains structure in the presence of the antibiotics which modify its molecular arrangement. The effects of the antibiotics differ due to their different physicochemical natures modifying the elastic properties of DPPC monolayers. NR data analysis showed that Clarithromycin, as a bulky hydrophobic molecule, merged into the hydrocarbon tails region allowing its deoxy sugar units to be close to the polar headgroups. Clarithromycin is able to induce a considerable reduction in the tilt angle of the lipid tails as well as reducing the thickness and solvent penetration of the polar headgroups. On the other hand, the smaller Levofloxacin produces a larger effect on the isotherm profile at high drug concentration (10% w/w), causing a delay in the LE-LC phase transition, hinders the phospholipid molecular organization, and induces a considerable decrease in the compressional modulus. The NR results indicate that Levofloxacin co-localizes mainly affecting the polar headgroups since it slightly increases both tail and head groups thickness as well as reduces the solvent penetration of the polar region and the acyl tail tilt. The presence of both antibiotics also induces the roughening at the head-to-tail region of the mixed monolayers, when compared with pure DPPC monolayers, which confirms their insertion. These effects corroborate changes in the packing and the lateral organization of the DPPC

molecules, as well as the integration of these antibiotics into the monolayer. Further, the stability, functionality and the monolayer to multilayer transition process in the DPPC monolayer ('collapse mechanism'), was not compromised at any drug concentration studied. We believe that this work can contribute to a better understanding and control of the molecular basis related to the interaction of these antibiotics with membrane models and thus, in the design of new strategies in respiratory medicine.

6.5

Conflicts of interest

The authors declare there are no conflicts of interest related to this manuscript.

6.6

Acknowledgments

The authors are thankful to the Brazilian funding agencies FAPERJ (Grant No. 210.558/2015, and E-26/010.001241/2016), FAPESP (Grant No. 2013/14262-7 and 210.558/2015), CNPq (Grant No. 465259/2014-6) for financial support in the form of a PhD studentship for S.O-C and CAPES for a sandwich doctorate scholarship (No.88881.132891/2016-01). We acknowledge Dr. Cristiano R. W. Magalhães (Aché Laboratórios Farmacêuticos), who supplied the antibiotics active samples. We would also like to thank ISIS Pulsed Neutron and Muon source for the beamtime (experiment number RB1710178) and the SURF beamline staff for their assistance in collecting the NR data. Thanks are also extended to Edler's research group from the University of Bath for their assistance in developing this work.

Physical-chemistry interaction studies in lipid monolayer membrane models have a deep role in the structural description and dynamics of biological membranes and contribute to understanding how its specific composition and organization can modulate biophysical processes at the nanoscale, thus allowing to improve the design of drug delivery systems. Although there are very few reports in literature about the physical-chemical characteristics of lung surfactant monolayers related to the specific introduction of Clarithromycin and Levofloxacin antibiotics, our findings clearly lead to structurally describe the behavior of the mixed systems in order to demonstrate its potential efficiency in *in vivo* systems.

Our data from experimental and complementary theoretical approaches shows that Levofloxacin, at fractions up to 10% w/w does not disrupt the stability nor the surface elasticity of Curosurf monolayers, even being certainly inserted in the film, since it causes an evident expansion in the surface pressure isotherms. PM-IRRAS, molecular dynamics, and BAM studies indicate that the drug is placed between lipid headgroups and its insertion causes a delay in the monolayer-to-multilayer phase transition, at 10% w/w of the drug, due to the presence of few aggregates. Also, in DPPC monolayers, which mimics the lung surfactant membrane at the air-water interface, it is evident that Levofloxacin strongly interacts with the phospholipid since induces changes in its packing, organization, and surface elasticity. Surprisingly, these effects do not induce an anticipate collapse even at a high content of drug. As evidenced by NR measurements the drug is in fact co-located in the tail-to-head interface region as an increase in the headgroups roughness was observed. The antibiotic also reduces the hydration percentage of headgroups at low concentration and increases this percentage at high concentration in DPPC monolayers.

Again, Curosurf monolayers containing Clarithromycin does not show instability due to the antibiotic introduction, at least up to 10% w/w of the drug. PM-IRRAS data reveals that Clarithromycin, in fact, affects the head groups disposition due to the displacement of PO_2^- and C-O-C IR bands to higher wavenumber values. MD simulations corroborate the monolayer integrity at the biological relevant surface pressure 30 mNm^{-1} . In *in vitro* assays, the mixture Clarithromycin/Curosurf appears to enhance its antibacterial activity, especially against Gram-positive bacteria. Our approaches to study the effect of Clarithromycin with pure DPPC monolayers shows that the drug induces an ordering effect in the film since NR data reveals that the drug is co-localized within the lipid tails. However, Clarithromycin also orients its polar sugar groups close to the polar heads region and strongly interacts with them. Besides, NR data shows the lipid tails roughening and a notable reduction in tail tilting as the drug concentration increases.

In conclusion, our results demonstrate the suitability of both Levofloxacin and Clarithromycin antibiotics to be introduced in Curosurf preparations, in terms of drug delivery systems, for the treatment of lower respiratory tract infections. The mixed systems studied here promising enhanced therapeutic efficacy, suggesting its application in future *in vivo* assays.

References

ALHAJLAN, M.; ALHARIRI, M.; OMRI, A. Efficacy and safety of liposomal clarithromycin and its effect on *pseudomonas aeruginosa* virulence factors. **Antimicrobial Agents and Chemotherapy**, v. 57, n. 6, p. 2694–2704, 2013.

ALONSO, C. et al. More Than a Monolayer: Relating Lung Surfactant Structure and Mechanics to Composition. **Biophysical Journal**, v. 87, n. 6, p. 4188–4202, 2004.

BANASCHEWSKI, B. J. H. H. et al. Antimicrobial and Biophysical Properties of Surfactant Supplemented with an Antimicrobial Peptide for Treatment of Bacterial Pneumonia. **Antimicrobial Agents and Chemotherapy**, v. 59, n. March, p. AAC.04937-14, 2015.

BASABE-BURGOS, O. et al. Natural Derived Surfactant Preparation As a Carrier of Polymyxin E for Treatment of *Pseudomonas aeruginosa* Pneumonia in a Near-Term Rabbit Model. **Journal of Aerosol Medicine and Pulmonary Drug Delivery**, v. 31, n. 0, p. jump.2018.1468, 2018.

BENSIKADDOUR, H. et al. Characterization of the Interactions between Fluoroquinolone Antibiotics and Lipids: a Multitechnique Approach. **Biophysical Journal**, v. 94, n. 8, p. 3035–3046, 2008a.

BENSIKADDOUR, H. et al. Interactions of ciprofloxacin with DPPC and DPPG: fluorescence anisotropy, ATR-FTIR and ³¹P NMR spectroscopies and conformational analysis. **Biochimica et biophysica acta**, v. 1778, n. 11, p. 2535–43, nov. 2008b.

BERNHARD, W. Lung surfactant: Function and composition in the context of development and respiratory physiology. **Annals of Anatomy**, v. 208, p. 146–150, 2016.

BERQUAND, A. et al. Interaction of the macrolide antibiotic azithromycin with lipid bilayers: Effect on membrane organization, fluidity, and permeability. **Pharmaceutical Research**, v. 22, n. 3, p. 465–475, 2005.

BREZESINSKI, G. et al. Influence of ether linkages on the structure of

double-chain phospholipid monolayers. **Chemistry and Physics of Lipids**, v. 76, n. 2, p. 145–157, 1995.

BREZESINSKI, G.; MÖHWALD, H. Langmuir monolayers to study interactions at model membrane surfaces. **Advances in Colloid and Interface Science**, v. 100–102, p. 563, 2003.

BRINGEZU, F. et al. Changes in model lung surfactant monolayers induced by palmitic acid. **Langmuir**, v. 17, n. 15, p. 4641–4648, 2001.

BROWN, R. E.; BROCKMAN, H. L. Using monomolecular films to characterize lipid lateral interactions. **Methods in Molecular Biology**, v. 398, p. 41–58, 2007.

C. PEETLA, A. STINE, V. L. Biophysical interactions with model lipid membranes: applications in drug discovery and drug delivery. **Mol Pharm.**, v. 6, n. 5, p. 1264–1276, 2009.

CASALS, C.; CAÑADAS, O. Role of lipid ordered/disordered phase coexistence in pulmonary surfactant function. **Biochimica et Biophysica Acta - Biomembranes**, v. 1818, n. 11, p. 2550–2562, nov. 2012.

CECCARELLI, M. et al. Phospholipidosis effect of drugs by adsorption into lipid monolayers. **Colloids and surfaces. B, Biointerfaces**, v. 136, p. 175–84, 1 dez. 2015.

CHEOW, W. S.; CHANG, M. W.; HADINOTO, K. Antibacterial efficacy of inhalable levofloxacin-loaded polymeric nanoparticles against E. coli biofilm cells: The effect of antibiotic release profile. **Pharmaceutical Research**, v. 27, n. 8, p. 1597–1609, 2010.

CHEOW, W. S.; HADINOTO, K. Factors affecting drug encapsulation and stability of lipid-polymer hybrid nanoparticles. **Colloids and surfaces. B, Biointerfaces**, v. 85, n. 2, p. 214–20, 1 jul. 2011.

CHIMOTE, G.; BANERJEE, R. Effect of mycobacterial lipids on surface properties of Curosurf™: Implications for lung surfactant dysfunction in tuberculosis. **Respiratory Physiology & Neurobiology**, v. 162, p. 73–79, 2005a.

CHIMOTE, G.; BANERJEE, R. Effect of antitubercular drugs on dipalmitoylphosphatidylcholine monolayers: implications for drug loaded surfactants. **Respiratory physiology & neurobiology**, v. 145, n. 1, p. 65–77, 15 jan. 2005b.

CHIMOTE, G.; BANERJEE, R. Lung surfactant dysfunction in

tuberculosis: Effect of mycobacterial tubercular lipids on dipalmitoylphosphatidylcholine surface activity. **Colloids and surfaces. B, Biointerfaces**, v. 45, n. 3–4, p. 215–23, 10 nov. 2005c.

CHIMOTE, G.; BANERJEE, R. Evaluation of antitubercular drug-loaded surfactants as inhalable drug-delivery systems for pulmonary tuberculosis. **Journal of Biomedical Materials Research - Part A**, v. 89, n. 2, p. 281–292, 2009.

CHIRIAC, A. M.; DEMOLY, P. **Drug Allergy**. Third Edit ed. [s.l.] Elsevier Inc., 2015.

CLIFTON, L. A. et al. Lipid binding interactions of antimicrobial plant seed defence proteins: puroindoline-a and beta-purothionin. **Physical Chemistry Chemical Physics**, v. 13, n. 38, p. 17153–17162, 2011.

CLIFTON, L. A. et al. The role of protein hydrophobicity in thionin-phospholipid interactions: a comparison of $\alpha 1$ and $\alpha 2$ -purothionin adsorbed anionic phospholipid monolayers. **Physical chemistry chemical physics : PCCP**, v. 14, n. 39, p. 13569–79, 2012.

CLIFTON, L. A. et al. Asymmetric phospholipid: lipopolysaccharide bilayers; a Gram-negative bacterial outer membrane mimic. **Journal of The Royal Society Interface**, v. 10, n. 89, p. 20130810–20130810, 2013.

DALLOW, J. et al. Microbiological interaction studies between ceftazidime-avibactam and pulmonary surfactant and between ceftazidime-avibactam and antibacterial agents of other classes. **International journal of antimicrobial agents**, v. 44, n. 6, p. 552–6, dez. 2014.

DAVIES, J. T.; RIDEAL, E. K. **Interfacial phenomena**. second ed ed. New York: Academic Press, 1963.

DAVIS, R.; BRYSON, H. M. Levofloxacin A Review of its Antibacterial Activity, Pharmacokinetics and Therapeutic Efficacy. **Drugs**, v. 47, n. 4, p. 677–700, 1994.

DELEU, M.; PAQUOT, M.; NYLANDER, T. Fengycin interaction with lipid monolayers at the air-aqueous interface - Implications for the effect of fengycin on biological membranes. **Journal of Colloid and Interface Science**, v. 283, n. 2, p. 358–365, 2005.

DI COLA, E.; GRILLO, I.; RISTORI, S. Small angle X-ray and neutron scattering: Powerful tools for studying the structure of drug-loaded liposomes.

Pharmaceutics, v. 8, n. 2, p. 1–16, 2016.

DIETRICH, U. et al. Interaction of the MARCKS peptide with PIP₂ in phospholipid monolayers. **Biochimica et Biophysica Acta - Biomembranes**, v. 1788, n. 7, p. 1474–1481, 2009.

DIMER, F. et al. Inhalable Clarithromycin Microparticles for Treatment of Respiratory Infections. **Pharmaceutical Research**, v. 32, n. 12, p. 3850–3861, 2015.

DUAN, J. et al. Design, characterization, and aerosolization of organic solution advanced spray-dried moxifloxacin and ofloxacin dipalmitoylphosphatidylcholine (DPPC) microparticulate/nanoparticulate powders for pulmonary inhalation aerosol delivery. **International Journal of Nanomedicine**, v. 8, p. 3489–3505, 2013.

DUNCAN, S. L.; LARSON, R. G. Comparing experimental and simulated pressure-area isotherms for DPPC. **Biophysical journal**, v. 94, n. 8, p. 2965–2986, 2008.

DYNAROWICZ-ŁĄTKA, P. et al. Quantitative treatment of surface potentials in Langmuir films from aromatic amphiphiles. **Chemical Physics Letters**, v. 337, n. 1–3, p. 11–17, 2001.

DYNAROWICZ-ŁĄTKA, P. et al. BAM studies on the penetration of amphotericin B into lipid mixed monolayers of cellular membranes. **Applied Surface Science**, v. 246, n. 4, p. 334–341, jun. 2005.

EBARA, Y. et al. Interactions of Calcium Ions with Phospholipid Membranes. Studies on π -A Isotherms and Electrochemical and Quartz-Crystal Microbalance Measurements. **Langmuir**, v. 10, n. 7, p. 2267–2271, 1994.

ESTRADA-LÓPEZ, E. D. et al. Prednisolone adsorption on lung surfactant models: Insights on the formation of nanoaggregates, monolayer collapse and prednisolone spreading. **RSC Advances**, v. 7, n. 9, p. 5272–5281, 2017.

ESTRELA-LOPIS, I.; BREZESINSKI, G.; MÖHWALD, H. Miscibility of DPPC and DPPA in monolayers at the air/water interface. **Chemistry and Physics of Lipids**, v. 131, n. 1, p. 71–80, ago. 2004.

FA, N. et al. Decrease of elastic moduli of DOPC bilayers induced by a macrolide antibiotic, azithromycin. **Biochimica et biophysica acta**, v. 1768, n. 7, p. 1830–8, jul. 2007.

FAJARDO, C. et al. Surfactant versus Saline as a Vehicle for Corticosteroid

Delivery to the Lungs of Ventilated Rabbits. **Pediatric Research**, v. 43, p. 542, 1 abr. 1998.

FERRARA, A.; DOS SANTOS, C.; LUPI, A. Effect of some fractions of alveolar surfactant (phospholipids and SP-A) on the bactericidal activity of different antimicrobials against some respiratory pathogens. **Clinical Microbiology and Infection**, v. 7, n. 3, p. 114–119, 2001.

FERRERO, J. L. . et al. Metabolism and Disposition of Clarithromycin in man. **Drug metabolism and disposition**, v. 18, n. 4, p. 441–446, 1990.

FOLLOWS, D. et al. Multilayers at the surface of solutions of exogenous lung surfactant: Direct observation by neutron reflection. **Biochimica et Biophysica Acta - Biomembranes**, v. 1768, n. 2, p. 228–235, 2007.

FORIER, K. et al. Lipid and polymer nanoparticles for drug delivery to bacterial biofilms. **Journal of Controlled Release**, v. 190, p. 607–623, 2014.

FRESTA, M. et al. Combining Molecular Modeling with Experimental Methodologies : Mechanism of Membrane Permeation and Accumulation of Ofloxacin. **Bioorganic & Medicinal Chemistry**, v. 10, p. 3871–3889, 2002.

FULLAGAR, W. K.; HOLT, S. A; GENTLE, I. R. Structure of SP-B/DPPC mixed films studied by neutron reflectometry. **Biophysical journal**, v. 95, n. 10, p. 4829–36, 2008.

GABRIELSON, J. et al. Evaluation of redox indicators and the use of digital scanners and spectrophotometer for quantification of microbial growth in microplates. **Journal of Microbiological Methods**, v. 50, n. 1, p. 63–73, 2002.

GANDHI, S. et al. Calcium-channel blocker-clarithromycin drug interactions and acute kidney injury. **JAMA - Journal of the American Medical Association**, v. 310, n. 23, p. 2544–2553, 2013.

GÉLISSE, P. et al. Carbamazépine et clarithromycine: Une interaction médicamenteuse cliniquement significative. **Revue Neurologique**, v. 163, n. 11, p. 1096–1099, 2007.

GEORGIEV, G. D.; GEORGIEV, G. A.; LALCHEV, Z. Interaction of gentamicin with phosphatidylserine/phosphatidylcholine mixtures in adsorption monolayers and thin liquid films: Morphology and thermodynamic properties. **European Biophysics Journal**, v. 39, n. 9, p. 1301–1312, 2010.

GERALDO, V. P. N. et al. Langmuir films containing ibuprofen and phospholipids. **Chemical Physics Letters**, v. 559, p. 99–106, 20 fev. 2013.

GERICKE, A.; FLACH, C. R.; MENDELSON, R. Structure and orientation of lung surfactant SP-C and L-alpha-dipalmitoylphosphatidylcholine in aqueous monolayers. **Biophysical journal**, v. 73, n. 1, p. 492–499, 1997.

GOLDMAN, R. C. et al. Role of Protonated and Neutral Forms of Macrolides in Binding to Ribosomes from Gram-Positive and Gram-Negative Bacteria. **Antimicrobial Agents and Chemotherapy**, v. 34, n. 3, p. 426–431, 1990.

GOTO, T. E. et al. CdSe magic-sized quantum dots incorporated in biomembrane models at the air-water interface composed of components of tumorigenic and non-tumorigenic cells. **Biochimica et Biophysica Acta - Biomembranes**, v. 1858, n. 7, p. 1533–1540, 2016.

GRANCELLI, A. et al. Interaction of 6-fluoroquinolones with dipalmitoylphosphatidylcholine monolayers and liposomes. **Langmuir**, v. 18, n. 24, p. 9177–9182, 2002.

GREENWOOD, D. **Antimicrobial Drugs: Chronicle of a Twentieth Century Medical Triumph**. 1. ed. Oxford: Oxford University Press, 2008.

GREENWOOD, D.; IRVING, W. L. Antimicrobial agents. **Medical Microbiology**, p. 54–68, 1 jan. 2012.

GRIESE, M. Pulmonary surfactant in health and human lung diseases: State of the art. **European Respiratory Journal**, v. 13, n. 6, p. 1455–1476, 1999.

GRIFFITH, E. C. et al. Oxidized aromatic-aliphatic mixed films at the air-aqueous solution interface. **Journal of Physical Chemistry C**, v. 117, n. 43, p. 22341–22350, 2013.

GULER, D. et al. Effects of Ether vs. Ester Linkage on Lipid Bilayer Structure and Water Permeability. **Chem Phys Lipids**, v. 160, n. 1, p. 33–44, 2009.

HAC-WYDRO, K. et al. Interactions of amphotericin B derivative of low toxicity with biological membrane components--the Langmuir monolayer approach. **Biophysical chemistry**, v. 116, n. 1, p. 77–88, 1 jun. 2005a.

HAC-WYDRO, K. et al. How does the N-acylation and esterification of amphotericin B molecule affect its interactions with cellular membrane components-the Langmuir monolayer study. **Colloids and surfaces. B, Biointerfaces**, v. 46, n. 1, p. 7–19, 25 nov. 2005b.

HAC-WYDRO, K.; DYNAROWICZ-ŁATKA, P. Nystatin in Langmuir

monolayers at the air/water interface. **Colloids and Surfaces B: Biointerfaces**, v. 53, p. 64–71, 2006.

HAITSMA, J.; LACHMANN, U.; LACHMANN, B. Exogenous surfactant as a drug delivery agent. **Advanced Drug Delivery Reviews**, v. 47, n. 2–3, p. 197–207, 25 abr. 2001.

HAN, M.-L. et al. Investigating the Interaction of Octapeptin A3 with Model Bacterial Membranes. **ACS Infectious Diseases**, v. 3, n. 8, p. 606–619, 11 ago. 2017.

HAZELL, G. et al. Langmuir monolayers composed of single and double tail sulfobetaine lipids. **Journal of Colloid and Interface Science**, v. 474, p. 190–198, 2016.

HERTING, E. et al. Combined treatment with surfactant and specific immunoglobulin reduces bacterial proliferation in experimental neonatal group B streptococcal pneumonia. **American Journal of Respiratory and Critical Care Medicine**, v. 159, n. 6, p. 1862–1867, 1999.

HESS, B. et al. GRGMACS 4: Algorithms for highly efficient, load-balanced, and scalable molecular simulation. **Journal of Chemical Theory and Computation**, v. 4, n. 3, p. 435–447, 2008.

HIDALGO, A. A. A. et al. Thermodynamic and infrared analyses of the interaction of chlorpromazine with phospholipid monolayers. **Journal of Physical Chemistry B**, v. 110, n. 39, p. 19637–19646, 2006.

HIDALGO, A.; CRUZ, A.; PÉREZ-GIL, J. Barrier or carrier? Pulmonary surfactant and drug delivery. **European journal of pharmaceutics and biopharmaceutics : official journal of Arbeitsgemeinschaft für Pharmazeutische Verfahrenstechnik e.V**, v. 95, n. Pt A, p. 117–27, set. 2015.

HIRANO, T. et al. Mechanism of the inhibitory effect of zwitterionic drugs (levofloxacin and grepafloxacin) on carnitine transporter (OCTN2) in Caco-2 cells. **Biochimica et Biophysica Acta - Biomembranes**, v. 1758, n. 11, p. 1743–1750, 2006.

HUSSEIN, N. et al. Surface chemistry and spectroscopy studies on 1,4-naphthoquinone in cell membrane models using Langmuir monolayers. **Journal of Colloid and Interface Science**, v. 402, p. 300–306, 15 jul. 2013.

ISKANDER, S. **Axisymmetric drop shape analysis (ADSA) and lung surfactant**. [s.l.] University of Toronto, 2011.

JABŁONOWSKA, E.; BILEWICZ, R. Interactions of ibuprofen with Langmuir monolayers of membrane lipids. **Thin Solid Films**, v. 515, p. 3962–3966, 2007.

JAGALSKI, V. et al. Biophysical study of resin acid effects on phospholipid membrane structure and properties. **Biochimica et Biophysica Acta - Biomembranes**, v. 1858, n. 11, p. 2827–2838, 2016.

JESÚS VALLE, M. J. DE; GONZÁLEZ LÓPEZ, F.; SÁNCHEZ NAVARRO, A. Pulmonary versus systemic delivery of levofloxacin: The isolated lung of the rat as experimental approach for assessing pulmonary inhalation. **Pulmonary Pharmacology & Therapeutics**, v. 21, n. 2, p. 298–303, 1 abr. 2008.

JYOTI, A. et al. An investigation of the compression rate dependence on the surface pressure-surface area isotherm for a dipalmitoyl phosphatidylcholine monolayer at the air/water interface. **Colloids and Surfaces A: Physicochemical and Engineering Aspects**, v. 116, n. 1–2, p. 173–180, 1996.

KANEKO, T.; DOUGHERTY, T. J.; MAGEE, T. V. Macrolide Antibiotics. **Comprehensive Medicinal Chemistry II**, p. 519–566, 1 jan. 2007.

KHARASCH, V. S. et al. Pulmonary surfactant as a vehicle for intratracheal delivery of technetium sulfur colloid and pentamidine in hamster lungs. **The American review of respiratory disease**, v. 144, n. 4, p. 909–913, 1991.

KISELEV, M. A. Methods for lipid nanostructure investigation at neutron and synchrotron sources. **Physics of Particles and Nuclei**, v. 42, n. 2, p. 302–331, 2011.

KLOPFER, K. J. J.; VANDERLICK, T. K. K. Isotherms of Dipalmitoylphosphatidylcholine (DPPC) Monolayers: Features Revealed and Features Obscured. **Journal of Colloid and Interface Science**, v. 182, n. 1, p. 220–229, 1 set. 1996.

KORCHOWIEC, B. et al. A Langmuir film approach to elucidating interactions in lipid membranes: 1,2-dipalmitoyl-sn-glycero-3-phosphoethanolamine/cholesterol/metal cation systems. **Chemistry and Physics of Lipids**, v. 144, n. 2, p. 127–136, 2006.

KORCHOWIEC, B. et al. Glycolipid–cholesterol monolayers: Towards a better understanding of the interaction between the membrane components. **Biochimica et Biophysica Acta (BBA) - Biomembranes**, v. 1808, n. 10, p. 2466–2476, 1 out. 2011.

KOSOL, S. et al. Probing the interactions of macrolide antibiotics with membrane-mimetics by NMR spectroscopy. **Journal of Medicinal Chemistry**, v. 55, n. 11, p. 5632–5636, 2012.

KOTECKA, K.; KRYSINSKI, P. Effect of tetracycline antibiotic on the monolayers of phosphatidylcholines at the air–water interface. **Colloids and Surfaces A: Physicochemical and Engineering Aspects**, v. 482, p. 678–686, out. 2015.

KUO, H. T. et al. A follow-up study of preterm infants given budesonide using surfactant as a vehicle to prevent chronic lung disease in preterm infants. **The Journal of pediatrics**, v. 156, n. 4, p. 537–41, abr. 2010.

LAMBERT, A.; REGNOUF-DE-VAINS, J. B.; RUIZ-LÓPEZ, M. F. Structure of levofloxacin in hydrophilic and hydrophobic media: Relationship to its antibacterial properties. **Chemical Physics Letters**, v. 442, n. 4–6, p. 281–284, 2007.

LODE, H.; ALLEWELT, M. Role of newer fluoroquinolones in lower respiratory tract infections. **The Journal of antimicrobial chemotherapy**, v. 50, n. 1, p. 151–154, 2002.

LOIRA-PASTORIZA, C.; TODOROFF, J.; VANBEVER, R. Delivery strategies for sustained drug release in the lungs. **Advanced Drug Delivery Reviews**, v. 75, p. 81–91, 2014.

LOPEZ-RODRIGUEZ, E.; PÉREZ-GIL, J. Structure-function relationships in pulmonary surfactant membranes: from biophysics to therapy. **Biochimica et biophysica acta**, v. 1838, n. 6, p. 1568–85, jun. 2014.

MACHADO-FERREIRA, E. et al. Bacteria associated with amblyomma cajennense tick eggs. **Genetics and Molecular Biology**, v. 38, n. 4, p. 477–483, 2015.

MAGET-DANA, R. The monolayer technique: a potent tool for studying the interfacial properties of antimicrobial and membrane-lytic peptides and their interactions with lipid membranes. **Biochimica et Biophysica Acta (BBA) - Biomembranes**, v. 1462, n. 1–2, p. 109–140, 15 dez. 1999.

MENDELSON, R.; MAO, G.; FLACH, C. R. Infrared reflection-absorption spectroscopy: Principles and applications to lipid-protein interaction in Langmuir films. **Biochimica et Biophysica Acta - Biomembranes**, v. 1798, n. 4, p. 788–800, 2010.

MICHEL, J. P. et al. Disruption of Asymmetric Lipid Bilayer Models Mimicking the Outer Membrane of Gram-Negative Bacteria by an Active Plasticin. **Langmuir**, v. 33, p. 11028–11039, 2017.

MITSCHER, L. A. Bacterial topoisomerase inhibitors: Quinolone and pyridone antibacterial agents. **Chemical Reviews**, v. 105, n. 2, p. 559–592, 2005.

MOGHADDAM, P. H. et al. Development of a nano–micro carrier system for sustained pulmonary delivery of clarithromycin. **Powder Technology**, v. 239, p. 478–483, maio 2013.

MOHAMMAD-AGHAIE, D. et al. Molecular dynamics simulations of liquid condensed to liquid expanded transitions in DPPC monolayers. **Journal of Physical Chemistry B**, v. 114, n. 3, p. 1325–1335, 2010.

MONTERO, M. T.; HERNÁNDEZ-BORRELL, J.; KEOUGH, K. M. W. Fluoroquinolone–Biomembrane Interactions: Monolayer and Calorimetric Studies. **Langmuir**, v. 14, n. 9, p. 2451–2454, 1998.

MONTERO, M. T.; MERINO-MONTERO, S.; VINUESA, T. Interfacial Membrane Effects of Fluoroquinolones as Revealed by a Combination of Fluorescence Binding Experiments and Atomic Force Microscopy Observations. **Langmuir**, v. 22, n. 18, p. 7574–7578, 2006.

MORENO-SASTRE, M. et al. Pulmonary drug delivery: A review on nanocarriers for antibacterial chemotherapy. **Journal of Antimicrobial Chemotherapy**, v. 70, n. 11, p. 2945–2955, 2015.

MOSMANN, T. Rapid colorimetric assay for cellular growth and survival: Application to proliferation and cytotoxicity assays. **Journal of Immunological Methods**, v. 65, n. 1–2, p. 55–63, 1983.

MUKHERJEE, S. et al. Physicochemical studies on goat pulmonary surfactant. **Biophysical chemistry**, v. 134, n. 1–2, p. 1–9, abr. 2008.

MUNIC, V. et al. Intensity of macrolide anti-inflammatory activity in J774A.1 cells positively correlates with cellular accumulation and phospholipidosis. **Pharmacological Research**, v. 64, n. 3, p. 298–307, 2011.

NATARAJAN, C. K. et al. Surfactant therapy and antibiotics in neonates with meconium aspiration syndrome: A systematic review and meta-analysis. **Journal of Perinatology**, v. 36, n. S1, p. S48–S53, 2016.

NELSON, A. Co-refinement of multiple-contrast neutron/X-ray reflectivity data using MOTOFIT. **Journal of Applied Crystallography**, v. 39, n. 2, p. 273–

276, 2006.

NEVILLE, F. et al. A comparative study on the interactions of SMAP-29 with lipid monolayers. **Biochimica et Biophysica Acta - Biomembranes**, v. 1798, n. 5, p. 851–860, 2010.

NICOLSON, G. L. The Fluid-Mosaic Model of Membrane Structure: Still relevant to understanding the structure, function and dynamics of biological membranes after more than 40 years. **Biochimica et Biophysica Acta (BBA) - Biomembranes**, v. 1838, n. 6, p. 1451–1466, 2014.

ORTIZ-COLLAZOS, S. et al. Langmuir films and mechanical properties of polyethyleneglycol fatty acid esters at the air-water interface. **Colloids and Surfaces A: Physicochemical and Engineering Aspects**, v. 498, p. 50–57, 2016.

ORTIZ-COLLAZOS, S. et al. Interaction of levofloxacin with lung surfactant at the air-water interface. **Colloids and Surfaces B: Biointerfaces**, v. 158, p. 689–696, 2017a.

ORTIZ-COLLAZOS, S. et al. Interaction of levofloxacin with lung surfactant at the air-water interface. **Colloids and Surfaces B: Biointerfaces**, v. 158, p. 689–696, 2017b.

PADILLA-CHAVARRÍA, H. I.; GUIZADO, T. R. C.; PIMENTEL, A. S. Molecular dynamics of dibenz[a,h]anthracene and its metabolite interacting with lung surfactant phospholipid bilayers. **Physical Chemistry Chemical Physics**, v. 17, n. 32, p. 20912–20922, 2015a.

PADILLA-CHAVARRÍA, H. I. H. I.; GUIZADO, T. R. C. T. R. C.; PIMENTEL, A. S. A. S. Molecular dynamics of dibenz[a,h]anthracene and its metabolite interacting with lung surfactant phospholipid bilayers. **Physical Chemistry Chemical Physics**, v. 17, n. 32, p. 20912–20922, 2015b.

PANAIOTOV, I. et al. Interfacial reorganization of molecular assemblies used as drug delivery systems. **Chemistry**, v. 24, n. 6, p. 891–921, 2015.

PANTOJA-ROMERO, W. S. et al. Efficient molecular packing of glycerol monostearate in Langmuir monolayers at the air-water interface. **Colloids and Surfaces A: Physicochemical and Engineering Aspects**, v. 508, p. 85–92, 2016.

PARK, C. W. et al. Advanced spray-dried design, physicochemical characterization, and aerosol dispersion performance of vancomycin and clarithromycin multifunctional controlled release particles for targeted respiratory delivery as dry powder inhalation aerosols. **International Journal of**

Pharmaceutics, v. 455, n. 1–2, p. 374–392, 2013.

PARRA, E.; PÉREZ-GIL, J. Composition, structure and mechanical properties define performance of pulmonary surfactant membranes and films.

Chemistry and physics of lipids, v. 185, p. 153–75, jan. 2015.

PATEL, A. et al. Statin Toxicity From Macrolide Antibiotic Coprescription A Population-Based Cohort Study. **Annals of internal medicine**, v. 158, n. 12, p. 869–876, 2013.

PENFOLD, J. et al. Recent advances in the study of chemical surfaces and interfaces by specular neutron reflection. **J Chem Soc Faraday Trans**, v. 93, n. 22, p. 3899–3917, 1997.

PEREZ-GIL, J. El Sistema del Surfactante Pulmonar. **Investigación y Ciencia**, p. 38–45, 2010.

PÉREZ-GIL, J. Structure of pulmonary surfactant membranes and films: The role of proteins and lipid-protein interactions. **Biochimica et Biophysica Acta - Biomembranes**, v. 1778, n. 7–8, p. 1676–1695, 2008.

PÉREZ, S. et al. Influence of the saturation chain and head group charge of phospholipids in the interaction of hepatitis G virus synthetic peptides. **Journal of Physical Chemistry B**, v. 109, n. 42, p. 19970–19979, 2005.

PICARDI, M. V. et al. Phospholipid packing and hydration in pulmonary surfactant membranes and films as sensed by LAURDAN. **Biochimica et Biophysica Acta - Biomembranes**, v. 1808, n. 3, p. 696–705, 2011.

PINHEIRO, M. et al. Molecular interaction of Rifabutin on model lung surfactant monolayers. **Journal of Physical Chemistry B**, v. 116, n. 38, p. 11635–11645, 2012.

PINHEIRO, M. et al. Interplay of mycolic acids, antimycobacterial compounds and pulmonary surfactant membrane: A biophysical approach to disease. **Biochimica et Biophysica Acta (BBA) - Biomembranes**, v. 1828, n. 2, p. 896–905, 2013a.

PINHEIRO, M. et al. Effects of a novel antimycobacterial compound on the biophysical properties of a pulmonary surfactant model membrane. **International journal of pharmaceutics**, v. 450, n. 1–2, p. 268–77, 25 jun. 2013b.

POCIVAVSEK, L. et al. Glycerol-induced membrane stiffening: The role of viscous fluid adlayers. **Biophysical Journal**, v. 101, n. 1, p. 118–127, 2011.

POLIS, M. A. et al. Clarithromycin lowers plasma zidovudine levels in

persons with human immunodeficiency virus infection. **Antimicrobial Agents and Chemotherapy**, v. 41, n. 8, p. 1709–1714, 1997.

RAGHAVENDRAN, K.; WILLSON, D.; NOTTER, R. Surfactant Therapy of ALI and ARDS. **Crit Care Clin**, v. 27, n. 3, p. 525–559, 2012.

SALEM, I. I.; FLASHER, D. L.; DÜZGÜNEŞ, N. Liposome-Encapsulated Antibiotics. **Methods in Enzymology**, v. 391, p. 261–291, 1 jan. 2005.

SANDRINO, B. et al. Correlation of [RuCl₃(dppb)(VPy)] cytotoxicity with its effects on the cell membranes: An investigation using langmuir monolayers as membrane models. **Journal of Physical Chemistry B**, v. 118, n. 36, p. 10653–10661, 2014.

SCHLÜNZEN, F. et al. Structural basis for the interaction of antibiotics with the peptidyl transferase centre in eubacteria. **Nature**, v. 413, p. 814, 25 out. 2001.

SCHÜRCH, S.; BACHOFEN, H.; POSSMAYER, F. Surface activity in situ, in vivo, and in the captive bubble surfactometer. **Comparative Biochemistry and Physiology - A Molecular and Integrative Physiology**, v. 129, n. 1, p. 195–207, 2001.

SCHURCH, S.; LEE, M.; GEHR, P. Pulmonary surfactant: Surface properties and function of alveolar and airway surfactant. **Pure & Applied Chemistry**, v. 64, n. 11, p. 1745–1750, 1992.

SCHWEDE, T. et al. SWISS-MODEL: An automated protein homology-modeling server. **Nucleic Acids Research**, v. 31, n. 13, p. 3381–3385, 2003.

SEKAR, V. J. et al. Darunavir/ritonavir pharmacokinetics following coadministration with clarithromycin in healthy volunteers. **Journal of Clinical Pharmacology**, v. 48, n. 1, p. 60–65, 2008.

SEVCSIK, E. et al. Interaction of LL-37 with model membrane systems of different complexity: Influence of the lipid matrix. **Biophysical Journal**, v. 94, n. 12, p. 4688–4699, 2008.

SHARMA, P. C.; JAIN, A.; JAIN, S. Fluoroquinolone antibacterials: A review on chemistry, microbiology and therapeutic prospects. **Acta Poloniae Pharmaceutica - Drug Research**, v. 66, n. 6, p. 587–604, 2009.

SINGER, S. J.; NICOLSON, G. L. The Fluid Mosaic Model of the Structure of Cell Membranes. **Science**, v. 175, n. 4023, p. 720–731, 1972.

SORIANO, G. B. et al. Interaction of non-aqueous dispersions of silver

nanoparticles with cellular membrane models. **Journal of Colloid and Interface Science**, v. 496, p. 111–117, 2017.

SOUZA, L. M. P. et al. Penetration of antimicrobial peptides in a lung surfactant model. **Colloids and Surfaces B: Biointerfaces**, v. 167, p. 345–353, 2018.

STEFANIU, C.; BREZESINSKI, G.; MÖHWALD, H. Polymer-capped magnetite nanoparticles change the 2D structure of DPPC model membranes. **Soft Matter**, v. 8, n. 30, p. 7952, 2012.

STEPANIĆ, V. et al. Physicochemical profile of macrolides and their comparison with small molecules. **European Journal of Medicinal Chemistry**, v. 47, n. 1, p. 462–472, 2012.

STERGIOPOULOU, T. et al. Comparative pharmacodynamic interaction analysis between ciprofloxacin, moxifloxacin and levofloxacin and antifungal agents against *Candida albicans* and *Aspergillus fumigatus*. **Journal of Antimicrobial Chemotherapy**, v. 63, n. 2, p. 343–348, 2009.

STEVENS, M. G.; OLSEN, S. C. Comparative analysis of using MTT and XTT in colorimetric assays for quantitating bovine neutrophil bactericidal activity. **Journal of Immunological Methods**, v. 157, n. 1–2, p. 225–231, 1993.

TAKESHITA, N.; OKUNO, M.; ISHIBASHI, T. Molecular conformation of DPPC phospholipid Langmuir and Langmuir–Blodgett monolayers studied by heterodyne-detected vibrational sum frequency generation spectroscopy. **Phys. Chem. Chem. Phys.**, v. 19, n. 3, p. 2060–2066, 2017.

TIETZ, A. et al. Fulminant liver failure associated with clarithromycin. **Annals of Pharmacotherapy**, v. 37, n. 1, p. 57–60, 2003.

TOGAMI, K.; CHONO, S.; MORIMOTO, K. Aerosol-based efficient delivery of clarithromycin, a macrolide antimicrobial agent, to lung epithelial lining fluid and alveolar macrophages for treatment of respiratory infections. **Journal of aerosol medicine and pulmonary drug delivery**, v. 25, n. 2, p. 110–5, 2012.

TOIMIL, P. et al. Monolayer and Brewster angle microscopy study of human serum albumin-Dipalmitoyl phosphatidyl choline mixtures at the air-water interface. **Colloids and Surfaces B: Biointerfaces**, v. 92, p. 64–73, 2012.

TORRES, A.; LIAPIKOU, A. Levofloxacin for the treatment of respiratory tract infections. p. 1203–1212, 2012.

TSANOVA, A.; GEORGIEV, G. A.; LALCHEV, Z. In vitro application of langmuir monolayer model to study in vivo biological systems. **Biotechnology and Biotechnological Equipment**, v. 26, p. 185–190, 2014.

TYTECA, D. et al. The macrolide antibiotic azithromycin interacts with lipids and affects membrane organization and fluidity: Studies on langmuir-blodgett monolayers, liposomes and J774 macrophages. **Journal of Membrane Biology**, v. 192, n. 3, p. 203–215, 2003.

VAKNIN, D. et al. Structural properties of phosphatidylcholine in a monolayer at the air/water interface: Neutron reflection study and reexamination of x-ray reflection measurements. **Biophysical Journal**, v. 59, n. 6, p. 1325–1332, 1991.

VAN'T VEEN, A. et al. Pulmonary surfactant as vehicle for intratracheally instilled tobramycin in mice infected with *Klebsiella pneumoniae*. **British journal of pharmacology**, v. 119, n. 6, p. 1145–1148, 1996.

VAN 'T VEEN, A. et al. Exogenous pulmonary surfactant as a drug delivering agent: influence of antibiotics on surfactant activity. **British journal of pharmacology**, v. 118, n. 3, p. 593–8, 1996.

VARDAKAS, K. Z. et al. Respiratory fluoroquinolones for the treatment of community-acquired pneumonia: a meta-analysis of randomized controlled trials. **CMAJ : Canadian Medical Association journal = journal de l'Association medicale canadienne**, v. 179, n. 12, p. 1269–77, 2008.

VELDHUIZEN, E. J. .; HAAGSMAN, H. P. Role of pulmonary surfactant components in surface film formation and dynamics. **Biochimica et Biophysica Acta (BBA) - Biomembranes**, v. 1467, n. 2, p. 255–270, ago. 2000.

VELDHUIZEN, R. et al. The role of lipids in pulmonary surfactant. **Biochimica et Biophysica Acta (BBA) - Molecular Basis of Disease**, v. 1408, n. 2–3, p. 90–108, 19 nov. 1998.

VIEIRA, L.; SCHENNACH, R.; GOLLAS, B. In situ PM-IRRAS of a glassy carbon electrode/deep eutectic solvent interface. **Physical Chemistry Chemical Physics**, v. 17, n. 19, p. 12870–12880, 2015.

WANG, Y. E. et al. Biophysical interaction between corticosteroids and natural surfactant preparation: implications for pulmonary drug delivery using surfactant as a carrier. **Soft Matter**, v. 8, n. 2, p. 504, 2012.

WEIDEMANN, G.; VOLLHARDT, D. Long range tilt orientational order

in phospholipid monolayers: a comparison of the order in the condensed phases of dimyristoylphosphatidylethanolamine and dipalmitoylphosphatidylcholine. **Colloids and Surfaces A: Physicochemical and Engineering Aspects**, v. 100, p. 187–202, 1995.

WIELAND, D. C. F. et al. Structure of DPPC–hyaluronan interfacial layers – effects of molecular weight and ion composition. **Soft Matter**, v. 12, n. 3, p. 729–740, 2016.

WINKEL, P. et al. Excess sudden cardiac deaths after short-term clarithromycin administration in the CLARICOR trial: Why is this so, and why are statins protective? **Cardiology**, v. 118, n. 1, p. 63–67, 2011.

WORLD HEALTH ORGANIZATION. 19th World Health Organization (WHO) Model list of essential medicines for children. n. March, p. 1–10, 2015.

WRIGHT, T. W. et al. Pulmonary inflammation disrupts surfactant function during *Pneumocystis carinii* pneumonia. **Infection and Immunity**, v. 69, n. 2, p. 758–764, 2001.

WÜSTNECK, R. et al. Interfacial properties of pulmonary surfactant layers. **Advances in colloid and interface science**, v. 117, n. 1–3, p. 33–58, 2005.

YE, T. et al. Inhalable clarithromycin liposomal dry powders using ultrasonic spray freeze drying. **Powder Technology**, v. 305, p. 63–70, 2017.

YEH, T. F. . et al. Early Intratracheal Instillation of Budesonide Using Surfactant as a Vehicle to Prevent Chronic Lung Disease in Preterm Infants: A Pilot Study. **Pediatrics**, v. 121, n. 5, p. e1310 LP-e1318, 1 maio 2008.

ZHANEL, G. G. et al. Fluoroquinolones Focus on Respiratory Tract Infections. **Drugs**, v. 62, n. 1, p. 13–59, 2002.

ZHANG, H. et al. On the low surface tension of lung surfactant. **Langmuir: the ACS journal of surfaces and colloids**, v. 27, n. 13, p. 8351–8358, 2011a.

ZHANG, H. et al. Comparative study of clinical pulmonary surfactants using atomic force microscopy. **Biochimica et biophysica acta**, v. 1808, n. 7, p. 1832–42, jul. 2011b.

ZUO, Y. Y. et al. Current perspectives in pulmonary surfactant — Inhibition, enhancement and evaluation. **Biochimica et Biophysica Acta (BBA) - Biomembranes**, v. 1778, n. 10, p. 1947–1977, 1 out. 2008.

A

Published papers

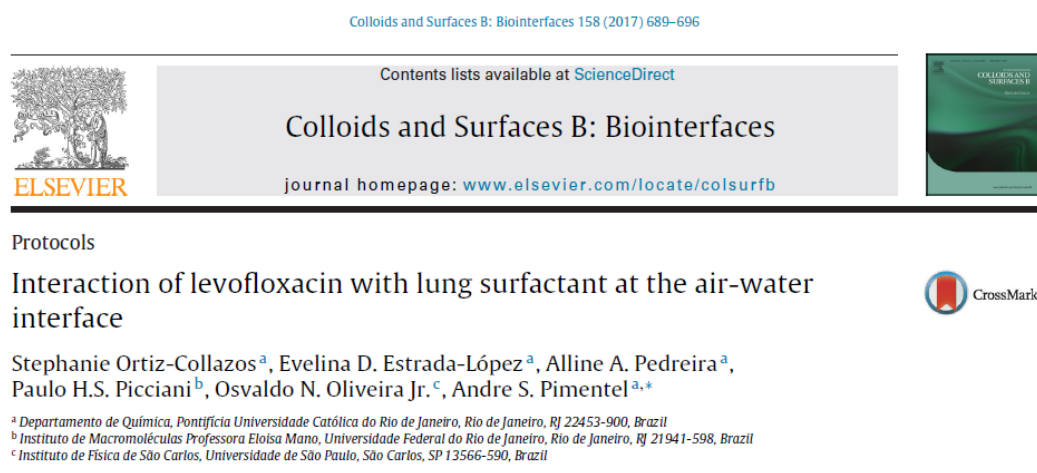


Figure A.1. Published paper: Chapter 4.

B

Submitted papers



Clarithromycin does not affect stability of a lung surfactant monolayer at the air-water interface

Journal:	<i>Journal of Biomolecular Structure & Dynamics</i>
Manuscript ID:	Draft
Manuscript Type:	Research Article
Date Submitted by the Author:	n/a
Complete List of Authors:	Collazos, Stephanie; Pontifícia Universidade Católica do Rio de Janeiro, Departamento de Química Pereira Souza, Lucas Miguel ; Pontifícia Universidade Católica do Rio de Janeiro, Departamento de Química Souza, Felipe; Pontifícia Universidade Católica do Rio de Janeiro, Departamento de Química Oliveira, Nathally; Universidade Federal do Rio de Janeiro Centro de Ciências da Saúde, Departamento de Genética, Instituto de Biologia Cavaleiro, Jéssica; Universidade Federal do Rio de Janeiro Centro de Ciências da Saúde, Departamento de Genética, Instituto de Biologia Soares, Carlos Augusto; Universidade Federal do Rio de Janeiro Centro de Ciências da Saúde, Departamento de Genética, Instituto de Biologia Piciani, Paulo Henrique; Universidade Federal do Rio de Janeiro, Instituto de Macromoléculas Professora Eloisa Mano Oliveira, Osvaldo; Universidade de São Paulo, Instituto de Física de São Carlos Pimentel, Andre Silva; Pontifícia Universidade Católica do Rio de Janeiro, Departamento de Química
Keywords:	Langmuir film, pulmonary system, antibiotic, macrolide, pneumonia

Figure B.1. Submitted paper 1: Chapter 5.

C

Supplementary material -1

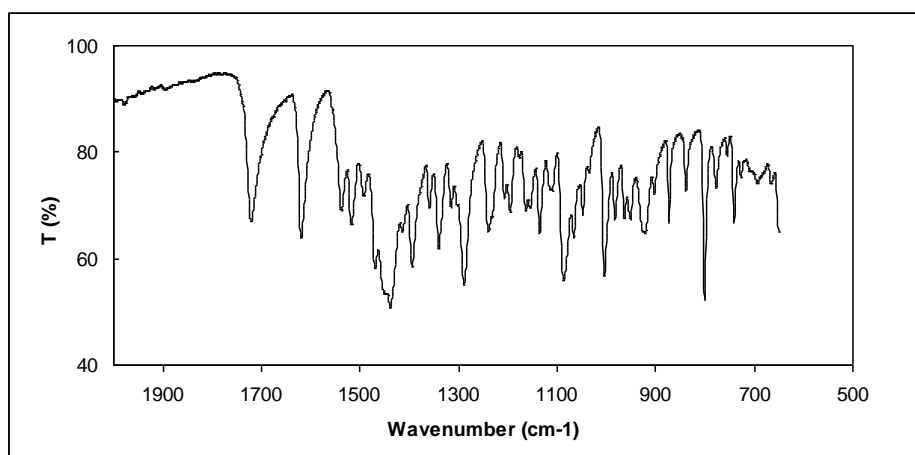


Figure C.1. The IR powder spectrum of pure Levofloxacin.

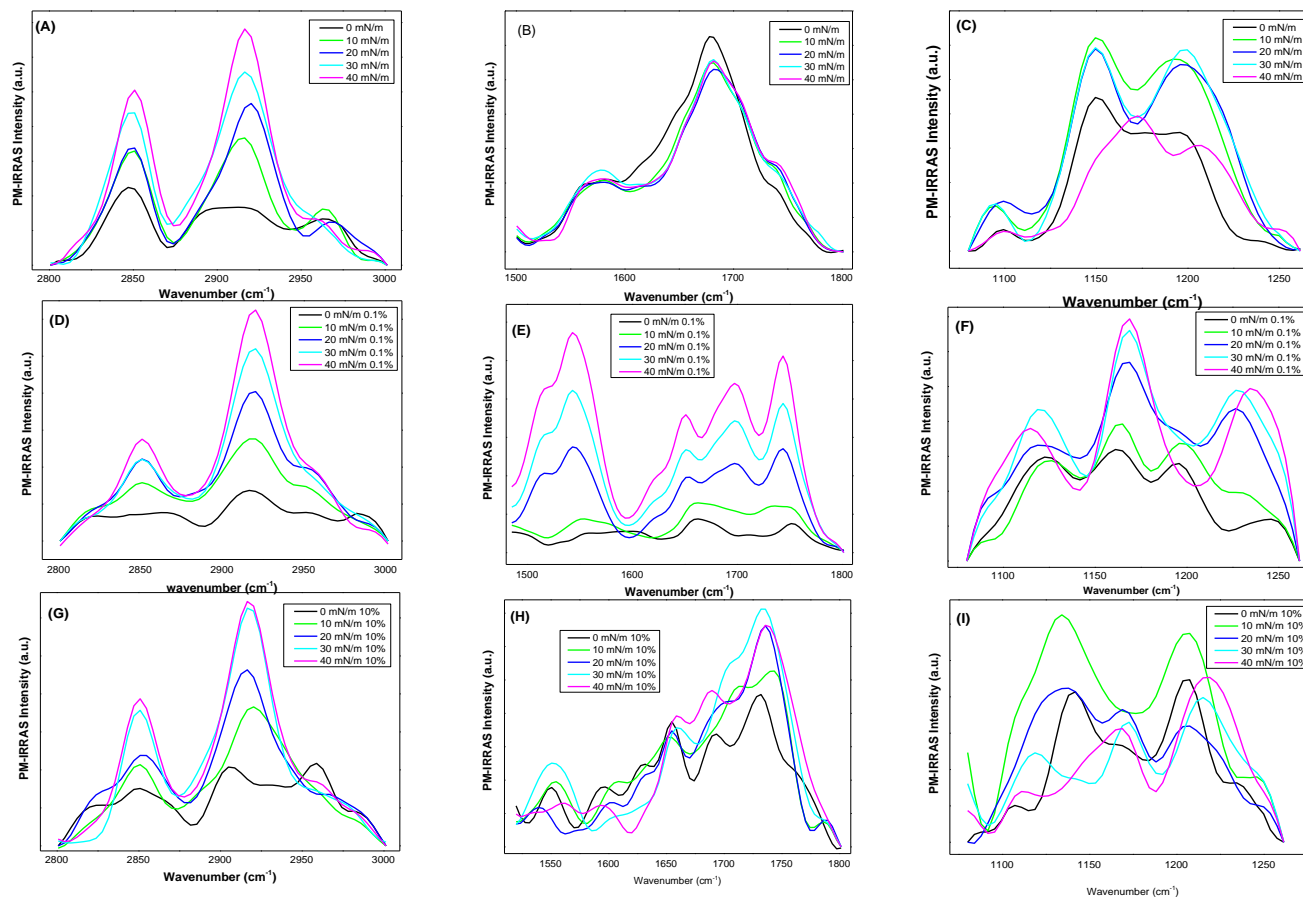


Figure C.2. PM-IRRAS spectra of Langmuir films of pure Curosurf (A, B, and C), Levofloxacin-Curosurf 0.1% w/w (D, E, and F), and Levofloxacin-Curosurf 10% w/w (G, H, and I) at surface pressures 0, 10, 20, 30 and 40 mN m^{-1} in the C-H region ($2800\text{--}3000\text{ cm}^{-1}$), C=O region ($1400\text{--}1800\text{ cm}^{-1}$), and C-O region ($1000\text{--}1300\text{ cm}^{-1}$).

D

Supplementary material -2

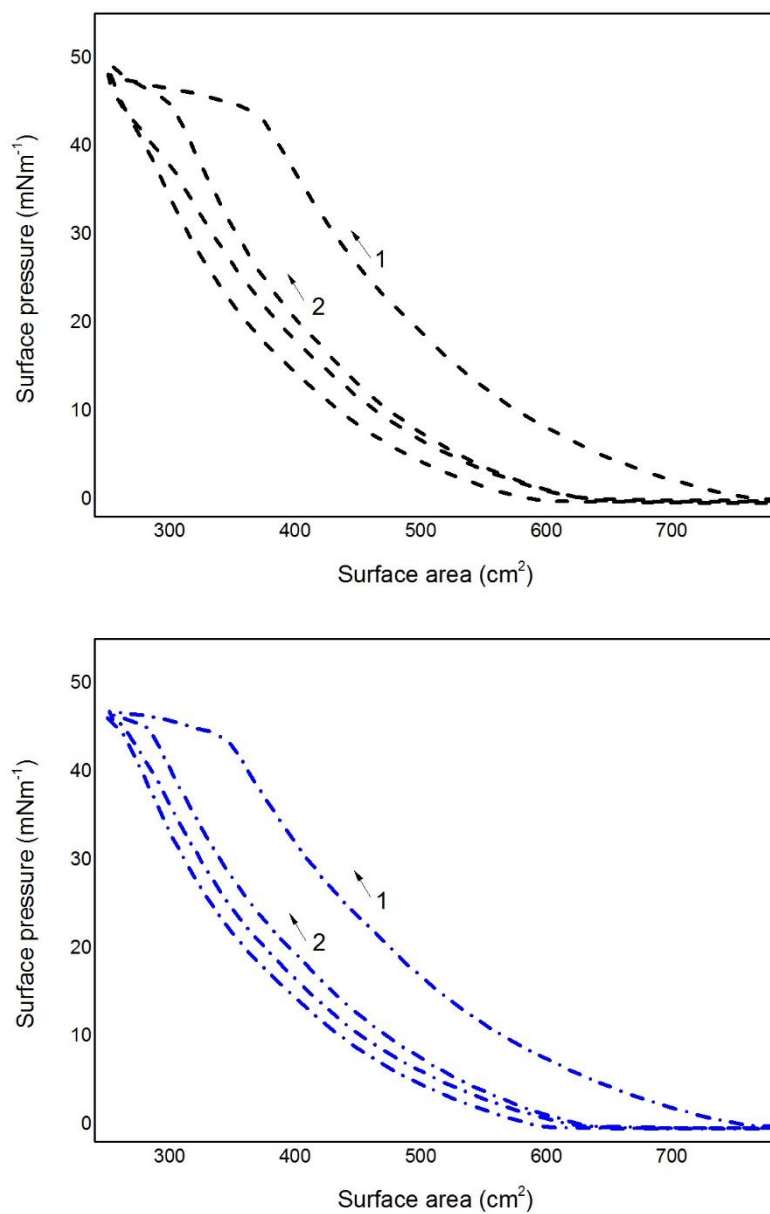


Figure D.1. Consecutive compression-expansion isotherms for pure Curosurf (black dashed line) and mixed Curosurf/Clarithromycin at 10% w/w. (blue dashed-dot line)

E Supplementary material -3

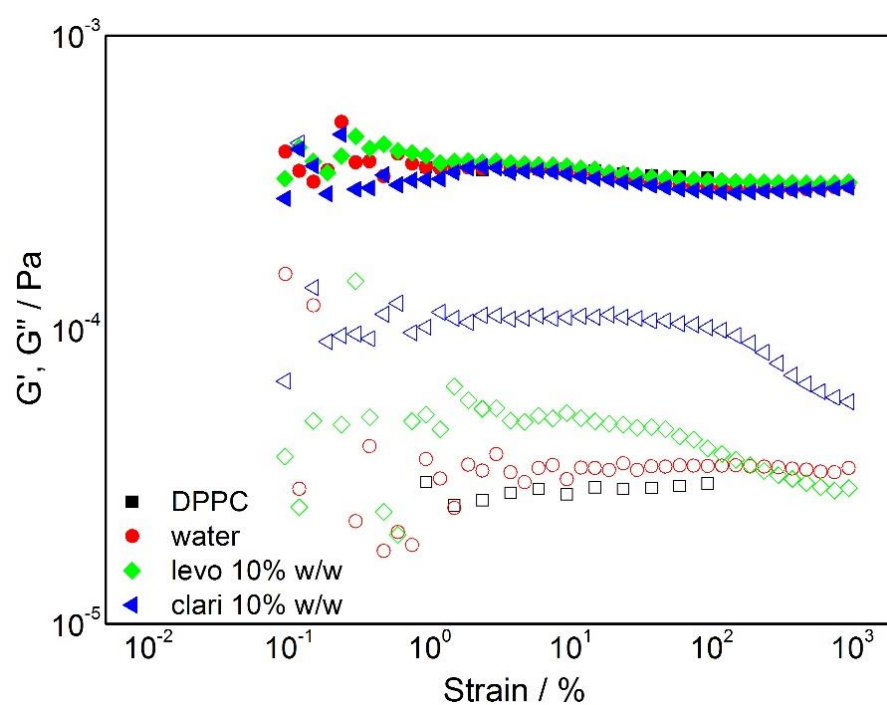


Figure E.1. Amplitude sweep of pure DPPC and mixed DPPC/antibiotics at 25°C using a DWR geometry at a strain amplitude of 1%. The full symbols represent the storage modulus G' and the empty symbols represent the loss modulus G'' , respectively.

Table E.1. BAM images for pure DPPC and mixed DPPC/Levofloxacin monolayers at 0.1, 1 and 10 % w/w under different surface pressures. All BAM images have a 25 μm scale bar at the left hand corner.

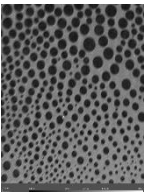
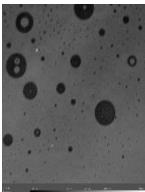
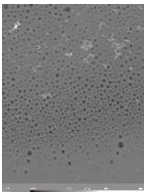
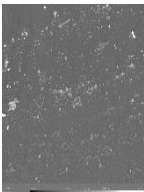
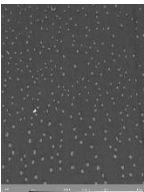
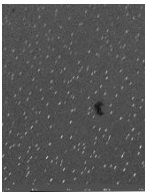
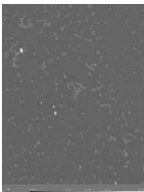
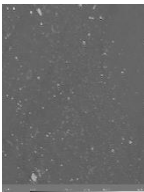
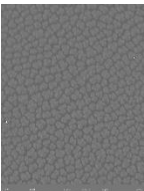
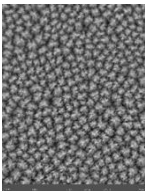
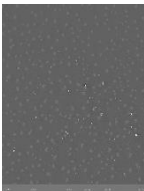
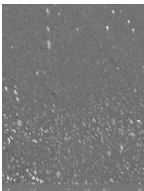
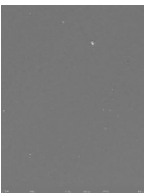
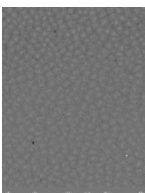
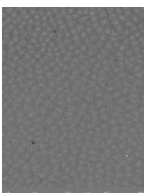
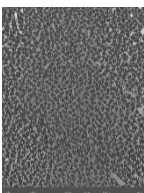
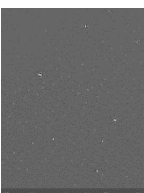
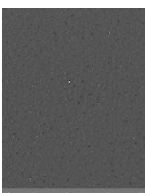
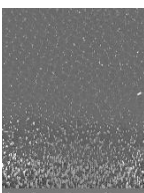
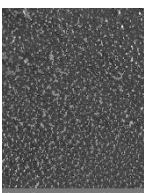
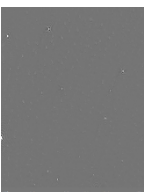
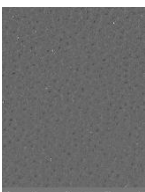
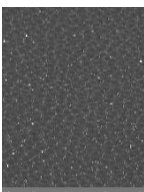
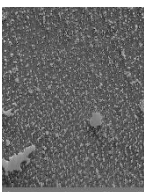
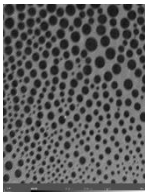

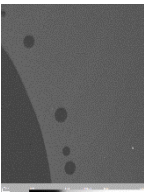
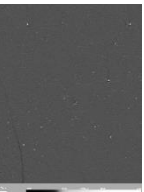
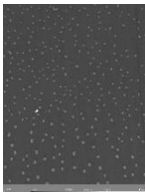
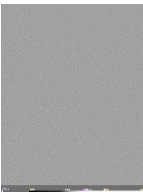

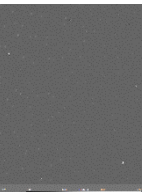
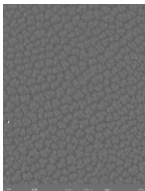
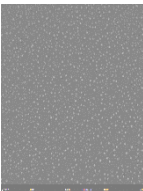
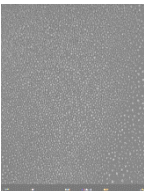
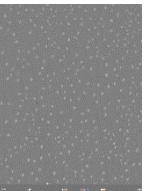
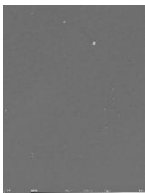
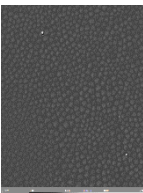
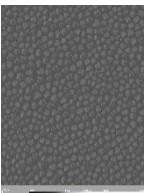
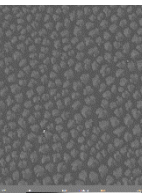
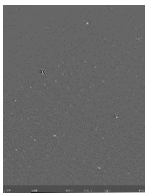
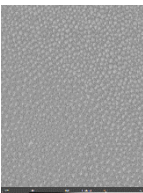
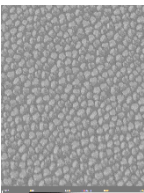
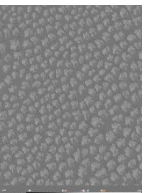
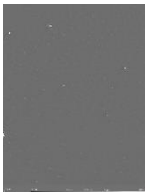
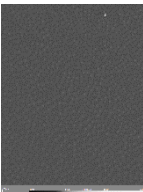
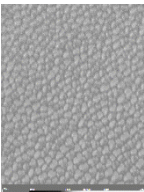
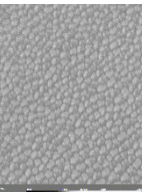
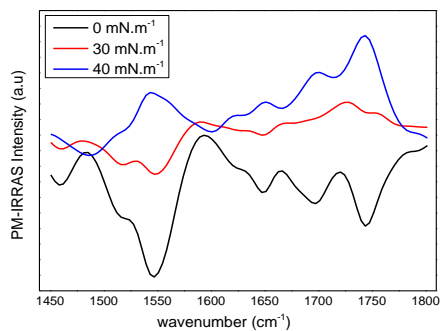
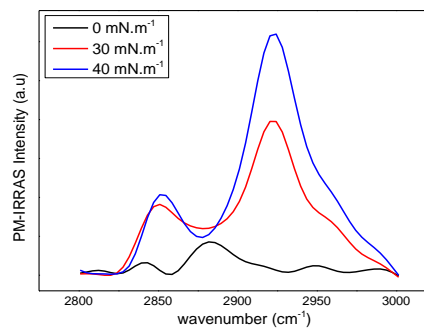
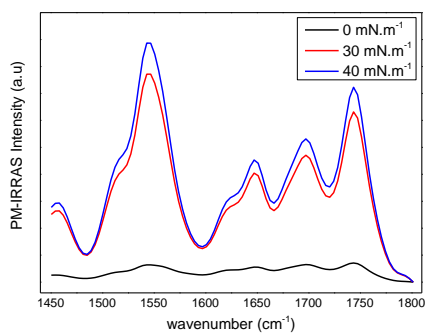
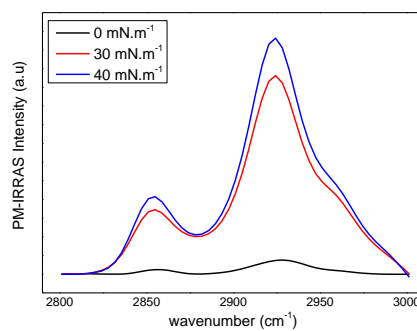
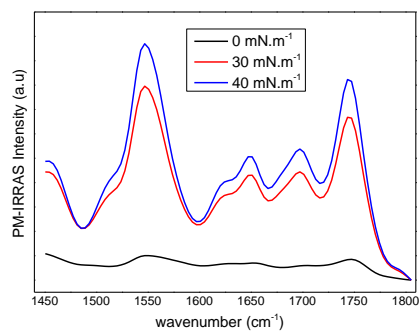
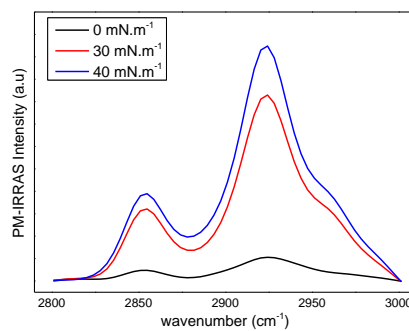
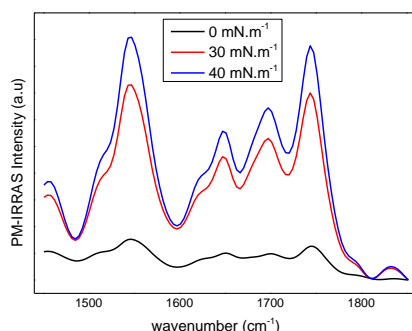
Surface pressure (mNm^{-1})	Pure h-DPPC	h-DPPC/Levofloxacin		
		0.1 %	1 %	10 %
0				
5				
10				
20				
30				
40				

Table E.2. BAM images for pure DPPC and mixed DPPC/Clarithromycin monolayers at 0.1, 1 and 10 % w/w under different surface pressures. All BAM images have a 25 μm scale bar at the left hand corner.

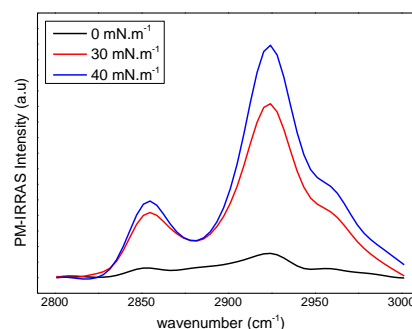
Surface pressure (mNm^{-1})	Pure h-DPPC	h-DPPC/Clarithromycin		
		0.1 %	1 %	10 %
0				
5				
10				
20				
30				
40				

DPPC**A****B****DPPC-Clari 0.1%****C****D****DPPC-Clari 10%****E****F**

DPPC-Levo 0.1%

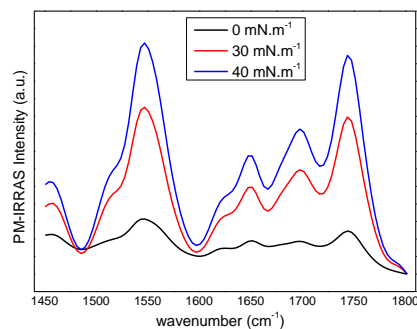


G

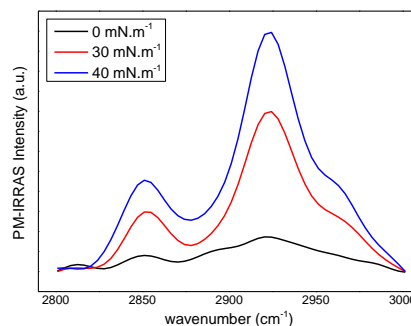


H

DPPC-Levo 10%



I



J

Figure E.2. PM-IRRAS spectra of DPPC at surface pressures of 0, 30 and 40 mNm⁻¹ for 1450 to 1800 cm⁻¹ region (A) and 2800 to 3000 cm⁻¹ (B) region. DPPC + 0.1% (w/w) Clarithromycin at surface pressures of 0, 30 and 40 mNm⁻¹ for 1450 to 1800 cm⁻¹ region (C) and 2800 to 3000 cm⁻¹ (D) region. DPPC + 10 % (w/w) Clarithromycin at surface pressures of 0, 30 and 40 mNm⁻¹ for 1450 to 1800 cm⁻¹ region (E) and 2800 to 3000 cm⁻¹ (F) region. DPPC + 0.1% (w/w) Levofloxacin at surface pressures of 0, 30 and 40 mNm⁻¹ for 1450 to 1800 cm⁻¹ region (G) and 2800 to 3000 cm⁻¹ (H) region. DPPC + 10 % (w/w) Levofloxacin at surface pressures of 0, 30 and 40 mNm⁻¹ for 1450 to 1800 cm⁻¹ region (I) and 2800 to 3000 cm⁻¹ (J) region.

Table E.3. Fitting parameters for a DPPC monolayer using two isotopic contrasts at surface pressures of 5, 20 and 30 mNm⁻¹.

Layer	Contrast	Model: Surface pressure/mNm ⁻¹									Area per lipid/ Å ² (30 mNm ⁻¹)	
		5			20			30			Exp.	Calc.
		t/Å	σ/Å	%Hyd	t/Å	σ/Å	%Hyd	t/Å	σ/Å	%Hyd		
1-Tails	h-DPPC on D ₂ O	8.0 ± 0.5	4.0 ± 0.2	-	12 ± 0.7	3.9 ± 0.4	-	16 ± 0.7	3.0 ± 1	-	46.2 ± 0.1	52.9 ± 0.3
	d-DPPC on ACMW										Alkyl tail tilt angle (relative to the surface normal)	
2-heads	h-DPPC on D ₂ O	12.0 ± 1	4.0 ± 0.3	70 ± 8	11 ± 1.0	3.8 ± 0.4	55 ± 5	11 ± 2	3.5 ± 1	38 ± 9	33.3°	
	d-DPPC on ACMW											

Table E.4. Fitting parameters for a DPPC/Clarithromycin (CLA) monolayer using three isotopic contrasts at surface pressures of 5, 20 and 30 mN m⁻¹. θ is the alkyl tail tilt angle relative to the surface normal.

Layer	Contrast: d-DPPC on D ₂ O or ACMW h-DPPC on D ₂ O	Model: Surface pressure/mNm ⁻¹									Area per lipid/ Å ² (30 mNm ⁻¹)		θ (°)
		5			20			30			Exp.	Calc.	
		t/Å	σ/Å	%Hyd	t/Å	σ/Å	%Hyd	t/Å	σ/Å	%Hyd			
1-Tails	CLA/DPPC 0.1 %	8.7 ± 0.6	5.8 ± 0.8	-	14 ± 0.5	5.5 ± 0.5	-	17.7 ± 0.3	5.0 ± 0.5	-	41.6 ± 0.1	48.0 ± 0.2	22.4
2-Heads	CLA/DPPC 0.1 %	11 ± 0.5	5.5 ± 1	60 ± 5	12 ± 0.5	5.0 ± 1	44 ± 4	9 ± 0.4	5.0 ± 0.5	16 ± 5			
1-Tails	CLA/DPPC 1 %	8.3 ± 0.5	4.5 ± 0.5	-	14 ± 0.7	4.9 ± 0.6	-	18 ± 0.6	5.5 ± 0.4	-	40.9 ± 0.1	47.5 ± 0.1	20.0
2-Heads	CLA/DPPC 1 %	10 ± 1	3.8 ± 0.8	50 ± 2	11 ± 0.3	5.2 ± 0.7	38 ± 2	10 ± 0.3	5.3 ± 0.3	24 ± 4			
1-Tails	CLA/DPPC 10 %	8.7 ± 0.2	5.5 ± 0.5	-	14 ± 0.2	4.4 ± 0.4	-	19 ± 0.3	4.5 ± 0.4	-	39.6 ± 0.2	46.4 ± 0.1	7.17
2-Heads	CLA/DPPC 10 %	12 ± 1	5 ± 0.3	60 ± 3	11.8 ± 0.4	5.0 ± 1	47 ± 3	9.1 ± 0.4	4.5 ± 0.5	19 ± 3			

Table E.5. Fitting parameters for a DPPC/Levofloxacin (LEV) monolayer using different isotopic contrasts at surface pressures of 5, 20 and 30 mN m⁻¹. θ is the alkyl tail tilt angle relative to the surface normal.

Layer	Contrast: d-DPPC on D ₂ O or ACMW h-DPPC on D ₂ O	Model: Surface pressure/mNm ⁻¹									Area per lipid/ Å ² (30mNm ⁻¹)		θ (°)	
		5			20			30			Exp.	Calc.		
		<i>t</i> /Å	<i>σ</i> /Å	%Hyd	<i>t</i> /Å	<i>σ</i> /Å	%Hyd	<i>t</i> /Å	<i>σ</i> /Å	%Hyd				
1-Tails	LEV/DPPC 0.1 %	9.5 ± 0.2	5 ± 0.5	-	14 ± 0.4	5.3 ± 0.5	-	18 ± 0.3	4.8 ± 0.3	-	40.7 ± 0.1	46.0 ± 0.2	±	15.0
2-Heads	LEV/DPPC 0.1 %	12 ± 0.3	5 ± 0.5	64 ± 4	10 ± 1	4.8 ± 0.5	38 ± 5	10 ± 0.2	4.7 ± 0.3	24 ± 2				
1-Tails	LEV/DPPC 1 %	8.2 ± 0.4	5.2 ± 0.4	-	15 ± 0.6	5.0 ± 1	-	17 ± 0.5	3.6 ± 1	-	45.0 ± 0.3	50.0 ± 0.1	±	26.8
2-Heads	LEV/DPPC 1 %	11 ± 1	5.8 ± 0.3	60 ± 4	12 ± 0.5	4.5 ± 0.4	42 ± 6	11 ± 1	4.0 ± 1	34 ± 4				
1-Tails	LEV/DPPC 10 %	8.0 ± 0.2	5.5 ± 0.3	-	15 ± 0.5	4.7 ± 0.7	-	18 ± 0.3	3.7 ± 1	-	43.2 ± 0.3	50.5 ± 0.3	±	20.0
2-Heads	LEV/DPPC 10 %	13 ± 0.4	5.2 ± 0.5	63 ± 3	12 ± 1	5.0 ± 1	49 ± 5	13 ± 0.7	3.9 ± 1	45 ± 4				